Implications for loss of gap junctional intercellular communication in skin derived tumor cells

Inaugural-Dissertation

zur

Erlangung des Doktorgrades der Mathematisch-Naturwissenschaftlichen Fakultät der Heinrich-Heine-Universität Düsseldorf

vorgelegt von

Dragana Mitic

aus Belgrad

Düsseldorf 2006

Gedruckt mit der Genehmigung der
Mathematisch-Naturwissenschaftlichen
Fakultät der Heinrich-Heine-Universität Düsseldorf

Referent: Prof. Dr. Peter Brenneisen
Koreferent: Univ.-Prof. Dr. Joachim Ernst

01. 06. 2006.

Mojim roditeljima

Zusammenfassung

Aus Connexinuntereinheiten aufgebaute *gap junctions* sind direkte Zell-Zellkontakte, die den passiven Austausch von Ionen und kleinen Molekülen erlauben und somit die zelluläre Homöostase regulieren können. Tumorzellen verlieren die Fähigkeit zur direkten Zell-Zell-Kommunikation (ZZK). Die Fähigkeit von Zellen, funktionsfähige *gap junctions* zu bilden, hängt nicht nur von der Expression von Connexinen, sondern auch von dem regulierten, fein abgestimmten Zusammen- und Abbau der gap junctions, von der Stabilität der Connexine und vom Zusammenspiel mit Adhäsionsmolekülen ab. Die gap junctions der Hautzellen sind hauptsächlich aus Connexin 43 (CX43) zusammengesetzt.

In dieser Untersuchung wird deutlich, dass die direkte ZZK in Tumorzellen der Haut komplett unterbunden ist. Hierfür verantwortlich ist weniger eine verminderte Expression von Cx43, als vielmehr eine veränderte intrazelluläre Lokalisation und Phosphorylierung von Cx43.

Verschiedene experimentelle Ansätze sollten Einblicke in die zugrunde liegenden Mechanismen geben. Eine veränderte Expression von Adhäsionsmolekülen und Zytoskelettproteinen, die am Transport und der Bildung von funktionsfähigen gap junctions beteiligt sind, ist in den untersuchten Tumorzellen im Vergleich zu normalen Zellen nicht vorhanden, was deren Bedeutung im Rahmen des Verlustes der ZZK ausschließt. Die Überexpression von exogenem Cx43 unterstützt diese These.

Obwohl aus der Literatur bekannt ist, dass ein verändertes Phosphorylierungsmuster von Cx43 Einfluß auf deren Zusammen- und Abbau, deren Transport zur Membran und Aktivität hat, zeigt die Modulation der Proteinkinase A- und Phosphatase-Aktivität in Tumorzellen zwar eine veränderte Phosphorylierung von Cx43, aber keinen Einfluß auf die direkte Zell-Zell-Kommunikation. Dagegen wird deutlich, dass eine Zunahme der Proteasomen-abhängigen Endoplasmatisches Retikulum-assoziierten Degradation (ERAD) in Tumorzellen vermutlich zu veränderten Phosphorylierungsprozessen in diesen Zellen führt, die nachfolgend die nur intrazelluläre Lokalisation von Cx43 fördert. Dieses Prozess, in Kombination mit einer verminderten Expression von Cx43 führt zum Verlust der homologen und heterologen Zell-Zell-Kommunikation von Tumorzellen der Haut.

Table of contents

Acknowledgements

I would like to thank Prof. Dr. Peter Brenneisen for providing me with the opportunity to work on this subject and in his laboratory, for his guidance and advise, and for his support throughout the study.

I would like to thank to Prof. Dr. Dr. h. c. Helmut Sies for giving me the possibility to do my thesis in his Institute.

To Prof. Dr. Joachim Ernst, I would like to express my special gratitude for sharing the responsibility of this work.

My special thanks goes to all members of my lab - Lirija Alili, Bahar Cat, Esra Bilgic, Christel Werth and Claudia Wyrich, for good working atmosphere and for moral support whenever I needed it. To Dr. Holger Steinbrenner and Dr. Dominik Stuhlmann, I express special gratitude for all what I learned from them, for fruitful discussions, and special support during writing of my thesis. I wish to especially thank Dr. D. Stuhlmann for microinjection experiments.

I would like to thank to the other members of our Institute, present and former ones, for nice atmosphere and experimental advises, among all to Dr. Emanuela Camera, Dr. Niloofar Ale-Agha, Dr. Lars-Oliver Klotz, Dr. Steffanie Galban, Yasemin Ince, Silke DeSprit, Juan Carlos Carrilo, Philippe Walter and Elizabet Sauerbier.

To Marlies Scholtes, I thank for all administrative help and Thomas Becher for his entire computers help. And to Frau Cremer, for her care.

My sincerest gratitude goes to all my friends that I met here, in Germany, and for my old friends back home in Belgrade, for their constant support in all ways and by all means… just for being my friends.

On the end, with all my heart, I thank to my parents and to my brother, for their endless support and love, throughout all this years and over the countries…

Abbreviations

APS	Ammoniumpersulfate
bp	Base pairs
CAF network	Cortical Actin Filament network
cAMP	adenosine-3´, 5´-cyclic monophosphate
CAMs	Cell Adhesion Molecules
Cx	Connexin
DAPI	4′, 6-diamidino-2-phenylindole
DMEM	Dulbecco's modified Eagle's medium
DMSO	Dimethylsulfoxide
EDTA	Ethylene glycol-O, O'-bis-(2-aminoethyl)-N, N, N'-tetraacetic acid
EGF	Epidermal growth factor
EGFP	Enhanced green fluorescent protein
EMT	Epithelial mesenchymal transition
ER	Endoplasmatic reticulum
ERAD	Endoplasmatic reticulum associated degradation
FCS	Fetal calf serum
GJ	Gap junction
GJIC	Gap junctional intercellular communication
HaCaT	Immortalized keratinocyte line
HDF	Human dermal fibroblasts
kDa	10^3 Dalton
min	minute
NHEK	Normal human epidermal keratinocytes
OA	Okadaic acid
PBS	Phosphate-buffered saline
PDGF	Platelet derived growth factor
PKA	Protein kinase A
PM	Plasma membrane
PP	Protein phosphatase
rpm	revolutions per minute
SCL-1	Squamous cell carcinoma tumor line

Suc-LLVY-AMC	N-Succinyl-Leu-Leu-Val-Tyr-7-amino-4-methylcoumarin
TGF-ß1	Transforming growth factor- ß1
TPA	12-O-Tetradecanoylphorbol-13-acetate
UTR	Untranslated region

1. Introduction

Cells in tissues and organs co-ordinate their activities by communicating directly with each other via specialised junctions.

The three major classes of cell junctions, defining the structure and function of epithelial cells are (Fig. 1):

- Anchoring junctions
- Tight junctions
- Gap junctions

Anchoring junctions and tight junctions hold cells together into tissues, while gap junctions permit the rapid diffusion of small water-soluble molecules between the cytoplasm of adjacent cells.

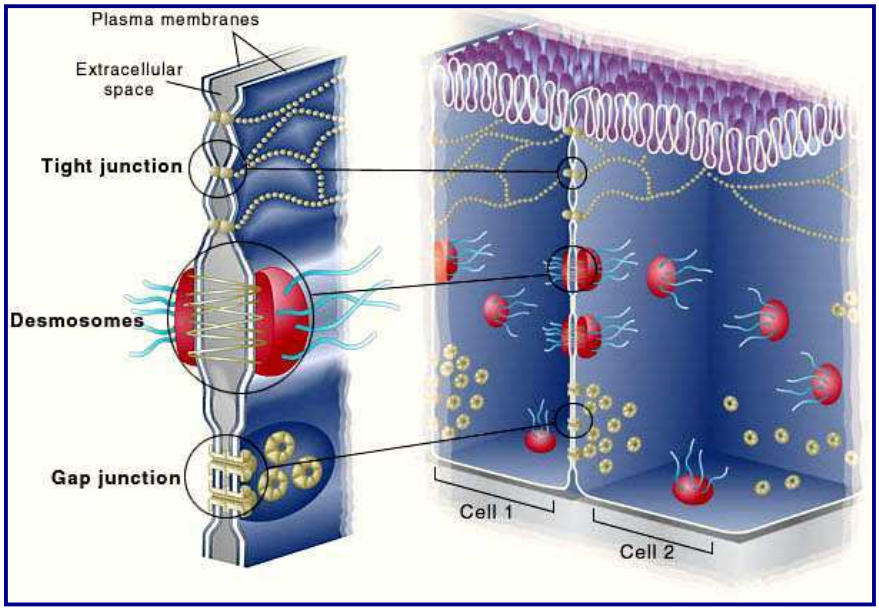

Fig. 1. The major classes of cell junctions

Of the three types of **anchoring junctions** present in epithelial cells, two participate in cell-cell adhesion (*adherens junctions* and *desmosomes*), whereas the third participate in cell-matrix adhesion (*hemidesmosomes*). Anchoring junctions give

strength and rigidity to a tissue and they transmit information between the extracellular and the intracellular space.

Tight junctions prevent the diffusion of macromolecules and to a certain level interrupt the diffusion of small water-soluble molecules and ions across epithelial cell layers into the intercellular space. In addition, they maintain the polarity of epithelial cells, restricting diffusion of membrane proteins and glycolipids.

1.1 Gap junctions- structure and function

Gap junctions (GJ) are morphologically defined as specialized contacts between cells mediating the direct exchange of small molecules in order to coordinate behaviour of multicellular systems. Gap junctions of Vertebrates are found in most cell types, except in skeletal muscle fibers, certain neurons, circulating blood cells (erythrocytes and platelets) and sperm.

Gap junctions are plasma membrane microdomains constructed of assemblies of gap junctional channels, which directly link the cytoplasms of neighbouring cells. Each gap junction channel is comprised of two hemichannels or connexons and each connexon is formed by the aggregation of six protein subunits known as connexins (Willecke et al., 2002) (Fig. 2).

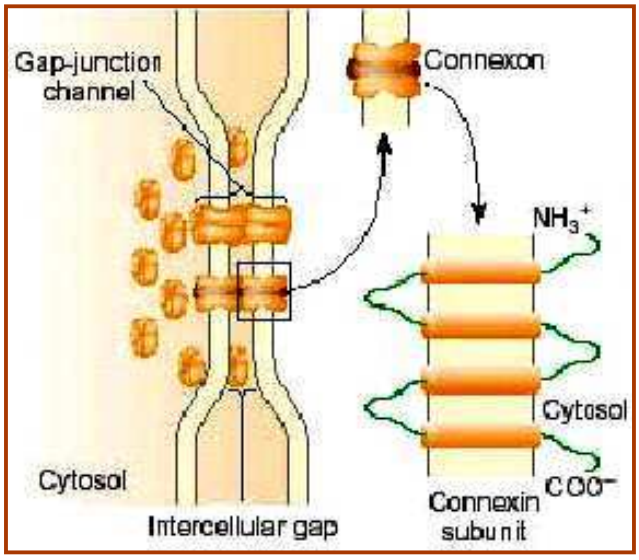

Fig. 2. Structure of gap-junction channel

The channels have a diameter of 1,5-2 nm, depending on the type of the junction-forming proteins and permit direct diffusion of ions and small molecules (<1,2 kDa) such as water, sugars, nucleotides, amino acids, fatty acids, small peptides, secondary messengers (cAMP, IP3, Ca^{2+} ions), drugs and carcinogens. However, proteins, complex lipids, polysaccharides, RNA, and other large molecules are not able to pass. Channel passage does not require ATP and therefore appears to result from passive diffusion. This flux of molecules between cells via gap junction channels is known as gap junctional intercellular communication (GJIC).

Gap junctions have important physiological roles. The most ancient, widespread and important function for these channels is rapid equilibration of nutrients, ions and fluids between cells, which contributes to the overall homeostasis. GJ also serve as synapses in electrically excitable cells such as cardiac myocytes, smooth muscle cells and neurons. Electrical coupling via gap junctions allows faster cell-to-cell transmission of action potentials compared to chemical synapses, enabling myocytes to contract synchronously (Severs, 1999). GJIC may enhance the responsiveness of tissues to external stimuli, through the passage of second messengers such as cAMP, cGMP, calcium, and inositol phosphates from hormonally activated cells to quiescent cells (Lawrence et al., 1978). Gap junctional coupling has also been demonstrated in embryonic tissue and is assumed to trigger intercellular pathways for chemical and/or electrical development signals and to define the boundaries of developmental compartments (Kalimi et al., 1988).

1.1.1. Connexin - expression, gene regulation and mutations

Connexins (Cx) are proteins encoded by a large gene family, of which 20 human genes have been identified to date. They are located on several chromosomes, suggesting their random distribution throughout the genome. Human connexins are classified into three groups, either by molecular mass or by sequence similarities: gap junction α (GJA), gap junction β (GJB) or gap junction γ (GJC). Despite the presence of conserved sequences among different connexins, the diversity of these proteins is not due to alternative splicing of RNAs.

Connexins are expressed in a cell-, tissue-, and development- specific manner. In those cells where multiple connexins are expressed, gap junction hemichannels may

be comprised of more then one connexin (heteromeric connexons) or may be homomeric (Sosinsky G, 1995). Heteromeric channels may have different permeability and regulatory properties then homomeric ones. Hemichannels could form homotypic channels (made by the same connexons) or heterotypic channels consisting of two different connexons (Bukauskas et al., 1995). However, only certain heterotypic pairings are capable to form functional channels (Bruzzone et al., 1996).

The structures of nearly all connexin genes are similar, consisting of two exons separated by a long intron (White et *al*, 1995). The first exon is rather short (about 100bp), and as it contains no protein coding information, the complete reading frame is within the second exon (Fig. 3).

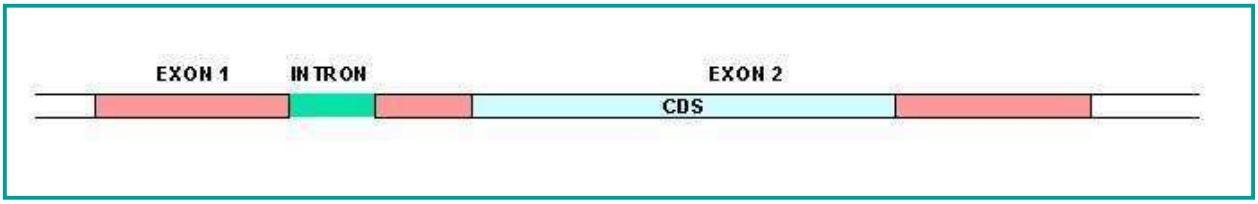

Fig. 4. Structure of connexin gene

The promoter of Cx43 contains a TATA box located near the transcriptional start site and an activator protein-1 site (AP-1, heterodimer of c-Fos and c-Jun) further upstream. Putative responsive elements in connexin promoters include Sp1 site, T cell factor/lymphoid enhancer binding factor, E-box, half-palindromic ERE sites (estrogen-responsive elements), AP-2, cAMP-responsive element binding protein, and Ets-1 sites (Carystinos et al., 2003). Several physiological, pharmacological and dietary factors alter the expression of connexins, and they often affect connexin expression in a cell-specific manner. Connexin mRNA and protein stability also appear to be important in the expression of connexin. Sequences located in the 3'-UTR of the Cx43 mRNA seem to have a role in stabilization of this mRNA (Stahl et al., 2000; Teicher et al., 1999).

Several mutations in different connexin genes were described and demonstrated to be associated with human inherited diseases. Mutations in connexin genes could influence the gating properties of the channel, the trafficking of connexins and the assembly of gap junctions. Mutation in human Cx32 gene cause Charcot-Marie-Tooth disease (X-type) (CMTX), an inherited demyelination disorder of the peripheral nervous system characterized by progressive wasting of distal muscles in the limbs

(Bergoffen et al., 1993). Mutations in Cx26 gene are responsible for the most frequent non-syndromic sensorineural hearing defect in humans (Kelsell et al., 1997) and could also exhibit alterations in the epidermis (Richard et al., 1998). Mutations in Cx31 and Cx30 gene also lead to hearing defects (Liu et al., 2000; Grifa et al., 1999). Defects in connexin 26, 31, 30 or 30.3 have been described to cause the inherited human skin disease *Erythrokeratodermia variabilis* (EKV) (as reviewed in Richard, 2000).

1.1.2. Formation and degradation of gap junctions

Assembly of gap junction channels is a complicated, highly regulated process that includes biosynthesis of the connexin subunit proteins on endoplasmatic reticulum membranes, oligomerization of compatible subunits into hexameric hemi-channels (connexons), delivery of the connexons to the plasma membrane, docking of compatible connexons in the extracellular space at distinct locations and arrangement of channels into the GJ channel aggregates (so-called plaques). Likewise, the coordinated removal of channels into the cytoplasm and the following degradation of their components are strictly controlled (Fig. 5).

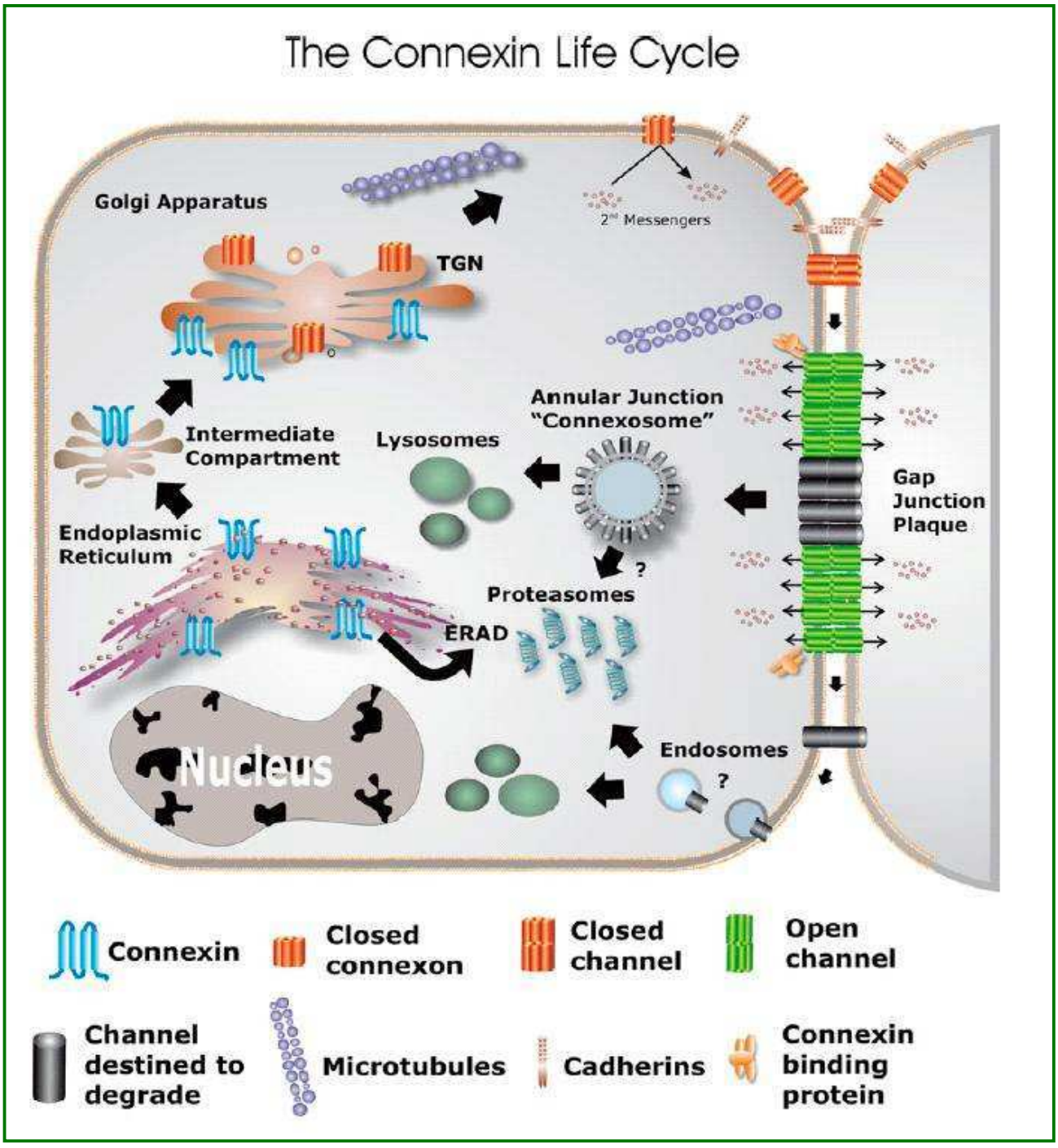

Fig. 5. The connexin life cycle (Laird et al., 2006)

1.1.2.1. Connexin polypeptide biosynthesis

Like other transmembrane proteins (and secretory proteins), connexins are synthesized by ribosomes that are bound to the endoplasmatic reticulum (ER) membrane. At their amino-terminus or further downstream they encode hydrophobic signal sequences recognized and bound by a signal recognition particle (SRP). This interaction is required for docking of the SRP/ribosome/nascent-polypeptide-chain/mRNA complex to a protein channel in the ER membrane (Sec 61 complex or translocon) (Gorlich et al., 1993; High et al., 1993; Kalies et al., 1994). When protein synthesis has been completed, secretory proteins are released into the lumen of ER, while membrane proteins are translocated out of the channel lumen into the hydrophobic ER membrane environment (Mothes et al., 1997). Charged residues within hydrophobic trans-membrane regions of connexins might be shielded from this bilayer environment through oligomerization.

During integration of a nascent connexin polypeptide into the ER membrane they achieve their specific trans-membrane topology. Connexin proteins have four trans-membrane domains (TM1-TM4), two extracellular loops (E1 and E2), and cytoplasmically located amino- and carboxyl termini (Falk et al., 1994; Falk et al., 1998) (Fig. 6).

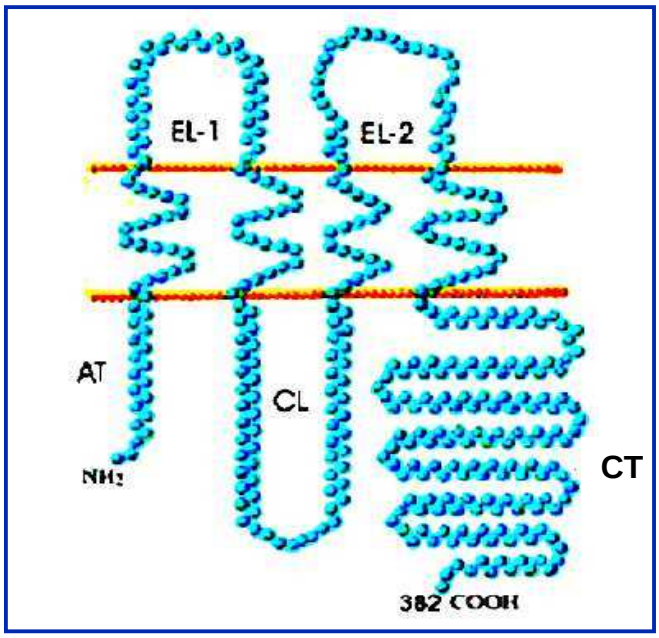

Fig. 6. Topology of connexin structure
(AT-Amino terminus; EL-1, EL-2- Extracellular loop 1,2; CL-Cytoplasmatic loop; CT- Carboxyl terminus)(modif. from Laird et al., 2006)

Connexins, like all membrane proteins with N-terminus facing the cytoplasm, use internal trans-membrane segments, structurally similar to N-terminal signal peptides of proteins, for SRP-binding, targeting and anchoring of the proteins in the membrane bilayer (signal anchor, SA sequences). Only N-terminal SPs are cleaved from pre-proteins by the ER lumenal protease SPase during or short after translocation while internal SA sequences are preserved (as reviewed in High et al., 1991; Zerial et al., 1986). In cell-free translation assays with connexins, cryptic cleavage of those internal SA sequences by SPase at the end of the first trans-membrane spanning domain occurred very efficiently (Falk et al., 1994), indicating the requirement of additional factors, such as chaperons, for successful connexin membrane integration. Those chaperons might prevent SPase from accessing the cryptic sites by accurately positioning TM regions within the membrane bilayer.

1.1.2.2. Connexin phosphorylation

The most important and remarkable posttranslational modification of all connexin proteins, except Cx26, is phosphorylation and a number of potential phosphorylation sites are found in their C-terminal tail. Many connexins exhibit a basal constitutive level of phosphorylation, but generally phosphorylation is induced or changed by the activation of proper signal transduction pathways. A modified phosphorylation pattern is often accompanied by changes in the level of GJIC. Thus, kinases are directly or indirectly involved in the regulation of GJIC and their action is balanced by protein phosphatases. Phosphorylation has been implicated in several stages of connexin lifecycle, such as trafficking, assembly/disassembly, and degradation, as well as in the gating of hemichannels or intact gap junction channels. Most studies in this field has been focused on Cx43. Activation of several kinases including protein kinase A (PKA), protein kinase C (PKC), $p34^{cdc2}$/cyclin B kinase, casein kinase 1 (CK1), mitogen-activated protein kinase (MAPK) and $pp60^{src}$ kinase can lead to phosphorylation of the majority of the 21 serine (Ser) and two tyrosine (Tyr) residues in the C-terminal region of connexin 43 (as reviewed in Solan et al., 2005; Cruciani et al., 2002) (Fig. 7).

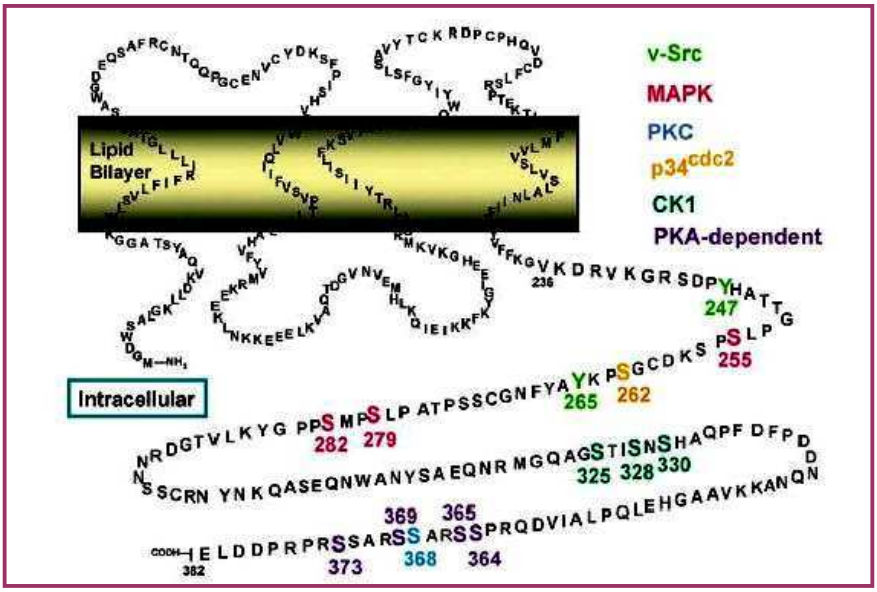

Fig. 7. Phosphorylation sites in Cx43. Phosphorylation sites targeted by known kinases are indicated by different colors (Src, lime green; MAPK, red; PKC, blue; p34cdc2, orange; CK1, dark green; PKA-dependent, purple) (Lampe and Lau, 2000)

Cx43 displays multiple protein isoforms when analysed by SDS-PAGE, including a faster migrating form that includes non-phosphorylated (P0 or NP) Cx43, and at least one of the two slower migrating forms, termed P1 and P2. Both P1 and P2 co-migrate with P0 following dephoshorylation by alkaline phosphatase (Musil et al., 1990).
In general, the action of kinases is usually counteracted and balanced by protein phosphatases. Modulation of the enzymatic activity of protein phoshatases 1 and 2A (PP1 and PP2A), as well as PP2B, was shown to alter phoshorylation status of connexin and to influence gap junction processing and function (as reviewed in Herve and Sarrouilhe, 2002).

1.1.2.3 Assembly, trafficking and insertion of connexins into the plasma membrane

For many oligomeric membrane proteins, assembly in the ER is necessary for further trafficking and delivery to the plasma membrane (Hurtley et al., 1989; Ellgaard et al., 2003). However, assembly of connexins has been shown to occur after exit from ER, probably in trans-Golgi network (TGN) (Musil et al., 1993), or also in the ER-Golgi-intermediate compartment (ERGIC) (reviewed in Evans et al., 1999). Using genetically engineered connexins, encoding ER-retention signals, evidence for an

isoform-specific site of connexon assembly has been obtained with Cx32 assembling in the ER/ERGIC and Cx43 assembling in the TGN (Das Sarma et al., 2001).

Trafficking to the cell surface is normally accomplished by the budding of secretory- and membrane-protein-containing vesicles from the ER, which then fuse with subsequent intracellular membrane compartments, the Golgi stacks, the TGN, and finally the plasma membrane (PM). Cx polypeptides follow the general intracellular transport route referred to as the secretory pathway (Rothman et al., 1996; Pfeffer et al., 1987). In that contest, no gap junction channel assembly or gap junction plaque formation was observed in cells treated with drugs that interfere with the secretory pathway, such as brefeldin A (BFA), carbonyl cyanide *m*-chlorophenylhydrazone (CCCP) or in cells kept at non-permissive temperature (Musil et al., 1993; DeSousa et al., 1993; Laird et al., 1995). Multicolour time-lapse microscopy studies on the delivery of connexons assembled from GFP-tagged Cx43 in transfected HeLa cells revealed that connexons travelled in vesicles along microtubules from the Golgi to the plasma membrane (Lauf et al., 2002). Membranes of the rough ER can be located very close to the plasma membrane and therefore, connexons assembled in ER might go directly to PM. This observation might explain the delivery of connexons even when microtubules and Golgi membranes have been disrupted.

Connexons are delivered to plasma membrane as single particles or small groups, but not as large aggregates, and therefore, they can move laterally in the plane of the membrane. Once delivered to the plasma membrane, connexons can also function in intra-/extracellular signalling. Their suggested functions are diverse and include isosmotic cell volume regulation, inhibition of the activity of Ca^{2+} -channels and subsequent glutamate release at synapses located in outer retina, involvment in pro- and anti-apoptotic pathways, regulation of glutamate and aspartate release in astrocytes, and differentiation of teratocarcinoma progenitor cells into neuronal and nonneuronal cells (as reviewed in Goodenough et al., 2003; Ebihara, 2003; Bennett et al., 2003).

The remark that connexons are delivered to non-junctional membrane might provide the possibility of a two-step mechanism allowing connexons first to function in intra-/extracellular signalling and then in direct cell-cell communication.

Calcium-dependent cell adhesion molecules (CAMs) are enabling or at least facilitating docking of connexons, probably by bringing the membranes of neighbouring cells close enough to initiate connexon interaction. Transfection of

S180 cells, which synthesize Cx43 but fail to assemble gap junctions, with L-CAM, could induce gap junction formation (Musil et al., 1990), suggesting that adherens junctions act as a foci for gap junction formation. Also, calcium-dependent regulation of GJIC by E-cadherin was reported (Jongen et al., 1991). Binding of catenins to the membrane-associated guanylate kinase protein, zonula occludens-1 (ZO-1) is required for Cx43 transport to the PM during the assembly of gap junctions (Wu et al., 2003).

1.1.2.4. Aggregation of gap junction channels into a plaque and its structural composition

Gap junction channels aggregate to create characteristic two-dimensional arrays of channels, termed plaques. A single plaque might be composed of less then a dozen to many thousand individual channels, and it can spread from less then a 100 nm to several µm in diameter (McNutt et al., 1970; Forge et al., 2003).
Lipids surround the proteins of gap junction channels, and cholesterol is enriched in plaques (Malewicz et al., 1990). Recent reports describe specific association of Cx43, Cx32, Cx36 and Cx46 with lipid rafts, specialized membrane domains rich in cholesterol, sphingolipids, and signalling proteins (Simons et al., 2000), and their co-localization with the lipid raft marker protein caveolin-1 (Mograbi et al., 2003; Schubert et al., 2002). The preferential localization of different connexins in certain lipid environments could be involved in channel aggregation, mixing and segregation.

1.1.2.5. Gap junction removal and degradation

The half-life of connexins ranges from 1 to 5 h, both in vivo and in vitro. Gap junction channels, once formed, can not be separated again into hemi-channels under physiological conditions (Goodenough et al*.,* 1974; Ghoshroy et al., 1995). There are three pathways proposed for degradation of connexins and gap junctions: (1) lysosomal or proteasomal degradation of connexins in gap junctional plaques after endocytotic internalization (2) lysosomal degradation of connexin monomers or oligomers from an early secretory compartmant and (3) endoplasmatic reticulum-

associated degradation (ERAD) of misfolded/abnormally oligomerized proteins (Fig. 8).

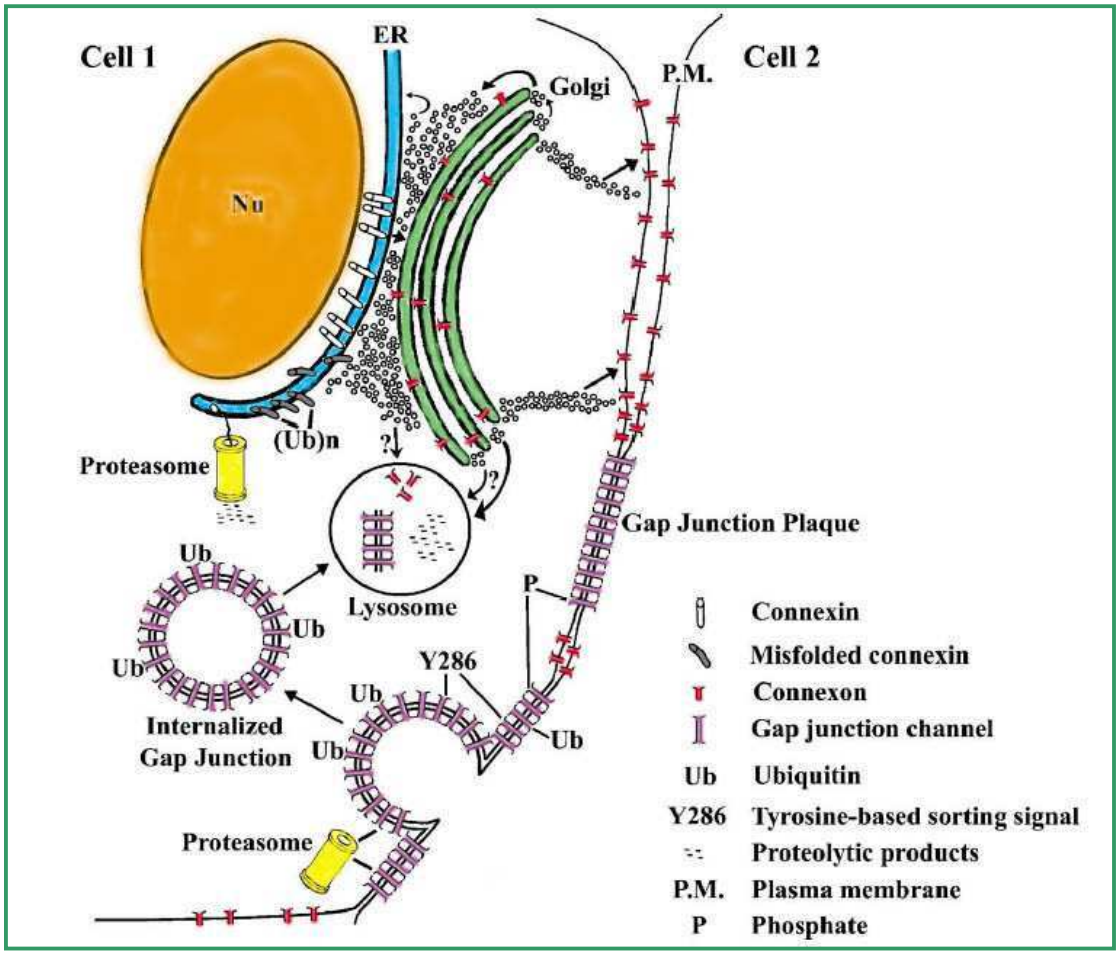

Fig. 8. Degradation of connexins and gap junctions (modif. from Berhoud et al., 2004)

The early degradation products of internalized gap junctions are called annular junctions, and they are generated by invagination, restriction, pinching off, and transport of both junctional membranes into the cytoplasm of one of the apposed cells (Larsen et al., 1978; Jordan et al., 2001). In this process, clathrin and actin filaments might be involved (Huang et al., 1996; Larsen et al., 1978). Once internalized, further degradation involves both lysosomal and proteasomal degradation pathways (reviewed in Spray, 1998; Laird, 1996), as it is described for Cx43 (Qin et al., 2003).

Phosphorylation of Cx43 by protein kinase C (PKC), extracellular signal-regulated kinases (ERK) and casein kinase 1 (CK1), have been described to induce gap

junction removal from the plasma membrane (Nguyen et al., 2003; Cooper et al., 2002; Lampe, 1994). Recently, a tyrosine-based sorting signal was characterized in the C-terminal domain of Cx43, which appears to be important for Cx43 stability and consequently GJIC, by targeting Cx43 for degradation in the endocytic/lysosomal compartment (Thomas et al., 2003). There is also possible role of a ZO-1 in Cx43 GJ turnover during cardiac development and disease processes (Barker et al., 2001; Barker et al., 2002).

Endoplasmatic reticulum associated degradation (ERAD) is carried out by the 26S proteasome, the multicatalytic protease complex. Major substrates for this type of degradation include proteins that are conformationally abnormal as a result of mutation, lack of assembly partner or imperfect folding. It was shown that ~40% or more of newly synthesized Cx43 and Cx32, are degraded in certain cell types even when the exit from ER is blocked (VanSlyke et al., 2000). This ER-associated turnover is sensitive to chemical inhibitors of the proteasome, but not to inhibitors of lysosome. ERAD of connexins could be a consequence of slow and/or inefficient folding.

1.2 Structure and function of human skin

The skin is the largest organ of the human body, accounting for about 15% of the body weight with a surface area of between 1.5-2.0m^2. The most important physiological function of the skin is the protection from the surrounding environmental factors- physical, chemical and microbial, serving as a barrier that keeps the internal systems intact. The other functions include temperature regulation, vitamin D synthesis, excretion of urea, and absorption of small amounts of oxygen, nitrogen and carbon dioxide.

The skin is composed of the *epidermis* and the *dermis*. Below these layers lies the subcutaneous fat tissue, *hypodermis*.

The **epidermis** is the most superficial layer of the skin and provides the first barrier of protection against invasion of foreign substances into the body. It consists of stratified squamous epithelium with an underlying basement membrane. The predominant cells, which make up the epidermis, are keratinocytes. In addition, dendritic cells-

melanocytes, Langerhans and Merkel cells (APUD cells) are present. The epidermis is further subdivided into four layers and these layers represent the stages in the differentiation/maturation of the keratinocytes (Fig. 9).

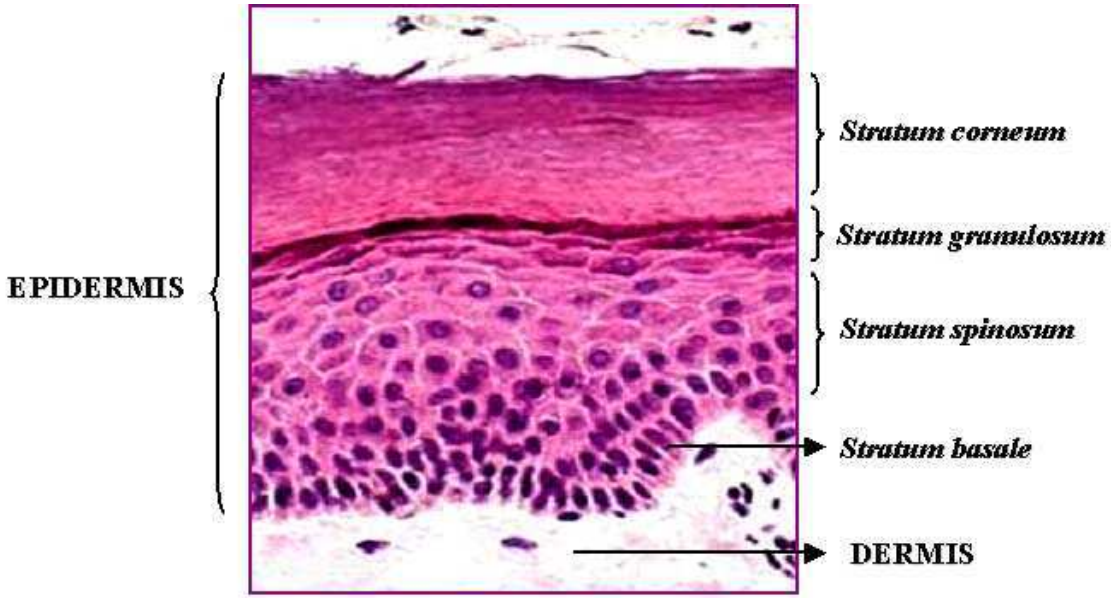

Fig. 9. Structure of human skin

The basal cell layer (*stratum basale* or *stratum germinativum*) consists mainly of one layer of basal keratinocytes, which are undergoing rapid cell division. Some of these cells represent epidermal stem cells supporting so-called epidermal proliferative units (Parkinson, 1992; Potten, 1974). The melanocytes are also present here and they make up 5-10% of the basal population.

The *stratum spinosum* consists of daughter basal cells, which have migrated upwards to form this multi-cell layer of polyhedral cells. Keratinocytes in this layer are synthesizing intermediate filaments composed of keratin, and those filaments are anchored to the desmosomes joining adjacent cells. In the cytoplasm of those cells, granules with lipids and lipoproteins are also presented. Langerhans cells (antigen-presenting cells) are found in this cell layer.

In the *stratum granulosum*, the cells become flattened and lose their nuclei, and keratohyaline granules can be seen in the cell cytoplasm.

The uppermost layer of the skin is the *stratum corneum*, the horny layer, representing the end result of keratinocyte differentiation. This layer consists of a sheet of

overlapping polyhedral cornified cells with no nuclei, whose cytoplasm is replaced by keratohyaline granules. Desmosomes between the adjacent cells cannot be found.

The **dermis** lies below the epidermis, and consists of connective tissue, and could be split into the *papillary* and *reticular* layer. This connective tissue is composed of cells, fibers and extracellular matrix. Extracellular matrix (ECM) mostly consists of ground substance, in which polysaccharides and protein form proteoglycan macromolecules, and structural glycoproteins (e.g. fibrillin, fibronectin). ECM is a dynamic structure that plays an important role in the cell's shape and activities. Spread through and attached to this matrix are protein fibers of several kinds, such as interstitial collagen fibers and elastic fibers, which are composed of elastin, and microfibrils. The major cellular forms are the fibroblasts, which secrete extracellular matrix proteins. Other dermal cells include mast cells, macrophages, lymphocytes and other leukocytes, and melanocytes. Dermis also contains sebaceous and sweat glands, blood and lymph vessels, nerves, neuron endings and epidermal appendages.

Basal membrane (BM) or *lamina basalis* is a specialized sheet-like structure, located between the epidermis and the dermis. The BM at the epidermal-dermal junction serves to tightly link the epidermis to the dermis. It restricts the passage of molecules between epidermis and dermis on the basis of size and charge, but allows the passage of migrating cells under normal (i.e. melanocytes and Langerhans cells) or pathological (i.e. lymphocytes, neutrophiles and tumor cells) conditions. It also influences the behaviour of keratinocytes by modeling cell polarity, proliferation, migration and differentiation (Burgeson and Christiano, 1997; Chan, 1997). BM is primarily composed of collagens, laminins, nidogen and perlecan. In normal human skin BM, type IV collagen is the predominant structural component, which self-assemble into a polygonal lattice network at neutral pH (Timpl et al., 1984; Yurchenco and Furthmayr, 1984; Yurchenco et al., 1992). Both fibroblasts and keratinocytes synthesize components of BM.

In human skin, the two most abundant connexins are Cx26 and Cx43. While Cx26 is mainly expressed in the epidermal basal layer, Cx43 is expressed throughout spinous and granular cell layers of the epidermis, focally in the basal layer, and in dermal fibroblasts (Richard, 2000; Salomon et al., 1994). Both connexins are differentially expressed in keratinocytes during development of the skin (Wiszniewski et al., 2000) (Fig. 10).

	Human	Rodent
Epidermis		
Basal cell layer	Cx26; (**Cx43**)	**Cx43**; Cx40; Cx37; (Cx31)
Spinous cell layer	**Cx43**>Cx31>Cx37	**Cx43**; Cx37; Cx31; Cx30.3
Granular cell layer	**Cx43**>Cx31>Cx37	Cx37; Cx31.1; Cx31; Cx30.3
Hair follicle	Cx26; **Cx43**	Cx31; Cx26; **Cx43**
Sebaceous glands	**Cx43**	Cx31>Cx40/**Cx43**
Eccrine sweat glands	Cx31; Cx26; (**Cx43**)	Cx31; Cx26
Dermal fibroblasts	**Cx43**; Cx40	**Cx43**

Fig. 10. Distribution of different connexins in human and rodent skin

1.3 Skin cancer

Skin cancer is the most common human cancer. Its development and progression is causally linked to exposure to ultraviolet (UV) radiation. Solar UV-radiation can be subdivided into UVC (200-280nm), UVB (280-320nm) and UVA (320-400nm). While UVC is absorbed by the atmospheric ozone layer, UVA and UVB radiation is reaching the earth's surface. Exposure to UVB and UVA is damaging the skin. UVB directly damages DNA and exploits chromopores for ROS generation. UVA has an effect on cellular targets involving photosensitizers and generation of ROS as well (de Gruijl, 2000). Both DNA damage and increase in ROS may result in persisting mutations and activation of signalling cascades which support tumor development and premature aging (Scharffetter et al., 1997, 2000; Brenneisen et al., 2002).

Ultraviolet radiation (UVR) can mutagenize several genes involved in the initiation, promotion and progression of skin cancer. The monoclonal expansions from polyclonal normal keratinocytes are initiated by UV-related genetic events in genes involved in tumor suppressing, oncogenic and cell-cycle control signalling pathways. Inactivation of *p53* tumor suppressor gene, resulting from point mutations, deletions or insertional mutations (Hussein et al., 2003) might be the earliest event in the development of skin cancer (Rebel et al., 2001). Additional genetic changes in other tumor suppressor genes such as *p16* and PTCH, protooncogenes *Bcl-2*, *Ras*, *c-Fos* and *c-Jun* will promote the clonal expansion of an initiated tumor cell and their

progression into malignant states (Hussein, 2005), which could be subdivided in melanoma and non-melanoma skin cancer.

Melanoma skin cancer (MSC) is a neuroectodermal tumor, which develops from pigment-producing melanocytes, and it is the most aggressive skin tumor.

1.3.1 Non-melanoma skin cancer (NMSC)

Among the NMSC, *basal cell carcinoma (BCC)* is the most frequent skin cancer, it is locally invasive and can cause massive tissue damage but hardly metastasise (Boukamp et al., 2005).

Squamous cell carcinoma (SCC) is a malignant tumor of keratinocytes of the spinous layer of the epidermis. Clinically, SCC presents crusting, erythematous ulcerated lesions with a granular friable (Fig. 11).

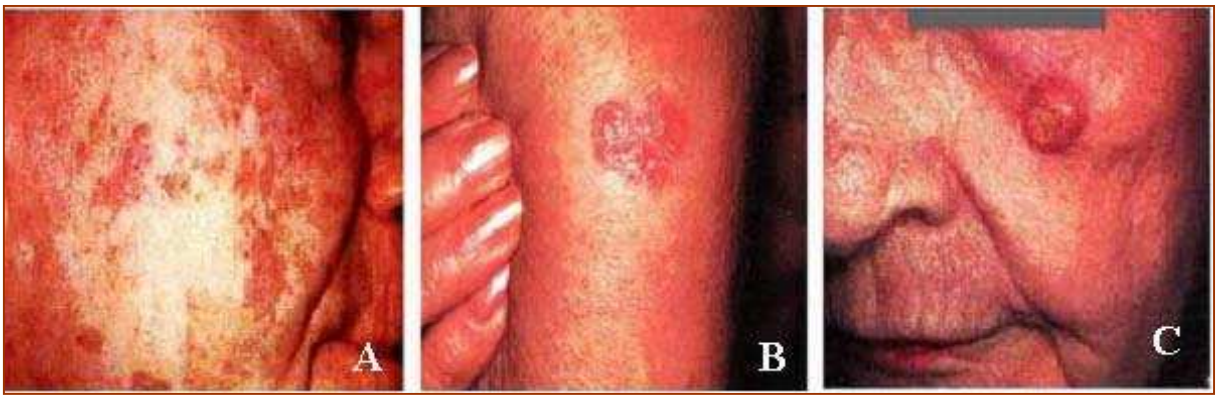

Fig. 11.
A-Actinic keratosis; B- Carcinoma in situ; C- Squamous cell carcinoma

It is the second most common form of the skin cancer among the Caucasians (Bernstein *et* al*.,* 1996), accounting for 20% of all cutaneous malignancies, and frequently arises at the sites of chronic UV damage (face, head, neck, back, hand, forearm). Evidently, the primary cause of cutaneuos SCC is cumulative sun exposure, but in addition also chronic exposure to heat, X- or gamma rays and arsenic could cause SCC (Cleaver et al., 2002). The contribution of the human

papilloma virus (HPV) in SCC development is still matter of debate. The incidence of metastasis of cutaneous SCCs is generally low (around 1%).

Almost 50% of all SCCs show mutations in p53 gene, specifically in codon 278, and this is mostly an UV-type specific mutation (Brash et al., 1996; Popp et al., 2002). The genetic changes during SCC development could be explained in a sequence-specific manner. The potential primary event is an UVB type specific mutation in p53 gene (Ling et al., 2001), which could be also found in actinic keratoses (AK), sun-induced precancerous skin lesions about 10% of which will develop into skin SCCs. Bowen disease or SCC *in situ* (CIS) represents a preinvasive stage of invasive skin SCCs.

1.4 Mechanism of tumor metastasis

A tumor is defined as an abnormal growth of the tissue, developing progressive through uncontrolled proliferation of appropriate cells. Malignant tumors differ from benign ones by their high and aggressive capacity to invade surrounding tissues and to metastasize.

The metastasis is a result of a multistep interaction between tumor cells and the permanently changing tumor microenvironment. The main steps in the development of metastasis are: (A) neoplastic transformation, proliferation and angiogenesis (B) detachment of tumor cells from primary lesion and invasion of the local stroma (C) aggregation of tumor cells in circulation (D) adherence of tumor cells to endothelial basement membrane (E) extravasation and (F) invasion and growth at a distant site (Ellenrieder et al., 1999).

The invasion of the tumor is the central point in metastasis. One of the first events in invasion is the loss of junctional contact between adjacent cells in epithelium by disruption of cell-cell and cell-extracellular matrix (ECM) adhesion. This is followed by production of proteolytic enzymes capable of degrading the ECM and the secretion of a variety of cytokines, which attract and activate stromal cells, and afterwards endothelial cells during angiogenesis. The alteration in the expression and function of cell adhesion molecules (CAMs), which are responsible for cell-cell atachment and cell-stroma interaction, leads to increased motility of tumor cells. Those CAMs are

belonging to cadherin family, integrin receptors family, IgG superfamily and/or selectin family.

Cadherins are a family of calcium-dependent cell adhesion molecules mediating mainly homotypic ***cell-cell interaction***. Most cadherins are type I transmembrane glycoproteins that are associated with the cytoskeleton through interactions with cytoplasmic proteins. The classic cadherins (E-, N- and P-cadherin) have a highly conserved cytoplasmic tail, which interacts with the actin cytoskeleton via the intercellular proteins α-, β- and γ-catenins (Wheelock et al., 1991). Catenins have a major role in regulating adhesive activity. The classic cadherins are a transmembrane component of adherens junction and they regulate the organization of the junctional complex in epithelial cells including desmosomes, tight junctions and gap junctions

As not only the disruption of cellular junctions, but also the disruption of ***cell-matrix association*** is important for tumor cell detachment of the primary tumor site, integrins play a pivotal role. Integrins are transmembrane receptor proteins, which mediate cell adhesion to ECM by recognizing a variety of ligands including extracellular matrix proteins, cell surface proteins and plasma proteins. They are composed of two non-covalently associated α and β subunits. The integrin family receptors are recognizing all major matrix components such as collagens, laminin, fibronectin and vitronectin as well as mediators of intercellular adhesion such as VLA-4 and the integrin of the β_2 subfamily (Clark et al., 1995). Alteration of expression and function of specific integrins may contribute to cancer progression (Schwartz, 1993) and this appears to be tumor-type and cell-type specific. Integrins could, additionally to their role in cell adhesion, transduce signals and influence on migration, differentiation and apoptosis of the cell.

An essential step in epithelial tumor metastasis is ***breaking of basement membrane*** and ***invasion*** of the surrounding stroma. Epithelial cancer cells are then being “captured” in extracellular matrix and surrounded by activated fibroblasts, endothelial cells, smooth muscle cells and inflammatory cells. These cell populations are recruited in the early phase of tumor progression by the secretion of cytokines, growth factors and chemokines, from the pre-malignant and pre-invasive epithelial cells. The stromal cells are participating in modification and/or degradation of ECM by production of proteases (Alessandro et al., 2002; Kerkelä et al., 2003; Johansson et al., 2000). There are three main families of proteases involved: (1) the serine proteases which include urokinase plasminogen activator (uPA), elastase, plasmin

and cathepsin G; (2) the matrix metalloproteinases (MMPs) which comprise gelatinases, interstitial collagenases, stromelysins and matrilysin; and (3) the cystein proteases, the cathepsins B and L.

1.5 Cell-cell communication and carcinogenesis

It is known for nearly 40 years that gap junctional intercellular communication plays a key role in carcinogenesis and more generally in growth control (Loewenstein et al., 1966). From cell-cell communication point of view, cancer is a result of disruption of the homeostatic regulation of a cell's ability to respond appropriately to extracellular signals of the body (growth factors, hormones, neurotransmitters and cytokines) which trigger intracellular signals via second messengers such as cAMP, Ca^{2+}, DAG, NO, ceramides, as well as intercellular communication by gap junctions (Trosko et al., 1998). Disruption of one of these communication processes results in abnormal homeostasis and supports pathological processes such as tumor development. Cancer cells have disrupted gap junctional intercellular communication. The ability of cells to form and maintain GJIC is not only dependent on connexin gene expression, but also rely on cell-cell adhesion, GJ assembly/disassembly, connexin stability and channel gating. Therefore disruption of GJIC during carcinogenesis often involves these regulatory mechanisms. It was hypothesized that reduction of GJIC in neoplastic and carcinogen-treated cells contributes to dysregulated cellular growth by isolating cells from their neighbours (Loewenstein, 1979; 1990). By ultrastructural, biochemical and immunological studies, and by introduction of fluorescent and radioactive tracers and determination of their passage into adjacent cells, it was shown that the majority of neoplastic cells have fewer and smaller gap junctions, express less connexins and have reduced GJIC compared to normal counterparts (Loewenstein, 1981; Cesen-Cummings et al., 1998; Weinstein et al., 1987; Yamasaki, 1990; Stuhlmann et al., 2003).

Many chemical carcinogens, which act as tumor promoters (but not directly damage DNA) inhibit GJIC in cultured cells and cells within target tissues (Trosko et al., 1987; Klaunig et al., 1990; Budunova et al., 1994). These compounds include pesticides such as DDT, dieldrin and lindane; pharmaceuticals such as phenobarbital and

diazepam; dietary additives such as saccharin and butylated hydroxytoluen; then dioxin; and peroxisome proliferators such as clofibrate.

In contrast, mutagenic carcinogens do not inhibit GJIC; instead they induce neoplastic transformation by activating proto-oncogenes and inactivating tumor suppressor genes (Trosko et al., 1990). Some oncoproteins, including Ras, Neu and Src could block GJIC.

Many growth factors such as EGF, PDGF, bFGF, HGF, TGF-α and TGF-ß applied to cultured cells, inhibit GJIC (Ruch, 1994; Stuhlmann et al., 2004). This effect occurs rapidly with minutes to hours or is detected after days. Inhibition of GJIC by EGF is related to stimulation of connexin phosphorylation by MAPK and closure of gap junctional channels (Kanemitsu et al., 1993). PDGF induce rapid inhibition of GJIC coincident with Cx43 phosphorylation and bFGF coincident with decreased Cx43 expression (Shiokawa-Sawada et al., 1997).

Many growth inhibitors and anticancer agents increase GJIC and connexin expression. Retinoids, carotenoids, green tea extract, certain flavonoids, dexamethasone and cAMP analogues and agonists increase connexin expression and gap junction formation in tissues (Ren et al., 1994; Rogers et al., 1990; Mehta et al., 1989; Zhang et al., 1992) or block the inhibitory effects of tumor promoters on GJIC (Ruch et al., 1989; Sigler et al., 1993; Chaumontet et al., 1994). Also, tumor suppressor gene products could inhibit neoplastic transformation by enhancing GJIC (Weinberg, 1993).

2. Aim of the study

Starting from a concept that most tumor cells show a disruption of the direct cell-to-cell communication, the present study investigates potential molecular parameters underlying the impairment of gap junctional intercellular communication in two immortalized cell lines of the human skin.

More in detail, the main focus was to examine the expression and localization of Connexin 43 protein, the major connexin in skin cells.

In addition, several molecular parameters involved in trafficking and assembly of gap junctional proteins, were studied by biochemical and molecular biological approaches.

On the one hand, it involves molecules of the adhesion system, known to be involved in forming of gap junctions, as well as cytoskeletal structures such as microtubules and actin network, known to be partially involved in trafficking of gap junctional proteins.

Finally, the effects of posttranslational modifications of connexin 43 were examined, in context of connexin turnover to be responsible for loss of GJIC in skin derived SCL-1 tumor cells.

3. Materials and Methods

3.1. Materials

Substances

Agarose electrophoresis grade,	Biozyme
Albumine from bovine serum (BSA) 98%,	Sigma
Ampicilin,	Roche
Antarctic Phosphatase,	New England Biolabs
APS,	Fluka
Bacto-Agar, Difco Laboratories,	Detroit Michigan USA
Bovine pituitary extract,	Gibco-Invitrogen
$CaCl_2$,	Merck
Calf Intestinal Phosphatase (CIP),	New England Biolabs
Canamycin,	Roche
Canthaxanthin,	Sigma
Cell culture material,	Greiner bio-One GmbH
Chemiluminicscence film,	Amersham Biosciences
DAPI,	Molecular Probes
DMEM (Dulbecco's Modified Eagle's Medium),	Sigma
DMSO,	Roth
dNTP mix,	Peqlab
EDTA electrophoresis grade,	ICN Biomedicals
Endotoxin-free Plasmid DNA Maxi prep,	Macherey-Nagel
Epoxomicin,	Sigma
Ethanol, 99% absolut,	Merck
Ethidiumbromide,	Molecular Probes
Expand High Fidelity PCR System,	Roche
FCS (Foetal Calf Serum),	PAA Laboratories GmbH
Fluoromount G,	Southern Biotechnologies
Forskolin,	Fluka-BioChemica

FuGENE 6,	Roche
Gentamycin solution,	Sigma
Glutamax,	Invitrogen
IPTG,	Roth
Keratinocyte-SFM(Serum-Free Keratinocyte Medium)	Gibco-Invitrogen
Lactacystin,	Alexis Biochemicals, San Diego CA
LB Broth base,	Gibco Invitrogen
Lucifer Yellow CH,	Sigma
Methanol p.A.,	Merck
Nitrocellulose-Membrane Hybond-C Extra,	Amersham Biosciences
Non-fat dried milk,	Roth
Normal goat serum,	Sigma
Nuclease-free H_2O,	Promega
NucleoSpin® Extraction Kit,	Macherey-Nagel
Okadaic acid, sodium salt,	Sigma
Oligo (dT) primer,	Roche
OptiMEM medium,	Gibco Invitrogen
Paraformaldehide,	Merck
Penicilin/Streptomycin,	PAA Laboratories GmbH
Phalloidin-FITC,	Sigma
Ponceau S,	Sigma
QIAprep Spin Mini prep,	Qiagen
Recombinant Epidermal Growth Factor (rEGF),	Gibco Invitrogen
RNeasy Mini Kit,	Qiagen
Rotiphorese Gel 40 (37,5:1),	Roth
S.O.C. medium,	Invitrogen
SDS Ultra Pure >99%,	Roth
Suc-LLVY-AMC,	Affiniti, Exeter, UK
SuperScript II Reverse Transcriptase,	Invitrogen
SuperSignal West Pico/Femto,	Pierce
T4 DNA-Ligase,	Promega
Taq DNA polymerase,	Qiagen
Temed p.A. 99%,	Roth
Tetrahydrofuran,	Fluka

Tris Pufferan® 99,9%,	Roth
Triton X-100,	Roche
Trypsin/EDTA,	PAA Laboratories GmbH
Whatman-filterpapier	Roth
X-Gal,	Roth

Buffers

Anode buffer I	0,3M Tris 10% (v/v) MeOH pH 10,4
Anode buffer II	25mM Tris 10% (v/v) MeOH pH 10,4
Katode buffer	25mM Tris 10% (v/v) MeOH 40mM Glycin pH 9,4
4x Laemlie buffer	3M Tris (pH 6,8) 20% SDS ß-mercaptoethanol glycerol
McIlvaine buffer	50mM Citric acid 100mM Na_2HPO_4
PBS	140mM NaCl 10mM Na_2HPO_4

RIPA buffer	0,25% Deoxycholate 0,5% Igepal 150mM NaCl 50mM Tris-Cl pH 7,5
1x TAE buffer	40mM Tris 20mM Acetic acid 1mM EDTA
10x TBS-T buffer	50mM Tris 150mM NaCl 0,1% (v/v) Tween 20 pH 7,5

Equipment

Balance AB 204-S,	Mettler Toledo, Schweiz
CCD Camera (ORCA II) Digital Camera,	Hamamatsu, Japan
Centrifuge, Sorvall® RC 26 Plus,	DuPont
Clean Air Sterilebench,	Thermo Life Sciences
Diana III Raytest-Camera,	Diana
Electro-Blot-Device,	Roth
Electrophoresis power supply,	Consort
ELISA-Reader Victor 1420 multilabel counter,	Wallac Oy, Turku, Finnland
Filmcassette BAS Cassette 2040,	FujiFilm Photo Film GmbH
Fluorescence-/Lightmicroscope Axiovert 100 TV,	Carl Zeiss
Heat Block,	Peqlab
Heraeus Incubator,	Kendro
Magnetic-Stirrer,	Janke+Kunkel IKAMAG©RCT
Microwave,	Braun
Milli-Q device,	Millipore
Photometer Ultraspec 1000,	Pharmacia Biotech
Table centrifuges: 5417R, 5417C,	Eppendorf

T-gradient PCR cycler,	Biometra
Ultrasonic Disintegrator No.7100,	M.S.E., Lorch
Vortexer,	Janke+Kunkel Labortechnik
Waterbath,	Köttermann

Software

AIDA Image Analyzer v.3.1 (Scion Image)
Aqua Cosmos
Chromas
Diana III Camera Control
DNA STAR
Microsoft office
Prism 3.0

3.2. Cell culture

3.2.1. Characteristics and cultivation of utilized cells and cell lines

Normal human epidermal keratinocytes (NHEK) were prepared from foreskin biopsies of healthy donors (3-6 years old) as described (Glade et al., 1996) and grown in keratinocyte-SFM medium containing 0,09mM calcium, 0,2ng/ml human epidermal growth factor, 35µg/ml bovine pituitary extract (Invitrogen) and 5µg/ml of gentamycin (Sigma). They were used for experiments between passage 2 and 4. For some of the experiments, in order to induce differentiation and similar behaviour of keratinocytes like in normal stratified skin, NHEK were preincubated for 24h with increased calcium concentration (up to 1mM $CaCl_2x2H_2O$).

Human dermal fibroblasts (HDF) were established from foreskin biopsies of healthy donors as described (Fleischmajer et al., 1981) with an age of 4-6 years.

NHEK and HDF were both kindly prepared from foreskin biopsies by Claudia Wyrich.

The spontaneously immortalized human epidermal keratinocyte cell line HaCaT (Boukamp et al., 1988) was used as a model for tumor cells. HaCaT cells represent an early stage of skin cancer development and serve as an in vitro skin cancer progression model. HaCaT shows characteristics of normal keratinocytes such as normal keratinization, as well as some features of cancer cells such as UV-type specific mutations in both alleles of the p53 gene and chromosomal aberrations, common for SCCs.

SCL-1 tumor is poorly differentiated squamous cell carcinoma (SCC) derived from a face of a 74-year-old woman.

HeLa tumor line is human negroid cervical epithelial carcinoma, derived from cervix of a 35-year-old woman Henrietta Lacks.

HaCaT cells and SCL-1 line were kindly provided by Dr. Norbert E. Fusenig (Deutsches Krebsforschungszentrum, Heidelberg). HeLa cells were commercially available.

HDF, HaCaT, SCL-1 and HeLa were maintained in Dulbecco's modified Eagle's medium (DMEM) containing 10% (v/v) defined foetal calf serum (FCS) supplemented

with 2mM Glutamax (L-alanyl-L-glutamin), 400U/ml penicillin and 50mg/ml streptomycin.

Together with NHEK they were maintained in a humidified atmosphere of 5% CO_2 and 95% air at 37℃.

According to the experimental purposes, cells were grown until ~60-80% confluence.

For subcultivation, after reaching 80-90% of confluence, cells were first washed with PBS and then detached from the culture flask surface by applying Trypsin-EDTA (0,5g/L Trypsin; 0,2g/L Na-EDTA) diluted 1:1 with PBS (v/v). The Trypsin activity was abrogated after 2-5 min by adding DMEM containing 10% FCS, cells were resuspended and counted in special counting glass plate. Appropriate number of cells was seeded for further cultivation. For NHEK, additional centrifugation step for 5 min on 1200rpm was done prior to cell resuspension.

3.2.2. Freezing and thawing of the cells

After described inactivation of Trypsin, suspension of cells was centrifuged for 5 min at 1200rpm, and cell pellet was resuspended in freezing medium (DMEM-medium with 20% FCS and 10% DMSO). Approximately 10^6 cells were frozen in special cryovials on –80℃.

Frozen cells were thawed fast, on 37℃ and immediat ely transferred into culture flask. In order to reduce content of DMSO less than 1% and to avoid further membrane damage, medium was changed after 24h.

3.2.3. Incubation of cells with test compounds

The cells were grown in 3,5cm dishes until reaching 80-90% of confluency. They were incubated with test compounds, in a humidified atmosphere of 5% CO_2, at 37 ℃.

Neutralizing TGF-ß1 antibody

The stock of neutralizing TGF-ß1 antibody was 1mg/ml. It was diluted in DMEM without FCS, to final concentration of 2µg/ml. Cells were incubated for 24h prior the experiment.

Canthaxanthin

Tetrahydrofuran was used as a delivery solvent for canthaxanthin, forming a highly bio-available pseudo-solution of carotenoids in cell culture medium (Berthram, 2004). Cells were preincubated for 24h in DMEM with 3%FCS. Canthaxanthin, prepared as 10mM stock solution, was added in cell culture medium to a final concentration of 10µM, and additionally incubated for next 24h prior to the experiment.

Forskolin

Forskolin was prepared as 10mM stock, in absolute ethanol. It was diluted in DMEM without FCS, to a final concentration of 15µM. Cells were incubated for 24h, prior to the experiments.

Okadaic acid

Okadaic acid, sodium salt, was prepared as 100µM stock in DMSO. It was diluted in DMEM without FCS, to the final concentrations of 10 and 20nM. Cells were incubated for 6h prior to the experiment.

Epoxomicin

Epoxomicin was prepared as 10mM stock in DMSO. It was diluted in DMEM with 10% FCS, to the final concentration of 10 and 15µM. Cells were incubated for 6h prior to the experiment.

3.3. Communication assay (microinjection)

Determination of intercellular communication was performed by transfer of fluorescent dye, Lucifer Yellow CH, from a single microinjected cell to its neighbouring cells. Equipment used for measuring GJIC was consisted of Fluorescent microscope, Micromanipulator (Femtojet) and Microinjector (InjectMan).

50-200 femtoliter of Lucifer Yellow CH (10% in 0.33 M LiCL w/v) were loaded into the femtotips and dye was injected to a single cell in less than 50 hPa of pressure for duration of 0.5 seconds. The excitation wavelength of Lucifer Yellow CH is at 426 nm whereas emission maximum is at 540 nm. The fluorescent cells surrounding injected cell were counted 5 minutes after the injection and the mean values of 10 individual injections were determined.

3.4. SDS-PAGE

Cells were lysed in 1% SDS or RIPA buffer, and the protein concentration was determined by modified Lowry method (DC-Protein Assay, Bio-Rad). 20-50µg of cell lysates were mixed with 4x SDS-PAGE buffer (Laemlie buffer), heated at 65℃ for 10 minutes and subjected to 10% SDS-PAGE.

10 ml resolving gel

Component	8% gel	10% gel	12% gel	14% gel	15% gel
H_2O	5,3 ml	4,8 ml	4,3 ml	3,8 ml	3,55 ml
Rothiphorese gel 40	2 ml	2,5 ml	3 ml	3,5 ml	3,75 ml
1,5M Tris pH 8,8	2,5 ml	2,5 ml	2,5 ml	2,5 ml	2,5 ml
10% SDS	100 µl	100 µl	100 µl	100 µl	100 µl
10% APS	100 µl	100 µl	100 µl	100 µl	100 µl
TEMED	5 µl	5 µl	4 µl	4 µl	4 µl

5 ml stacking gel

Component	5% stacking gel
H_2O	3.53 ml
Rothiphorese gel 40	720 µl
1M Tris pH 6,8	650 µl
10% SDS	50 µl
10% APS	50 µl
TEMED	5 µl

The proteins were separated electrophoreticaly after 1-2h (I≈50mA, U≤200V app.) and as running buffer, 1x Tris/Glycin/SDS Running buffer was used.

Semi-dry electroblot of the proteins on nitrocellulose membrane (Hybond-C Extra, Amersham Biosciences) was performed for 2h (I≈60mA, U≤10V). The blotting is accomplished by putting the nitrocellulose membrane on two sheets of Wathman filter paper separately soaked with Anode buffer I and Anode buffer II, and overlaid with the SDS-PAGE gel and two sheets of Wathman filter paper soaked with Katode buffer. A heavy cover plate was then put on the entire assembly. In this way, a sandwich of nitrocellulose membrane and gel is compressed between two parallel electrodes.

The excess adsorption sites and unspecific binding on nitrocellulose were then blocked with a non-specific protein (Non fat dried milk solved in 1x TBS-T) for 1-2h at room temperature (RT). The blot was then incubated with appropriate antibody over night, at 4℃. After washing with 1x TBS-T (thoroug hly for 1h), the blot was incubated with anti-rabbit / mouse IgG antibody conjugated to horseradish peroxidase (HRP) (Dianova) for 1h at room temperature.

The chemiluminescent detection (SuperSignal West Pico / Femto, Pierce), followed after another washing step with 1x TBS-T (thoroughly for 1h). Afterwards, the nitrocellulose membrane was expose to the film (Amersham) 5min - 1,5h and analysed.

Specificity of primary antibody	Working dilution	Applied secondary antibody	Working dilution
Anti-Cx43 (Sigma)	1:1000-1:2000	HRP conjugated anti-rabbit IgG (Dianova)	1:5000-1:20000
Anti-E-cadherin (Santa Cruz)	1:500	HRP conjugated anti-mouse IgG (Dianova)	1:5000
Anti-N-cadherin (BD)	1:1000	HRP conjugated anti-mouse IgG (Dianova)	1:5000
Anti-ß-catenin (Abcam)	1:4000	HRP conjugated anti-rabbit IgG (Dianova)	1:20000
Anti-GFP (Sigma)	1:3000	HRP conjugated anti-rabbit IgG (Dianova)	1:20000

3.4.1. Dephosphorylation of proteins

Dephosphorylation of proteins prior to SDS-PAGE was performed on 50µg of protein sample, using 10 units of Antarctic Phosphatase (NE BioLabs), with 1X Antarctic Phosphatase Reaction Buffer, for 2h at 37℃.

3.5. Immunocytochemistry

Cells were grown on glass cover slips to ~80% confluence. After brief washing with PBS, cells were fixed or by MeOH (protein denaturation by coagulation) or with paraformaldehide (formation of crosslinkages).

Precooled MeOH was put on the cells for 10 minutes at –20℃ and afterwards briefly washed with PBS. Unspecific proteins were blocked with 3% (v/v) goat serum in 1x TBS-T, for 2-4 hours at room temperature.

Alternatively, cells were fixed with 3,7% paraformaldehide (diluted in PBS) for 15-20min at room temperature, washed briefly with PBS, and permeabilised with 0,1% Triton X-100/ 3% goat serum/ PBS (v/v) while blocking for 1h. Before applying primary antibody, they were briefly washed with PBS.

For immunodetection of specific protein, cells were incubated with appropriate primary antibody diluted in 1% (v/v) goat serum in 1x TBS-T, overnight at 4℃, under slight agitation. Frequent washing steps with 1x TBS-T followed for 1 hour.

While those antibodies were not directly labelled with an enzyme or fluorophore, labelled secondary antibodies generated against the immunoglobulins of the primary antibody source carried out detection. Secondary antibodies used were Alexa fluor 488- or 546-labelled goat anti-rabbit IgG or Alexa fluor 546- labelled goat anti-mouse IgG (Molecular Probes) diluted in 1% (v/v) goat serum in 1x TBS-T. Incubation was 1 hour at room temperature, followed by 1 hour frequent washing with 1x TBS-T.

Nuclear staining was obtained by incubation with 4′, 6-diamidino-2-phenylindole (DAPI, 0,5mg/ml in McIlvaine buffer) diluted in PBS, for 20 minutes, followed again by intense washing with 1x TBS-T. Coverslips were then mounted with Fluoromount G (Southern Biotechnologies) and analysed on a Zeiss Axiovert 100 TV inverted

fluorescent microscope with 63x oil objective, coupled to a CCD camera (ORCA II, Hamamatsu, Japan).

Specificity of primary antibody	Working dilution	Applied secondary antibody	Working dilution
Anti-Cx43 (Sigma)	1:1000	Alexa 488/546-coupled goat anti-rabbit IgG	1:1000
Anti-E-cadherin (Santa Cruz)	1:500	Alexa 488-coupled goat anti-mouse IgG	1:1000
Anti-N-cadherin (BD)	1:250-1:500	Alexa 488-coupled goat anti-mouse IgG	1:1000
Anti-ß-catenin (Abcam)	1:1000	Alexa 488- coupled goat anti-rabbit IgG	1:1000
Anti-α-tubulin (Santa Cruz)	1:2000	Alexa 488-coupled goat anti-mouse IgG	1:1000

3.5.1. Phalloidin labelling of actin

Cells were grown on glass cover slips to ~80% confluence. Following brief washing with PBS, they fixed with 3,7% paraformaldehide (diluted in PBS) for 15min at room temperature, washed briefly with PBS, and permeabilised with 0,1% Triton X-100/ 3% goat serum/ PBS (v/v) while blocking for 1h. Cells are stained with phalloidin-FITC conjugate diluted 1:500 in PBS, for 1h at RT. Afterwards, they were frequently washed with PBS for 1h, prior to nuclear staining with DAPI/PBS. Following steps are as described in chapter 3.5.

3.6. ELISA

Supernatants of confluent HDF, NHEK, HaCaT and SCL-1 cells were harvested at 24 h after serum starvation. The amount of secreted active and latent TGF-β1 was measured by a 96-well microplate enzyme linked immunosorbent assay (ELISA) system for active TGF-β1 according to the manufacturer's instruction (R&D systems).

MaxiSorb 96-well immuno-plate (Nunc) was coated with Capture Antibody (mouse anti-TGFß-1, 2µg/ml of PBS), and incubated overnight at RT. Each well was washed with Washing buffer three times prior blocking. While TGF-ß1 is presented in latent form, it is necessary to activate latent one to the immunoreactive by acidification.
100µl of 1N HCl was added to 500µl of sample, mixed and incubated for 10 min at RT. The reaction is then neutalized by adding 100µl of 1.2 N NaOH/ 0.5 M HEPES, mixed and assay was continued.
Plate was blocked with a Block buffer for at least 1h at RT. Washing is repeated and the plate was ready for assay. In each well, 100µl of undiluted sample was added and incubated 2h at RT. After washing, 100µl of Detection Antibody (biotinylated chicken anti-human TGF-ß1, 300ng/ml of Reagent Diluent), was added to each well and incubated further 2h at RT. Streptavidin-HRP was added to each well after washing, and incubated for additional 20 min at RT, followed by adding of 1:1 mixture of H_2O_2 and tetramethylbenzidin (v/v) of substrate solution. After 10-30 min incubation at RT, 2 N H_2SO_4 was added to stop reaction and plate was read using a microplate reader set to 450nm, to determine the optical density of each well.
Concentrations of total and active TGF-ß1 were calculated according to a standard curve of serial dilutions of a recombinant human TGF-ß1 (serial dilutions from 20-2000 pg/ml of Reagent Diluent)), which were treated in parallel with the samples.

3.7. Proteasome activity assay

Proteasomal acitivity in cell fractions was determined by cleavage of the fluorogenic precursor substrate N-Succinyl-Leu-Leu-Val-Tyr-7-amino-4-methylcoumarin (Suc-LLVY-AMC; Affiniti, Exeter, UK). 10 µM substrate was added to cellular lysates (~1x10^6 cells), and incubated in a reaction buffer (500 mM Hepes, 10 mM EDTA, 1% Triton X-100, pH 7.6). Fluorescent increase resulting from degradation of Suc-LLVYAMC at RT was measured after 24h by means of a fluorometer (LS-5, Lyminiscence Spectrometer, Perkin Elmer) at 340 nm excitation and at 460 nm emission. Each value of fluorescence intensity represents a mean value obtained from two independent experiments. After 2 hours of activity measurement, 10 µM

proteasome inhibitor lactacystin (Alexis Biochemicals, San Diego, CA) was applied to the substrate/lysate reaction as a specific control.

3.8. Basic molecular biology methods

3.8.1. RNA isolation from the cells

RNeasy Mini Kit (Qiagen) was used for total RNA isolation from cells, according to manufacture's protocol.
Briefly, samples are lysed, and homogenized by shredder columns, in the presence of a highly denaturing guanidine isothiocyanate (GITC)-containing buffer, which inactivates RNases. Appropriate binding conditions are achieved by adding ethanol, and the sample is then applied to a column, where total RNA binds to the silica-gel-based membrane. Contaminations are washed away with ethanolic buffers, and RNA is eluted with RNase-free water.
For assessing the concentration and purity of RNA in the sample, UV spectroscopy was used. The absorbance of a diluted RNA sample (1:50 in H_20) was measured at 260 and 280nm, and the nucleic acid concentration was calculated using the Lambert-Beer law

$$A=\varepsilon CI$$

(where A is absorbance, C is concentration, ε is the extinction coefficient and I is path length of the spectrometer cuvette)

which predicts a linear change in absorbance with concentration. Using this equation, an A260 reading of 1.0 is equivalent to ~40µg/ml single-stranded RNA. The A260/A280 ratio is used to assess RNA purity. An A260/A280 ratio of 1.82 is indicative of highly purified RNA.

3.8.2. Reverse transcription of mRNA (cDNA synthesis)

The synthesis of single-stranded cDNA, which could be used as a template for PCR, is enabled by reverse transcription (RT) of isolated RNA. Reverse transcription is an enzymatic-catalysed reaction in which RNA-dependent DNA-polymerase uses mRNA as a template for synthesis of single-stranded cDNA. The synthesis is initiated by binding of primers to the mRNA.
SuperScript II Reverse Transcriptase (Invitrogen Life Technologies) was used for transcription of RNA. 1 µg of total RNA together with 1 µl of Oligo (dT) 15-primer (50 pmol) and 1 µl of dNTP Mix (10 mM each) was pipetted in a 200 µl PCR tube, and filled with nuclease free H2O up to total volume of 12 µl. The mixture was then incubated 10 min at 65℃ and quickly chilled on ice . The following mixture was added:

4 µl 5x First-Strand Buffer
2 µl 0,1M DTT
0,5 µl (100U) Reverse Transcriptase (SuperScript II- RT)
1,5µl nuclease free H2O

This reaction mixture was incubated for 1 h at 42℃ and reaction was stopped by a 10 min incubation period at 72℃.

3.8.3. Polymerase chain reaction (PCR)

PCR is an *in vitro* method of amplification of a specific DNA segment. In each cycle of amplification, which consists of Denaturation of the template DNA, binding of the specific primers to their complementary strand (Annealing) and synthesis of the complementary strand directed by heat-stable*Taq*- DNA-polymerase (Elongation), we are getting higher amount of specifically defined DNA-fragment.
The PCR reaction had the following composition with a final volume of 20µl:

2 µl 10x QIAGEN PCR Buffer (contains also 15 mM MgCl2)	(final conc. 1x)
0,4 µl dNTP mix (10 mM each)	(final conc. 200µM each)
0,2 µl primer 1 (50µM)	(final conc. 0,5µM)
0,2 µl primer 2 (50µM)	(final conc. 0,5µM)
2 µl template DNA	(final conc. ≤ 1µg/ reaction)
6,1 µl dH2O	
0,1 µl Taq DNA Polymerase (Qiagen)	(final conc. 2,5 units/ reaction)

The sequences for forward and reverse primers are shown in table, together with positions in appropriate gene sequences.

Primer name	**Nucleotide sequence (5'-3')**	**Position in gene sequence**	**Accession number in Gene Databank**
HPRT-f	attctttgctgacctgctggatt	304-326	NM000194
HPRT-r	cttaggctttgtattttgcttttc	720-743	NM000194
Cx43cds-f	caactgctggagggaaggtgtg	260-281	NM000165
Cx43cds-r	caggtcatcaggccgaggtct	1327-1347	NM000165
ΨCx43-f	tcacctggcgtgacttcacttct	248-270	NG003029.1
ΨCx43-r	gtatcaagattcctctcacttgtg	1460-1483	NG003029.1
Cx43seq-f	ggcaacatgggtgactggagc	202-222	NM000165
Cx43seq-r	cccctccctctccacccatcta	1533-1554	NM000165
Cx43expr-f	**tacaggctcgagacc**atgggtgactgga	…208-220	NM000165
Cx43expr-r	**atggtggatccgc**gatctccaggtcatcagg	…1425-1443	NM000165

PCR was performed according to the following temperature profile: initial denaturation for 2 min at 94℃, cyclic repetition o f 1) denaturation for 20 sec at 94℃, 2) primer hybridisation (annealing) for 30 sec at primer-specific temperature (HPRT-55℃; Cx43cds- 57,9℃; Cx43seq- 56,5℃) 3) elongati on for 1 min 30 sec at 72℃, and final elongation for 10 min at 72℃. The cycle number for HPRT was 30, for Cx43cds, 39, and for Cx43seq, 40. Temperature profile for amplification of ΨCx43 was as the following: initial denaturation for 3 min at 95℃, 38 cyclic repetition of 1) denaturation for 30 sec at 95℃, 2) primer hybridis ation (annealing) for 2 min at 65℃ 3) elongation for 2 min at 72℃, and final elongati on for 10 min at 72℃. The PCR fragments were separated on a 1% agarose gel (w/v) in 1x TAE buffer and stained with EtBr (10 mg/ml stock concentration). The samples were mixed with DNA-probe

buffer and loaded on gel. The gel was run in 1x TAE buffer, by constant voltage of ~80V. Appropriate DNA molecular weight marker (Fermentas) was used to confirm fragment size. The fluorescence of intercalated EtBr was analysed by UV-light and photographically documented by AIDA image system (Raytest).

3.8.4. Molecular cloning

Molecular cloning (also referred as genetic engineering and recombinant DNA technology) is a method to insert a DNA segment of interest into an autonomously replicating DNA molecule, a so-called *cloning vector*, so that the DNA segment is replicated with the vector. Cloning of such a chimeric vector in a suitable host organism such as *E. coli*, results in the production of large amounts of the inserted DNA segment. Hereby, the circular DNA duplexes, plasmids, are used as cloning vectors.
The steps in molecular cloning procedure involve:

1. amplification of a DNA fragment of interest by High Fidelity PCR
2. elution of DNA fragment from the agarose gel
3. ligation of DNA fragment with appropriate vector
4. transformation of *E. coli* bacteria
5. isolation of plasmid DNA from *E. coli* suspension culture

High Fidelity PCR

The Expand High Fidelity PCR System (Roche) was used for amplification of the DNA fragment of interest for subcloning in pGEM-T vector (Promega) and in pEGFP-N1 vector (BD Clontech).
Two separate reaction mixtures (10µl each) were prepared on ice in 200 µl PCR tubes, and then combined just before starting of the PCR.

Master mix 1:	0,4 µl	dNTP mix (10 mM each)
	0,2 µl	primer 1 (50 µM)
	0,2 µl	primer 2 (50 µM)
	2 µl	template DNA
	7,2 µl	dH2O
Master mix 2:	2 µl	10x Expand High Fidelity Buffer
	7,8 µl	dH2O
	0,2 µl	Expand High Fidelity Enzyme Mix (final conc. 3,5 U/µl)

For cloning in pGEM-T vector, the reaction mixture was incubated and DNA was amplified according to temperature profile given in 3.8.3., while DNA amplification for subcloning to pEGFP-N1 was amplified according to following temperature profile: initial denaturation for 2 min at 94℃, 2 cyclic re petitions of 1) denaturation for 20 sec at 94℃, 2) primer hybridisation (annealing) for 30 sec at 55℃ 3) elongation for 1 min 30 sec at 72℃, then 30 cyclic repetitions of 1) de naturation for 20 sec at 94℃, 2) primer hybridisation (annealing) for 30 sec at 61℃ 3) elongation for 1 min 30 sec at 72℃ and final elongation for 10 min at 72℃. The P CR fragments were separated on a 1% agarose gel (w/v) in 1x TAE buffer and stained with EtBr (10 mg/ml). The samples were mixed with DNA-probe buffer and loaded on gel. The gel was run in 1x TAE buffer, by constant voltage of ~80V. Appropriate DNA molecular weight marker (Fermentas) was used to confirm fragment size.

Elution of DNA fragment from the agarose gel

The DNA fragments were cut with a scalpel from the agarose gel and eluted with NucleoSpin® Extraction Kit (Macherey-Nagel) according to the manufacturer's protocol. Briefly, gel slices are dissolved at 50℃ and loaded to a special column, where in a presence of chaotropic salt, DNA binds to a silica membrane. Contaminations are removed by washing with ethanolic buffer and DNA is finally eluted under low ionic strength conditions with 20µl of slightly alkaline buffer (5mM Tris-Cl, pH 8.5).

Ligation of DNA fragment with plasmid vector

The pGEM-T vector is a lynearised plasmid vector, with additional tymidin nucleotide on 3'-ends. During amplification of specific DNA fragment, *Taq* DNA-Polymerase is adding deoxyadenosine on 3'- ends of the fragments, which is then enabling direct ligation with the vector DNA.

For pEGFP-N1, specifically designed primers are introducing certain restriction sites (palindromic sequences recognized by specific restriction endonucleases) on the ends of DNA fragment of interest, so digestion of both plasmid vector and DNA fragment, with the same restriction enzyme, yield single-stranded ends that are complementary to each other (cohesive or "sticky" ends) and enable covalent joining of those two DNAs through the action of an enzyme named *DNA ligase*. Those specific primers created an additional restriction site for *Xho*I at the 5' end and for *BamH*I at the 3' end of Cx43, respectively. Both, the PCR products and the vector pEGFP-N1 were digested with *Xho*I and *BamH*I. The vector DNA digestion was followed by dephosphorylation with 10U of Calf Intestinal Phosphatase (CIP, NE BioLabs), 1 h at 37℃.

Afterwards, both the cleaved DNA fragment and vector DNA were clean-upped with NucleoSpin® Extraction Kit (Macherey-Nagel) according to the manufacturer protocol. Briefly, samples were mixed with binding buffer and loaded into a special column, where in a presence of chaotropic salt, DNA binds to a silica membrane. Contaminations are removed by washing with ethanolic buffer and DNA is finally eluted under low ionic strength conditions with 20µl of slightly alkaline buffer (5mM Tris-Cl, pH 8.5).

The ligation reaction (10 µl in total) was then set up in 200 µl PCR tube as follows and incubated 1h at RT, and then overnight at 16℃.

1 µl 10x T4 DNA-Ligase Buffer
1 µl T4 DNA-Ligase (3U/µl, Promega)
4 µl DNA fragment
3 µl plasmid DNA
1µl dH2O

Transformation of E. coli bacteria

For the transformation of 50 µl of E. coli bacterial strain K-12 (Fusion-Blue, BD Clontech), 5 µl of ligation mixture was used. The incubation of transformation mixture was 5 min on ice, followed by heat-shock transformation for 30 sec at 42℃, and again 2 min on ice. After addition of SOC medium, the mixture was shaken vigorously 1 hour at 37℃ at 250rpm.

Properly transformed bacterial cells are selected through use of antibiotics and/or chromogenic (colour-producing) substrates. For pGEM-T which is allowing blue-white screening, 200-400µl of the mixture was then spread on LB-Agar plate supplemented with 50 µg/ml Ampicillin, 0,5 mmol/l IPTG and 20 µg/ml X-Gal and incubated overnight at 37℃. Under this growth conditions, ba cteria transformed with re-ligated vector could express enzyme ß-galactosidase which yields blue products after hydrolysing X-Gal, are forming blue colonies, whereas bacteria transformed with vector-DNA fragment construct form colourless one. Positive colonies (colourless) are then selected for plasmid DNA isolation. pEGFP-N1 is carrying gene for resistance to Canamycin, so on LB-Agar with (100µg/ml) of Canamycin, just transformed bacteria, having plasmid DNA, would grow.

Isolation of plasmid DNA from E. coli bacteria

Selected bacterial colonies from LB-Agar plates were picked up and cultivated overnight in 5 ml LB-medium (containing 50-100 µg/ml of Ampicillin or Canamycin) in bacterial shaker. The bacterial suspension was then centrifuged by 4000 x g, 20 min, at 4℃. Plasmid DNA isolation was performed with QI Aprep Spin Mini prep (QIAGEN), according to the manufacturer protocol.

Pelleted bacterial cells were resuspended and lysed under alkaline conditions. The lysate is subsequently neutralized and adjusted to high-salt binding conditions. After lysate clearing, the supernatants were applied to columns and the sample plasmid DNA was adsorbed on silica membrane. Subsequent washings efficiently remove

endonucleases as well as salts, and plasmid DNA was eluted with 50µl of low-salt buffer (10 mM Tris-Cl, pH 8.5).

Plasmid DNA isolation for transfection experiments was performed using Endotoxin-free Plasmid DNA Maxi prep (Macherey-Nagel) according to the manufacturer protocol.

E.coli are Gram-negative bacteria, and therefore, major component of their cell wall is lipopolysaccaride (LPS), endotoxin, which is extremely potent stimulator of the mammalian immune system. LPS is a common contaminant of plasmid DNA preparations grown in E. coli. While DNA should be used for expression in mammalian cells, procedure for the endotoxin-free plasmid preparation must be performed.

The procedure is using modified alkaline/SDS lysis procedure for preparing the bacterial cell pellet for plasmid purification. Both chromosomal and plasmid DNA are denaturated. Then, Na-acetate is added to the denaturated lysate, and this cause the formation of precipitate containing chromosomal DNA and other cellular components. This buffer also neutralizes the lysate. Plasmid DNA, which remains in solution, can revert to its native supercoiled structure. After equilibration of appropriate column, plasmid DNA is bound to the anion-exchange resin and eluted after efficient washing of column, and endotoxins are removed in this step. After precipitation of the eluted DNA, it is dissolved in water for further use.

3.8.5. DNA sequencing

Sequencing of cloned DNA fragment (cdsCx43) in pGEM-T and pEGFP-N1, was done by BMFZ, using ABI PRISM® 3100 Genetic Analyser (16 capillary system).

The sequence result was then, using BLAST-Algorithm compared with already published original sequences in Gene-Databank of NCBI (www.ncbi.nim.nih.gov/blast).

3.8.6. Transient expression of cDNA encoding Cx43

Transfection is a method to introduce nucleic acids into the cells by using chemical reagents or by physical method. Lipofection technology is using cationic lipids for the delivery of nucleic acids to eykaryotic cells.

For transfection of HeLa, HaCaT and SCL-1 cells, lipofection reagent FuGENE 6 (Roche) was used. Cells were seeded in 3,5 cm dishes and growth to 60% confluence. Procedure was performed according to manufacturers protocol, with some optimised modifications. FuGENE 6 was diluted by direct pipetting of 3 µl in 97 µl of OptiMEM medium (Gibco Invitrogen), without allowing contact with the walls of the plastic tubes, and incubated 5 min at room temperature. 2 µg of DNA was added to diluted FuGENE 6 reagent, mixed and complex was incubated 30 min at room temperature. Growth medium was removed from the cells, washed away with PBS and cells were given 1ml of OptiMEM medium. The FuGENE 6 reagent : DNA complex was added on the cells, in a drop-wise manner and the cells were incubated 3-5 hours. After that period, the medium with transfection reagent and DNA was removed and replaced with serum-containing DMEM. Cells were then put back to incubator and analysed for gene expression after 24 hours.

Transfected cells were lysed with 1% SDS, and protein expression was analysed by immunobloting. *In vivo* imaging was performed on a Zeiss Axiovert 100 TV inverted fluorescent microscope with 63x/100x oil objective, coupled to a CCD camera (ORCA II, Hamamatsu, Japan).

4. Results

4.1. Gap junctional intercellular communication in normal and tumor cells

A common way of determining the level of gap junctional intercellular communication (GJIC) is by microinjection of fluorescent dye Lucifer Yellow into single cell. Active gap junctional channels permit passage of the dye into connected neighbouring cells, so the fluorescent signal is spreading. The number of fluorescent cells reflects the level of GJIC.

Primary human dermal fibroblasts (HDF) were used as a control, having the basal communication of 7–10 communicating cells, what makes them as a suitable control to measure and compare stimulatory and inhibitory effects on homologues GJIC. Measurement of GJIC was done in confluent monolayer cultures.

In order to study GJIC between normal human epidermal keratinocytes (NHEK), which reached up to 90 % confluency, single cells were microinjected with the dye. The same measurement of GJIC was done with HaCaT cells and SCL-1 tumor cells (Fig.1).

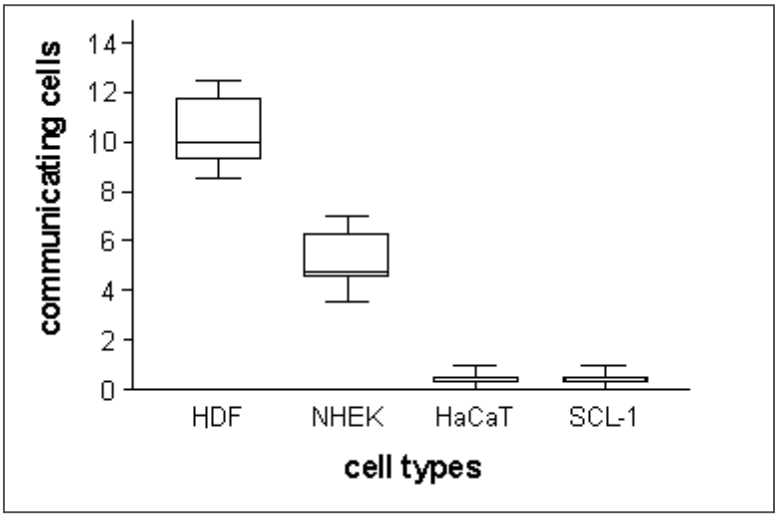

Fig. 1. GJIC capacity of different cell types

The number of stained collateral cells adjacent to the injected cell was used as a measure of GJIC. Box plots show a significant number of communicating fibroblasts (HDF), while lower GJIC is between NHEK. GJIC in HaCaT and SCL-1 cells was completely abrogated. The cells were maintained in DMEM + 10% FCS throughout the experiments. The upper and lower boundaries of the box are the upper and lower quartiles. The box length is the interquartile distance so the box contains the middle 50% of values (the horizontal line inside the box indicates the median). The vertical lines extend to maximum and minimum values. The values of the box plots represent the number of communicating cells of 20 microinjected cells (10 cells/dish).

While HDF and NHEK show homologous communication, measurement of GJIC revealed that GJIC between HaCaT cells was completely abrogated. In addition, in confluent monolayer cultures of SCL-1 tumor cells, microinjection of Lucifer Yellow dye in a single cell revealed no spreading of fluorescence, indicating complete loss of GJIC.

4.1.1. Effect of TGF-ß on GJIC in HaCaT and SCL-1 tumor cells

Interaction between tumor cells and stroma is crucial for tumor survival, invasion and metastasis. We could show that the squamous cell carcinoma line SCL-1 modulates homologues GJIC of dermal fibroblasts by growth factors, in a paracrine manner. In particular, transforming growth factor ß-1 (TGFß-1) was demonstrated to be involved in this paracrine effects. TGFß-1 released from SCL-1 tumor cells significantly downregulated homologues GJIC of dermal fibroblasts (Stuhlmann et al., 2003, 2004).

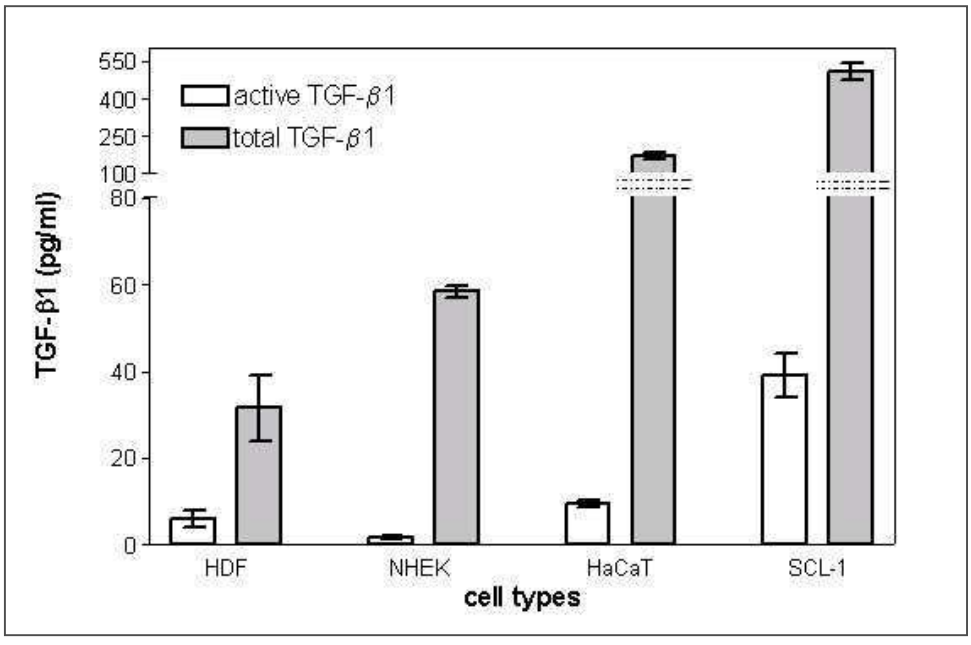

Fig. 2. Constitutive TGF-ß1 levels of different cells

Supernatants of human dermal fibroblasts (HDF), normal human epidermal keratinocytes (NHEK), HaCaT cells and SCL-1 tumor cells were harvested 24 h after incubation of the cells with serum-free cell culture medium and subjected to TGF-ß1 ELISA. Active and total TGF-ß1 amounts were determined as described in Materials and Methods. Data represent means±standard deviation for three independent experiments.

We first measured the total and active amount of TGF-ß1 in supernatants from normal and tumor cells, in order to show constitutive level of this factor. To differ between total and active growth factor, commercially available ELISA was used. Results demonstrated a higher amount of both total and active TGF-ß1 released from HaCat and SCL-1 cells, in comparison to HDF and NHEK (Fig. 2).

As in HaCaT and SCL-1 cells, homologues GJIC was completely abrogated, we addressed the question of whether TGFß-1 affects downregulation of GJIC in an autocrine manner.

In order to counteract a possible autocrine effect of TGFß-1, HaCaT and SCL-1 cells were incubated with neutralizing TGFß-1 antibody (2µg/ml) for 24h prior to microinjection. The number of stained cells adjacent to the injected single cell was counted (Fig. 3).

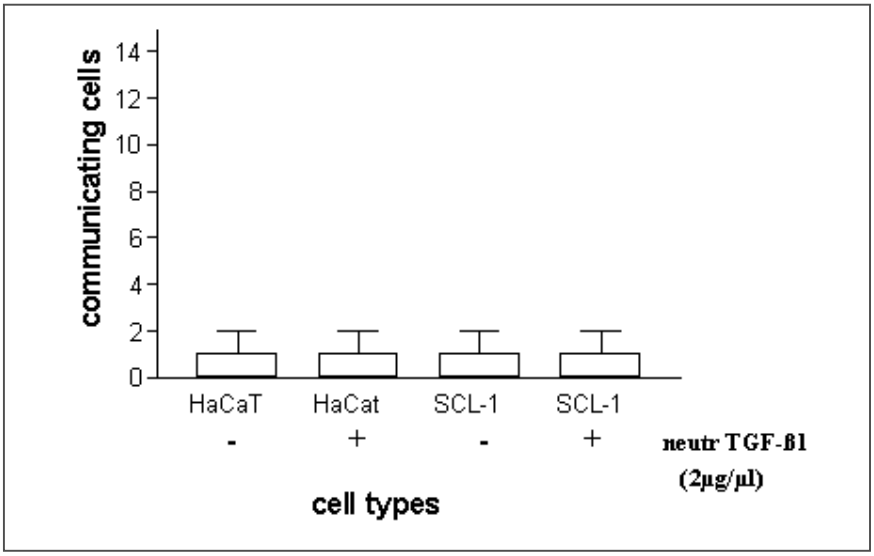

Fig. 3. Effect of neutralizing TGF-ß1 on GJIC

The number of stained collateral cells adjacent to the injected cell was used as a measure of GJIC. Box plots show abrogated GJIC between control HaCaT cells, and between SCL-1 cells (-). After 24h incubation with 2µg/µl of neutralizing TGF-ß1 (+), no change was demonstrated in GJIC. The cells were maintained in DMEM without FCS throughout the experiments. The values of the box plots represent the number of communicating cells of 20 microinjected cells (10 cells/dish).

In both HaCaT and tumor cells, no dye was transferred into neighbouring cells. This finding indicates that TGFß-1 does not exhibit an autocrine effect on homologous GJIC in HaCaT and SCL-1 tumor cells, pointing to other mechanisms responsible for that abrogation.

4.1.2. Effect of carotenoid *Canthaxanthin* on GJIC in HaCaT cells and SCL-1 tumor cells

Previous studies provide evidences that carotenoids could have cancer-protective effects, affecting cell proliferation (Tanaka et al., 1995). Carotenoid canthaxanthin stimulates GJIC in various cell systems and induce connexin transcriptional activation (Stahl and Sies, 2005; Hieber et al., 2000).
Communication assay was performed in order to study the effect of canthaxanthin on up-regulation of GJIC in HaCaT and SCL-1 cells. Communication-competent primary human dermal fibroblasts (HDF) were used as a control.

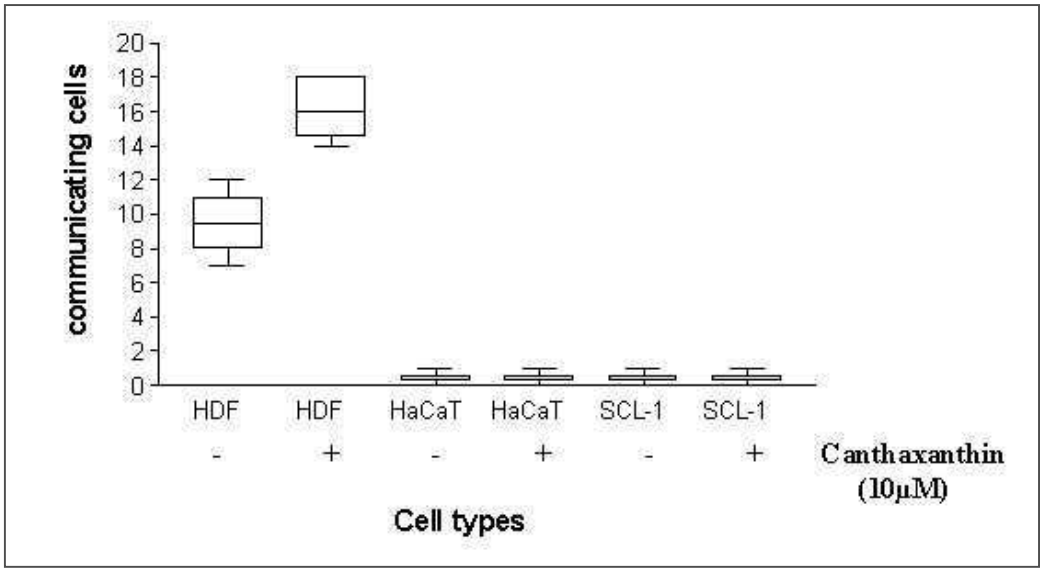

Fig. 4. Canthaxanthin effect on GJIC in different cell types
The number of stained collateral cells adjacent to the injected cell was used as a measure of GJIC. Box plots show a significant up-regulation of number of communicating fibroblasts after 24h treatment with canthaxanthin (HDF +), compared to untreated cells (HDF -). GJIC in HaCaT and SCL-1 cells was prior, as well as after treatment with canthaxanthin, completely abrogated. The cells were maintained in DMEM + 3% FCS throughout the experiments. The upper and lower boundaries of the box are the upper and lower quartiles. The values of the box plots represent the number of communicating cells of 20 microinjected cells (10 cells/dish).

HDF, HaCaT and SCL-1 cells were incubated with 10 µM of canthaxanthin for 24h prior to microinjection. Significant up-regulation of GJIC, measured by number of stained cells, was demonstrated in HDF. In both HaCaT and tumor cells, no spread of the dye was observed, indicating no effect of canthaxanthin on homologues GJIC (Fig. 4).

4.2. Connexin 43 steady-state mRNA levels in normal and tumor cells

Gap junctions in human skin are mainly composed of Connexin 43 (Cx43). As GJIC in tumor cells was not affected by carotenoids, a decrease in the Cx43 mRNA level was hypothesised to be responsible for its impaired GJIC. Therefore, normal human epidermal keratinocytes (NHEK) were compared with the immortalized keratinocyte cell line HaCaT and the tumor line SCL-1. In order to evaluate the steady-state mRNA levels, RT-PCR with specific primers, comprising the complete coding sequence (cds) of human Cx43, was performed (Fig. 5).

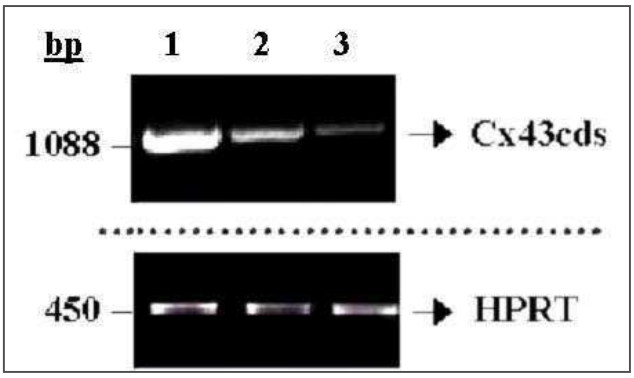

Fig.5. Cx43 steady-state mRNA level

Cx43 mRNA level was detected by RT-PCR .The ethidium bromide stained bands of 1088 bp correspond to the amplification products using Cx43cds- specific primers and total RNA extracted from normal keratinocytes (NHEK) (lane 1), HaCaT cells (lane 2) and SCL-1 tumor cells (lane 3). The housekeeping gene HPRT was used as an internal control to standardize the samples for mRNA content. Experiments were performed in triplicates.

Cx43 mRNA was detectable in all three tested cell types. The amount of full length Cx43cds in the transformed cell lines HaCaT (Fig. 5, lane 2) and SCL-1 (lane 3) is remarkably lower compared to the untransformed NHEK (lane 1). As there are no differences in electrophoretic mobility of the PCR products, a mutation, resulting in a truncated coding sequence, is not to be assumed.

While SCL-1 cells have high tumorigenic potential compared to the immortalized, but non-tumorigenic HaCaT cells, it could be presumed that the steady-state mRNA level of Cx43 decreases with increased tumorigenity of the cells.

4.3. Effect of phosphorylation on GJIC

Because a lack of transcription is not the reason for impaired cellular coupling and the low level of Cx43 mRNA does not explain the absence of GJIC in HaCaT and SCL-1, another decoupling mechanism was tested: the phosphorylation of Cx43.
Connexin 43 protein is posttranslationally modified by phosphorylation. In communication competent dermal fibroblasts, Cx43 protein expression results in a pattern of three bands, reflecting different phosphorylation status named P0 (unphoshorylated), P1 (phosphorylated), and P2 (higher phosphorylated), while in epidermal keratinocytes only P0 and P1 bands are detected. In this study, the Cx43 protein pattern was compared with the pattern of NHEK and HaCaT cells, using polyclonal antibody raised against an epitope in the C-terminus of Cx43 (Fig. 6).

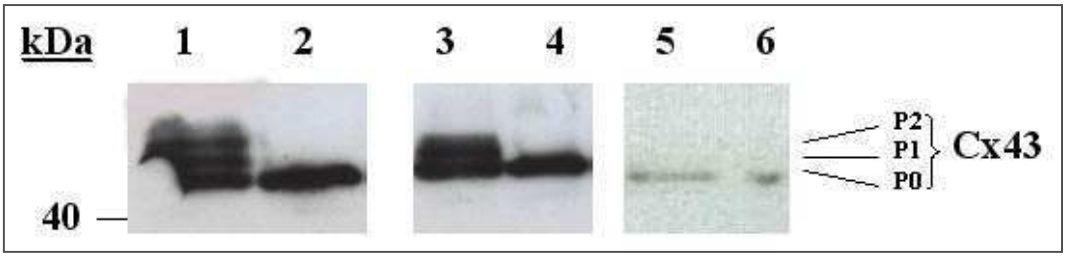

Fig. 6. Cx43 phosphorylation pattern in different cell types

Expression of Cx43 was analyzed by immunoblots using a specific Cx43 antibody. Lanes 1, 3 and 5 represent the Cx43 pattern (P0, P1, P2) of HDF, NHEK and HaCaT cells. To confirm the phosphorylated Cx43 protein, phosphatase treatment was performed (lanes 2, 4, 6).

In accordance with previous studies, Western blot analysis confirmed the three band pattern for Cx43 in HDF (Fig. 6, lane 1). To prove that the shift in electrophoretic mobility is due to higher phosphorylated Cx43 species, the lysate was treated with phosphatase for 2h prior to SDS-PAGE and Western blotting. Consistently, two upper bands accumulate to the lowest P0-band after dephoshorylation (lane 2).
Resting NHEK cells show a two band pattern for Cx43, composed of an unphosphorylated and phosphorylated band (lane 3). P1 was removed by phosphatase treatment (lane 4).

The spontaneously immortalized keratinocyte line HaCaT displays only a single band (lane 5), which was maintained after phosphatase digestion, proving it to be unphosphorylated (lane 6). Interestingly, the protein amount was significantly lower, compared with the HDF and NHEK.
In SCL-1 cells, protein amount was below the detection limit, although up to 50 µg of total protein was loaded for SDS-PAGE, and the most sensitive chemiluminesscent reagent was applied. This low amount of protein fits to the low mRNA level.

4.4. Immunolocalization of Connexin 43 in normal and tumor cells

GJIC is characterized by localization of connexin in the cell membrane. As transcription and translation of Cx43 are present in normal and tumor cells, localization of Cx43 was checked to figure out whether impaired communication in tumor cells is due to alterations in subcellular distribution.
Cx43 protein in confluent monolayer cultures of human dermal fibroblasts (HDF), used as a control, is present in a high amount and localized mainly in cell membranes (Fig. 7, A). In subconfluent monolayer cultures of NHEK, Cx43 is highly expressed and localized both on the cell membrane and inside the cell around the nucleus (B). In confluent monolayer cultures, NHEK undergo final differentiation. They show high expression of Cx43 localized only around the nuclei, which reflects decreased gap junctional intercellular communication (data not shown). For that reason, subconfluent monolayer cultures of keratinocytes were used for subsequent experiments.

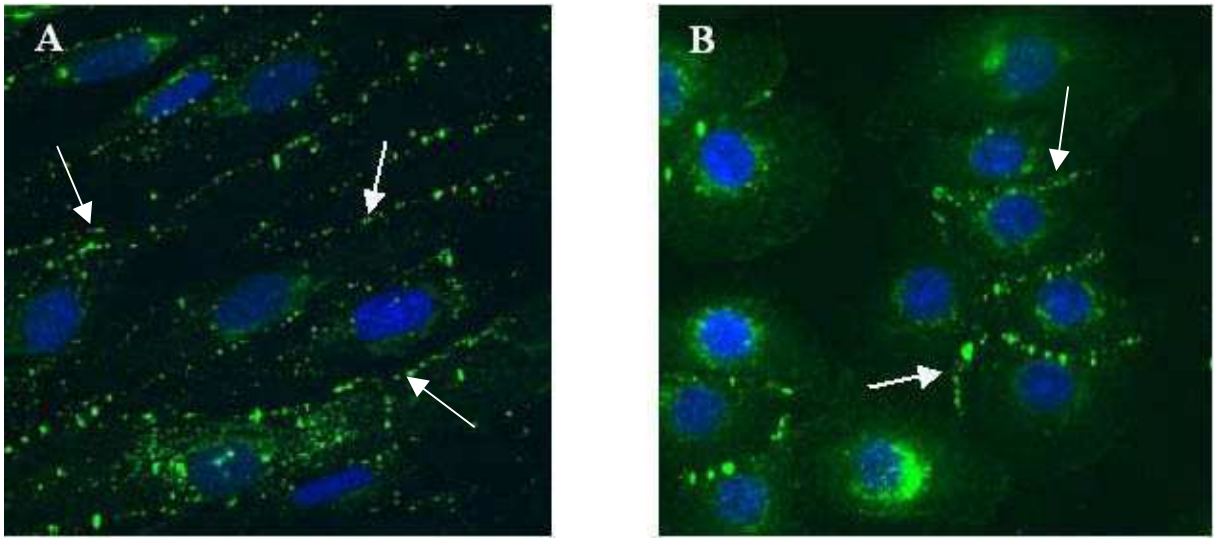

Fig. 7. Subcellular distribution of Cx43 in monolayer cultures of normal cells
(A) HDF and (B) NHEK were immunostained for Cx43. The green dots represent Cx43 protein. The arrows indicate Cx43 localized in the cell membrane. The blue DAPI staining reflects labeled nuclei.

In contrast, Cx43 protein in HaCaT cells (Fig. 8, A) and SCL-1 tumor cells (B) is mainly localized around the nuclei of the cells, with no staining in the cell membrane. This intracellular localization of Cx43 in tumor cells reflects the inability to form gap junctions at the membrane and loss of GJIC.

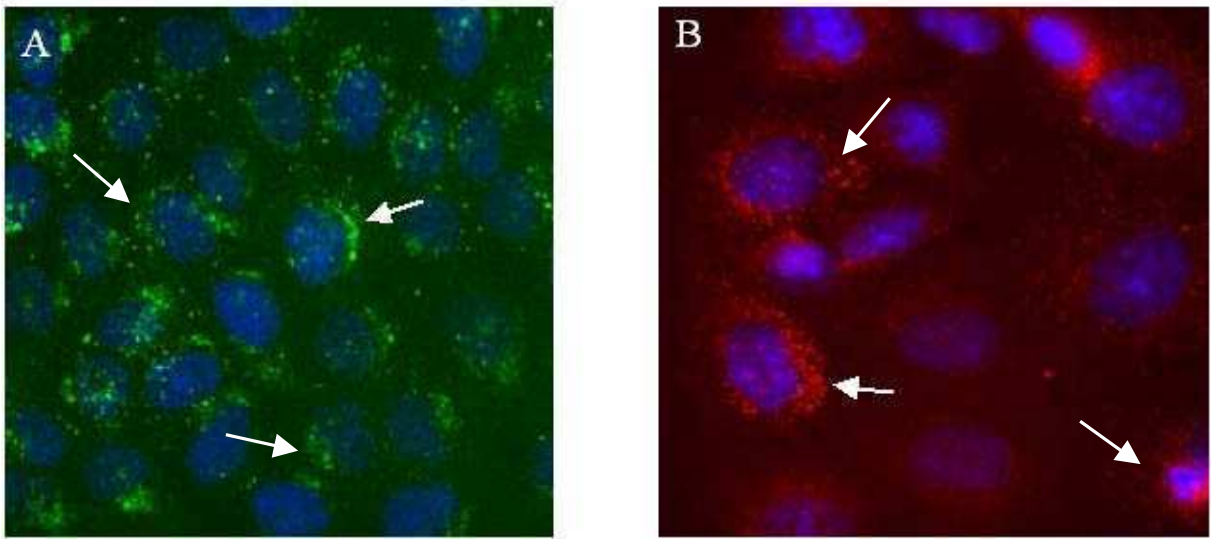

Fig. 8. Subcellular distribution of Cx43 in monolayer cultures of transformed cells
(A) HaCaT cells and (B) SCL-1 tumor cells were used for immunocytostaining of Cx43. Both HaCaT and SCL-1 showed high Cx43 fluorescence located around the nuclei but no signal in the membrane. Green dots (A) and red dots (B) represent Cx43 protein. The arrows indicate Cx43 localized around the nuclei. The blue staining (DAPI) reflects labeled nuclei.

4.5. Sequence analysis of Cx43cds from SCL-1 tumor cells

Point mutations in the coding sequences (cds) of connexins, causing amino acid exchange and possibly improper folding of the mature proteins, could influence trafficking and intracellular localization of some connexins. Therefore, the Cx43cds from SCL-1 tumor cells was cloned and sequenced

Mutations were described for some connexin genes expressed in skin (Rouan et al., 2001), which are associated with modified intracellular localization of connexin proteins. However, until yet, no connexin mutation is described to be involved in cancer development.

A databank search was done in the Genebank of the National Institute for Biological Information (NCBI) and in the Expert Protein System (ExPASy) of the Swiss Institute of Bioinformatics for available Cx43 sequences. Human Cx43 mRNA sequence was found (access N° NM000165), and specific primers co vering the Cx43 coding sequence were designed. The complete coding sequence comprising 1036 bp was amplified by RT-PCR, cloned into the pGEM-T vector and analyzed using an automatic fluorescence based sequencer (ABI). To minimize the risk of mistakes generated by Taq polymerase, a proofreading PCR system (Expand High Fidelity, Roche) was used for amplification.

Comparison of Cx43cds from human epidermal keratinocytes and SCL-1 tumor cells, revealed a point mutation in Cx43cds from SCL-1 cells, leading to a Valine-Alanin exchange in the amino acid chain at position 183 (Fig. 9).

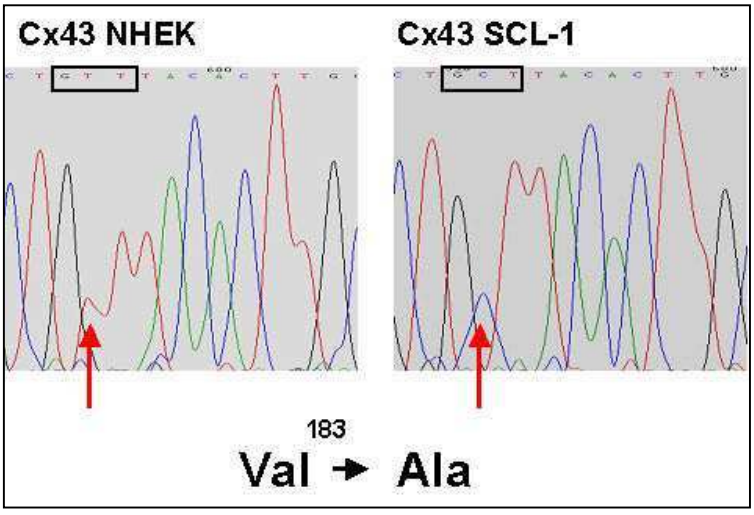

Fig. 9. Sequence analysis of the Cx43 coding sequence

Sequencing revealed a point mutation in the Cx43cds from SCL-1 cells, leading to Val/Ala exchange in the amino acid chain at position 183. The coding sequence of Cx43 gene was amplified by RT-PCR using total RNA extracted from NHEK and SCL-1 cells, and specific primers. Red arrows indicate the site of nucleotide base change (T→C).

Valine and Alanine are both characterized by the presence of an aliphatic side chain (non-polar side chain). Their residues are not described to be posttranslationally modified, so they have minor influence on secondary structure of the protein. Therefore, this Val-Ala exchange might not be relevant for Cx43 folding or its transport to the membrane.

4.6. Cx43 steady-state pseudogene mRNA levels

Up to now, connexin 43 is the only connexin, for which a corresponding pseudogene has been reported (Willecke et al., 1990). A pseudogene (Ψ gene) is usually considered to be a functionally inactive copy of a gene. As it is described to be associated with tumorigenesis, its expression has been studied herein.

Sequence comparison of the open reading frames (ORFs) revealed the presence of a *Nco*I restriction site at position 605 from the ATG start site in the ΨCx43 predicted mRNA sequence (access N° NG003029.1), which is absent in the Cx43 counterpart. Therefore, digestion of PCR product with *Nco*I was used to confirm the specific transcription of the pseudogene.

RT-PCR was performed on total RNA isolated from NHEK, HaCaT and SCL-1 cells, using specific primers, which amplify the region encompassing nucleotide positions 248 to 1483 in ΨCx43 (Fig. 10, A).

RT-PCR showed the presence of ΨCx43 mRNA in all studied cell types. The level of mRNA was slightly lowered in HaCaT cells (Fig. 10, A, lane 2) and SCL-1 tumor cells (A, lane 3), compared with NHEK (A, lane 1).

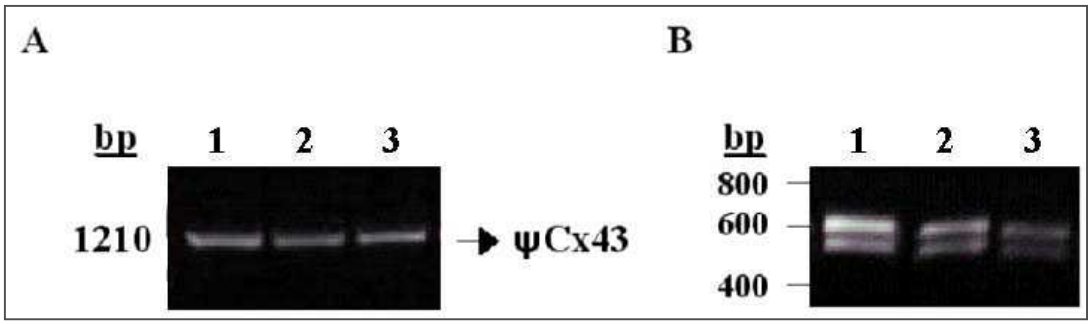

Fig. 10. ΨCx43 mRNA level in different cell types

(A) mRNA level of ΨCx43 was detected by RT-PCR .The ethidium bromide stained bands of 1210 bp correspond to the amplification products using ΨCx43- specific primers and total RNA extracted from normal keratinocytes (NHEK) (lane 1), HaCaT cells (lane 2) and SCL-1 tumor cells (lane 3). (B) The PCR products from the corresponding samples were digested with excess NcoI to confirm specificity of the ΨCx43 PCR amplification (lanes 1, 2, 3)

Digestion with *Nco*I restriction endonuclease confirmed ΨCx43 PCR amplification in all samples, yielding fragments with a size of 560bp and 650bp, respectively (Fig. 10, B).

As Cx43 gene and pseudogene show a high degree of homology, a specific antibody directed against an epitope of Cx43 pseudoprotein is still not available. This shortcoming restricts the research currently on transcriptional level. Therefore, it is not known whether ΨCx43 mRNA is translated in the cell, although in vitro translation for ΨCx43 has been demonstrated (Kandouz et al., 2004). A possible interference of ΨCx43 in transcription and/or translation of wtCx43, and formation of functional gap junctions, therefore resulting in down-regulation of GJIC, still remains to be elucidated, even though the data with GJIC competent NHEK (Fig. 10 A, lane 1; Fig.10 B, lane 1) might exclude that possibility.

The Cx43 is expressed in tumor cells and protein is intracellulary localized. As Cx43 is expressed, but not localized in the membrane of HaCaT and SCL-1 cells, additional proteins involved in transport of Cx43 to the membrane and forming of gap junctions, were investigated.

4.7. Expression and localization of adherens junction proteins in normal and tumor cells

4.7.1. E-cadherin/ß-catenin connection

The E-cadherin/ß-catenin complex mediates intercellular adhesion. In tumors, impaired adhesion between cells is thought to contribute to cancer invasion and metastasis. The cadherins are a transmembrane component of adherens junctions and regulate the organization and formation of gap junctions on the cell membrane, bringing adjacent cells in close contact. Several studies demonstrated an abnormal or reduced expression of E-cadherin, ß-catenin, or both, in various carcinomas (Pignatelli et *al*., 1994; Behrens, 1993; Oyama et al., 1994).

Human epidermal keratinocytes (NHEK) are used as normal counterpart cells for HaCaT and SCL-1 cells. Cell-cell adhesion in keratinocytes is related with their terminal differentiation and regulated by the extracellular calcium concentration. Normal primary keratinocytes isolated from human foreskin were cultured routinely under low calcium conditions (0,09 mM $CaCl_2x2H_2O$). These cells growth exponentially and, therefore, show almost no apparent cell-to-cell contact and no adherens junctions. By increasing the calcium concentration of the media, keratinocyte proliferation is retarded; the cells become adhesive and initiate terminal differentiation. In order to induce differentiation and similar behaviour of keratinocytes like in normal stratified skin, NHEK were preincubated for 24h with increased calcium concentration (up to 1 mM $CaCl_2$). Proliferation of HaCaT and SCL-1 cells is calcium-independent.

The expression of E-cadherin was investigated by immunoblotting using a monoclonal antibody raised against the human E-cadherin (Fig. 11). In differentiated NHEK (Fig. 11, lane 2), expression of E-cadherin was enhanced compared to non-differentiated cells (lane 1). The level of E-cadherin expression in both HaCaT (lane 3) and SCL-1 (lane 4) cells show higher E-cadherin expression in comparison to non-differentiated keratinocytes.

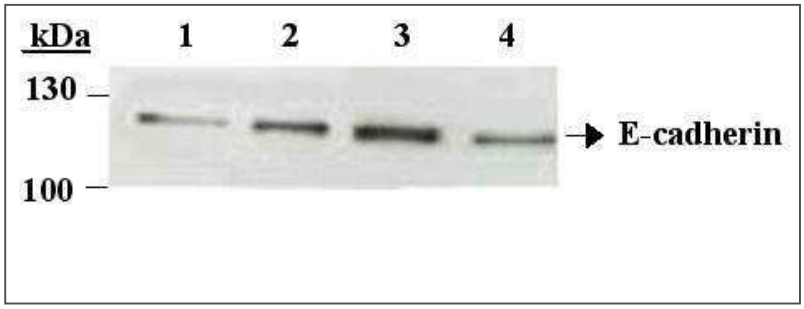

Fig. 11. Expression of E-cadherin in different cell types

Immunoblot analysis of E-cadherin expression revealed discrete band of 124 kDa in all cells. Lane 1 (low calcium) and lane 2 (high calcium) represent calcium-dependent expression of E-cadherin in NHEK. Lanes 3 and 4 represent expression of E-cadherin in HaCaT and SCL-1 cells, maintained in high calcium

Membrane localization of E-cadherin was confirmed by immunofluorescent staining in normal epidermal keratinocytes, HaCaT cells and SCL-1 tumor cells (Fig. 12).

Figure 12 (A, C), demonstrates light microscope images of calcium-dependent differentiation of keratinocytes. In medium with low calcium concentration, keratinocytes are morphologicaly looking more oval and not so close to each other (A). Under conditions of increased calcium they become flattened and form sheet-like clusters (C). While there is less expression on the membrane in non-differentiated NHEK (B), E-cadherin is highly expressed and localized at points of cell-cell contacts in differentiated cells (D). HaCaT cells (Fig. 13, A) and SCL-1 tumor cells (B), show elevated amounts of E-cadherin. In SCL-1 tumor cells, in some areas of the cells, more punctuate staining could be observed. These data suggest that alteration of E-cadherin expression in HaCaT and SCL-1 tumor cells is not the reason for GJIC downregulation.

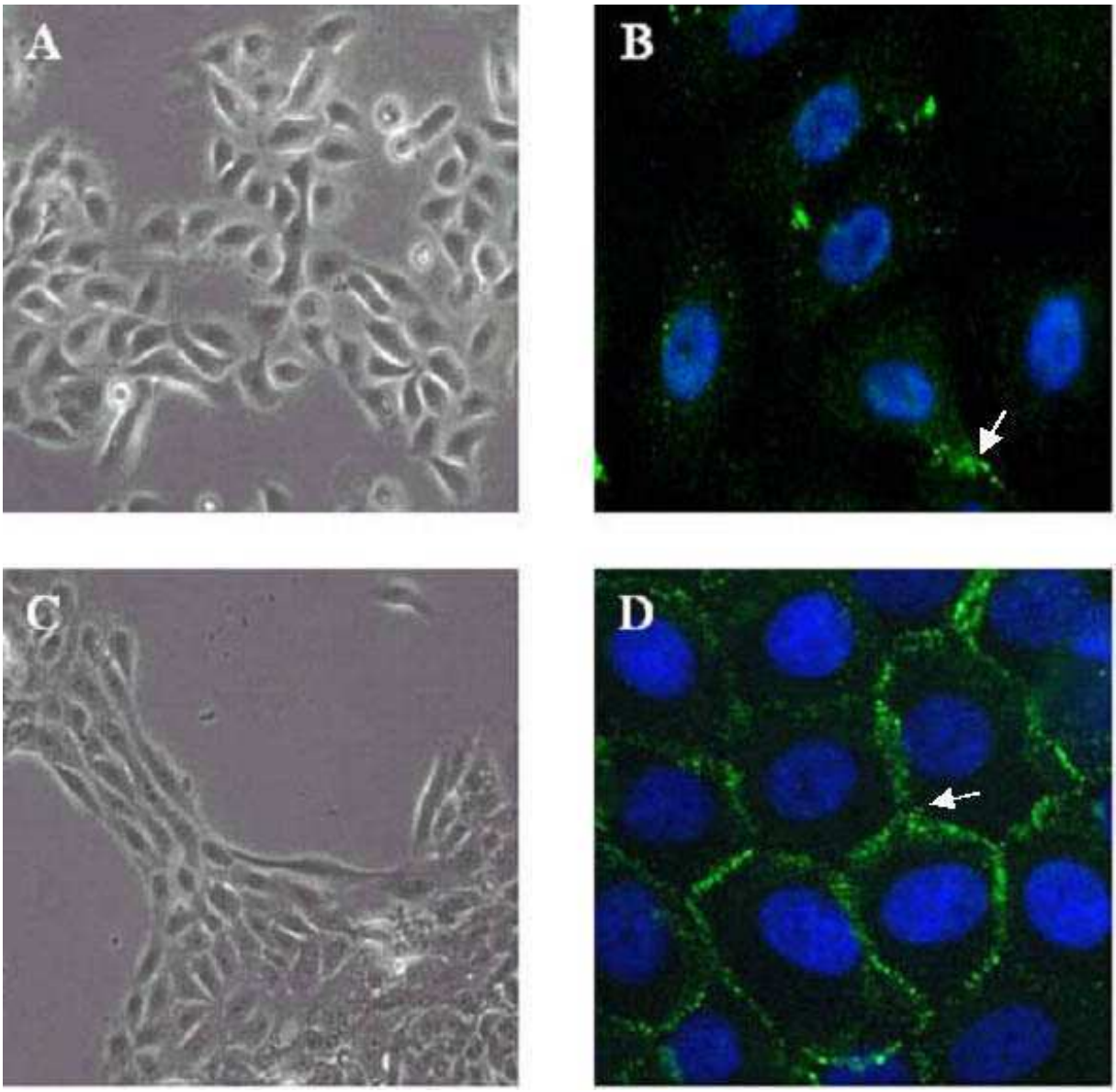

Fig. 12. Subcellular distribution of E-cadherin in monolayer cultures of normal epidermal keratinocytes (NHEK)
NHEK were immunostained for E-cadherin. A and C show the morphology of non-differentiated and differentiated NHEK. Epifluorescence reveals E-cadherin subcellular distribution in non-differentiated and differentiated NHEK (B and D). Green staining represents E-cadherin. The arrows indicate subcellular distribution of E-cadherin. The blue staining (DAPI) reflects nuclei.

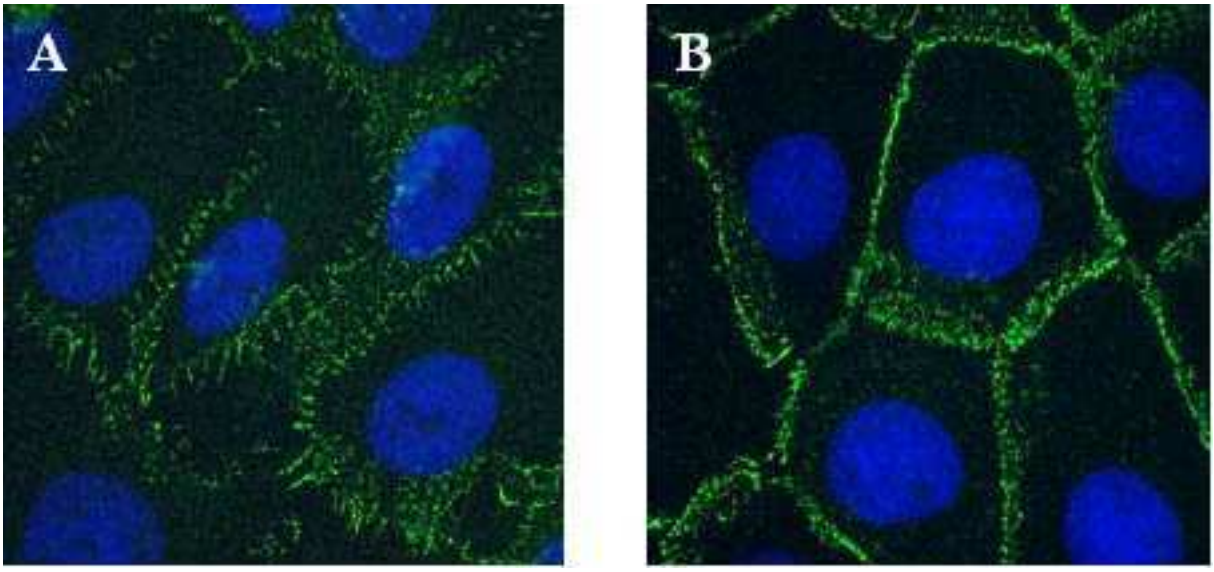

Fig. 13. Subcellular distribution of E-cadherin in monolayer cultures of transformed cells

HaCaT cells (A) and SCL-1 tumor cells (B) were immunostained for E-cadherin. The green staining represents E-cadherin, while the blue staining (DAPI) reflects nuclei.

Beta-catenin, in addition to its role in intercellular adhesion, regulates transcription of some genes involved in invasion and metastasis. Accumulation of free, unbound ß-catenin in the cytoplasm has been shown to potentiate the translocation of ß-catenin into the nucleus, augmenting its transcriptional activity (Morin et al., 1997).

To investigate whether ß-catenin in HaCaT and SCL-1 cells is relevant only in cell adhesion or whether the free unbound pool of ß-catenin could also be involved in forming of GJ in those cells, the following experiments were performed.

First, the expression of ß-catenin was studied. Immunoblots with a polyclonal antibody raised against a synthetic peptide corresponding to amino acids 768-781 of human ß-catenin, showed that expression of ß-catenin was enhanced in differentiated NHEK (Fig. 14, lane 2). In comparison to NHEK, the expression in HaCaT cells (lane 3) and SCL-1 tumor cells (lane 4) was even higher.

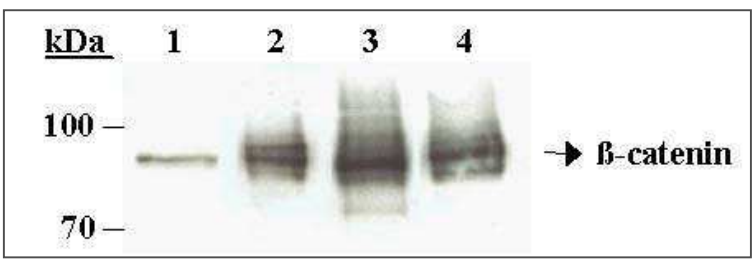

Fig. 14. Expression of ß-catenin in different cell types

Expression was analyzed by immunoblot using specific ß-catenin antibody, revealing band of 94 kDa. Lane 1 (low calcium) and lane 2 (high calcium) represent calcium-dependent expression in NHEK. Level of ß-catenin expression in HaCaT and SCL-1 cells is presented in lanes 3 and 4.

Immunocytochemical labeling of ß-catenin and analysis by fluorescent microscopy was performed in order to perceive the possible cytoplasmic localization of the unbound ß-catenin. Figure 15 shows images of non-differentiated (A) and differentiated NHEK (B), demonstrating increased appearance of ß-catenin in the supramembrane region of the differentiated cells. HaCaT cells (C) and SCL-1 tumor cells (D) also show strong ß-catenin distribution in supramembrane regions of the cells.

No intracellular localization and thus no free ß-catenin pool in cytoplasm of those cells was observed, indicating no influence on GJIC.

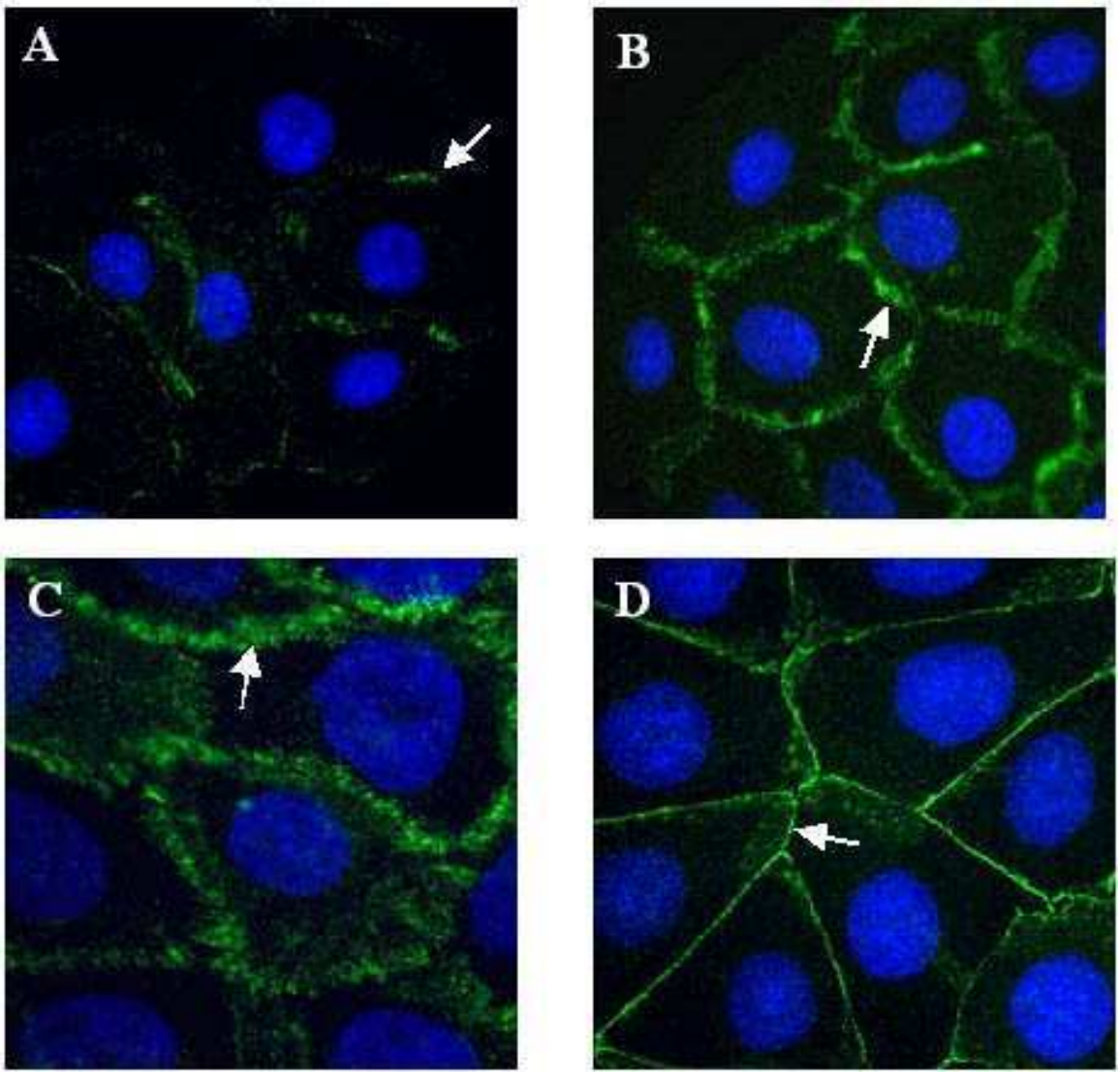

Fig. 15. Subcellular localization of ß-catenin in monolayer cultures of different cell types

Low expression of ß-catenin is observed in non-differentiated NHEK (A). Differentiated NHEK, HaCaT and SCL-1 cells show localization of ß-catenin in cell membrane (B, C, D). Green staining represents ß-catenin. The white arrows indicate presence of ß-catenin in the membrane. The blue staining (DAPI) reflects nuclei.

4.7.2. N-cadherin expression

During tumor progression, function of E-cadherin is frequently replaced or even overruled by the expression of N-cadherin. While E-cadherin promotes tight cell-cell adhesion, N-cadherin is responsible for both stable and labile cellular interactions, facilitating cell migration. Expression of N-cadherin in tumor cells is associated with its increased invasive and metastatic potential, even though cells continue to express E-cadherin (Hazan et al., 2000). In addition, it has been shown that cell surface trafficking of Cx43 and GJIC likely require the intracellular co-assembly of N-cadherin with Cx43 in mouse fibroblast line NIH3T3 (Wei et al., 2005).

Western blot analysis was performed to assess the expression of N-cadherin, by using a polyclonal antibody raised against the C-terminus of N-cadherin. As shown on Figure 16, normal epidermal keratinocytes do not express N-cadherin, independent of the differentiation state (lanes 1, 2). However, HaCaT cells (lane 3), and SCL-1 tumor cells (lane 4), express N-cadherin. Compared to HaCaT cells, lower expression of N-cadherin was seen in SCL-1 tumor cells.

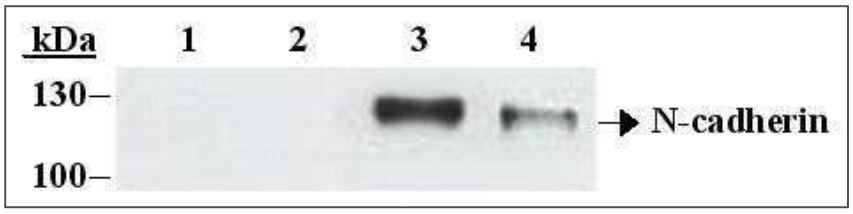

Fig.16. Expression of N-cadherin in different cell types

Immunobloting of N-cadherin expression revealed a discrete 130 kDa band. Lanes 1 and 2 represent expression in non-differentiated and differentiated NHEK, respectively. Lane 3 and 4 represent expression in HaCaT and SCL-1 cells.

Immunocytochemistry was performed to confirm localization of N-cadherin on the cell membrane. Figure 17 demonstrates absence of the N-cadherin expression in both non-differentiated (A) and differentiated epidermal keratinocytes (B). In contrast, N-cadherin is present in a high amount and localized in the cell membrane in HaCaT cells (C) and SCL-1 tumor cells (D).

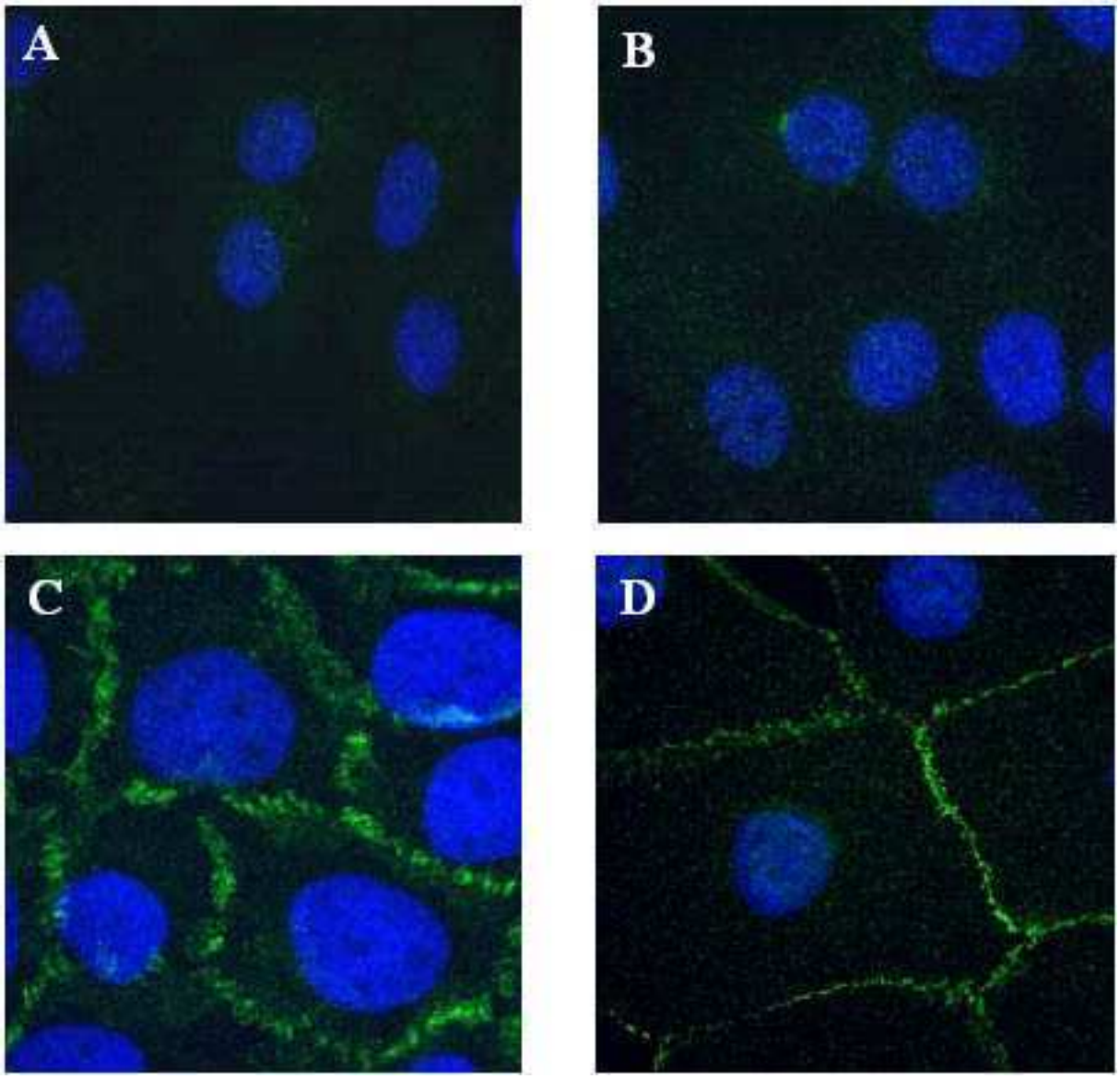

Fig. 17. Subcellular distribution of N-cadherin in different cell types
N-cadherin was immunocytochemically labeled and analyzed by epifluorescence. Non-differentiated as well as differentiated NHEK do not show any expression of N-cadherin (A and B). N-cadherin localize at cell-cell contacts in HaCaT and SCL-1 cells (C and D). Green staining represents N-cadherin. The blue DAPI staining reflects labeled nuclei.

In contrast to the described co-assembly of Cx43 with N-cadherin, necessary for trafficking of Cx43 to the cell surface and forming of GJ in some cells, NHEK do not express N-cadherin but nevertheless transport Cx43 and form functional gap junctions. The appearance of N-cadherin in HaCaT cells and SCL-1 tumor cells seems not to play a role in Cx43 trafficking. It rather might reflect their increased invasive potential. As the expression and localization of molecules involved in cell-

cell adhesion did not show relevant differences among the tested cell types, further experiments were performed focusing on the status of the cytoskeleton.

4.8. Cytoskeletal network in normal and tumor cells

4.8.1. Microtubules

Microtubules are formed from tubulin subunits. Each tubulin subunit is a heterodimer of two closely related globular proteins called α-tubulin and ß-tubulin.
In HeLa cells transfected with GFP-tagged Cx43, connexons are transported in vesicles along microtubules from the Golgi apparatus to the plasma membrane. Disruption of microtubules might inhibit connexon trafficking and formation of GJ on membrane (Lauf et al., 2002).
In order to examine the status of microtubules in tumor cells, the immunocytochemical labelling of α-tubulin was performed. Figure 18 shows that normal epidermal keratinocytes, used as control cells (A), as well as HaCaT cells (B) and SCL-1 tumor cells (C) displayed no difference in the distribution of microtubuli.

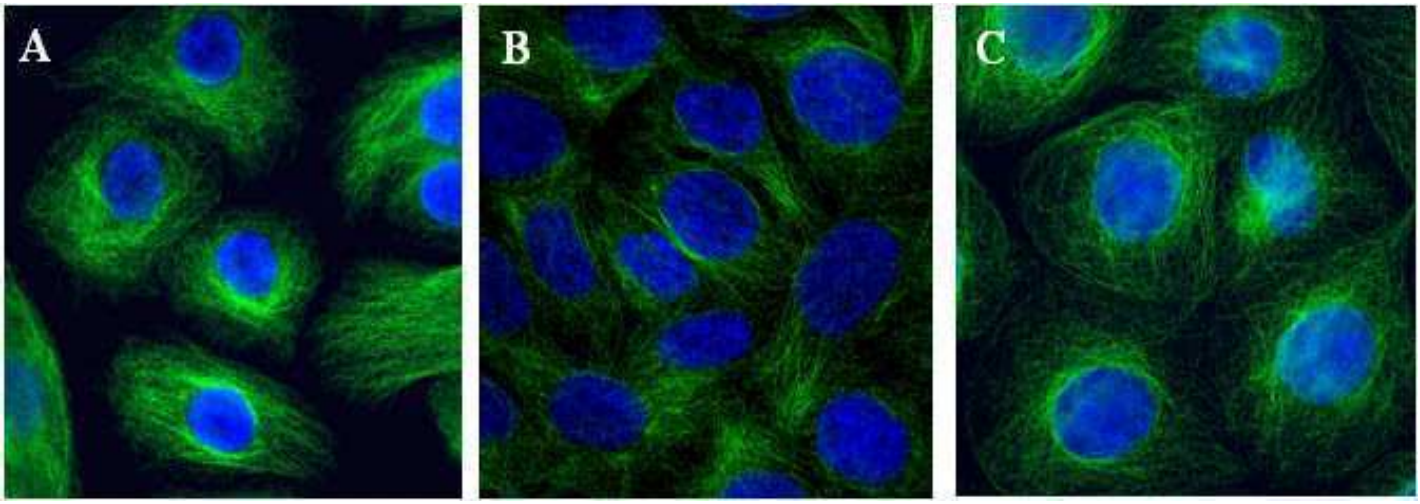

Fig. 18. Expression of α-tubulin in monolayer cultures of different cell types
NHEK, HaCaT and SCL-1 cells were immunostained for α-tubulin (A, B, C). Green stained fibers represent α–tubulin. The blue DAPI staining reflects labeled nuclei.

The similar pattern of α-tubulin in NHEK and keratinocyte-derived tumor cells, demonstrates that Cx43 trafficking in skin cells is not related to the state of microtubules.

4.8.2. Actin network

The actin cytoskeleton controls cell-cell and cell-matrix interactions and participates in transmembrane signalling. Intact actin filaments have been observed to be involved in the plasma membrane delivery of connexins, especially of Cx26 (Thomas et al., 2001).

UVA radiation reversibly damages actin cytoskeleton in epidermal keratinocytes, as shown by actin filament depolymerization and changes in cell morphology. Subsequently, a transient disruption of GJIC and loss of Cx43 localization on the membrane is observed in those cells (Provost et al., 2003).

Herein, the organization of actin cytoskeleton in normal and tumor cells was investigated by phalloidin labelling of actin, analyzed by fluorescent microscopy.

Non-differentiated NHEK (Fig. 19, A) show almost no polymerized actin, while in increased calcium environment (B), cortical actin filament (CAF) network is clearly seen at cell-cell contacts. HaCaT cells (C) mostly exhibit stress fibres (SF) of actin, while SCL-1 tumor cells (D) also show circumferential CAF network, similar as for differentiated NHEK (B).

This result indicates that in HaCaT cells and in SCL-1 tumor cells, other mechanisms are responsible for Cx43 trafficking, which are not affected by actin organization.

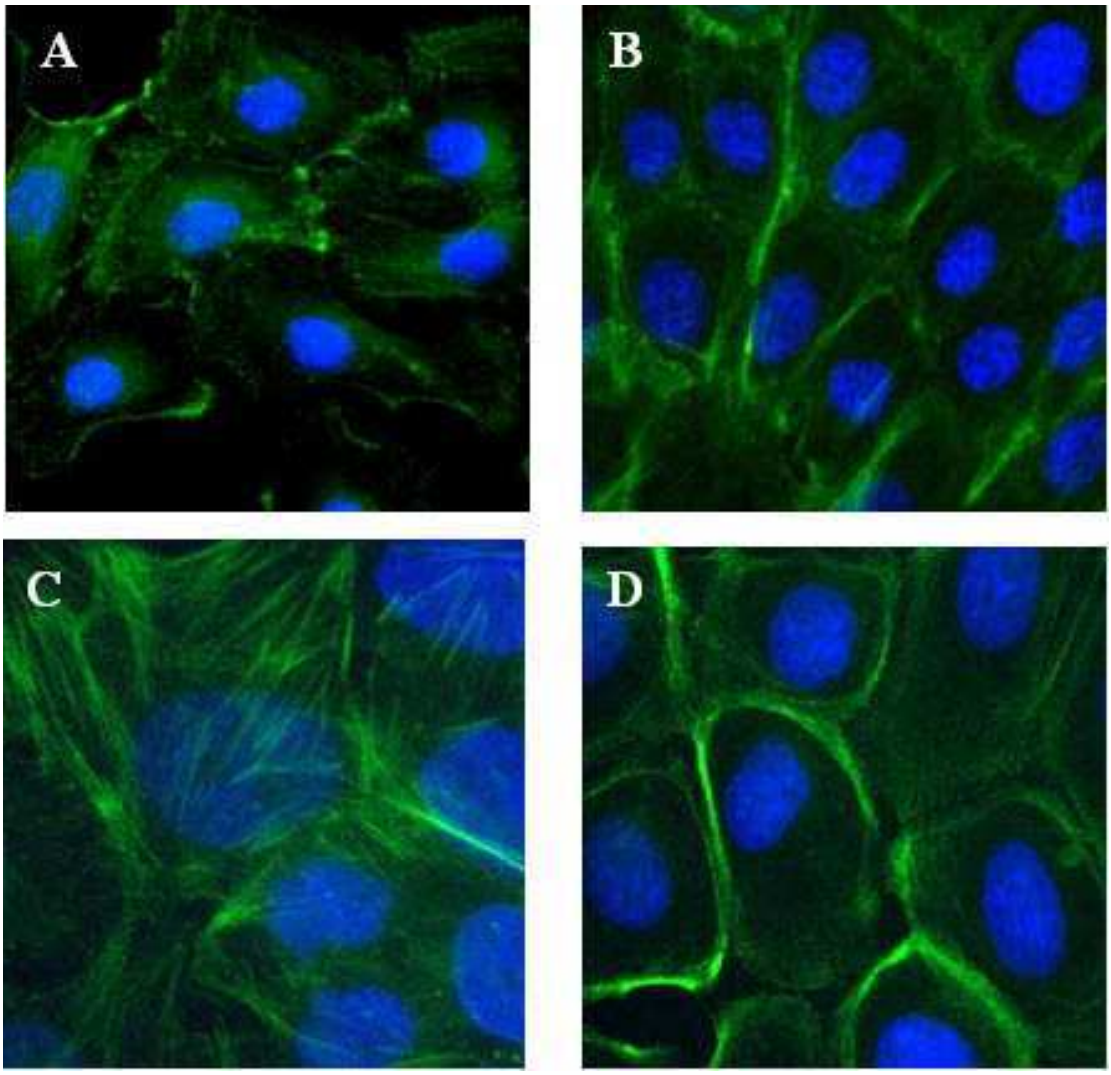

Fig. 19. Actin network in monolayer cultures of different cell types

Cells were labeled for F-actin using FITC-conjugated phalloidin. The green staining represents F-actin in non-differentiated (A) and differentiated NHEK (B) HaCaT (C) and SCL-1 cells (D). The blue staining (DAPI) reflects labeled nuclei.

4.9. Transient overexpression of Cx43-EGFP in tumor cells

In order to better characterize synthesis and trafficking of Cx43 in tumor cells, HaCaT and SCL-1 cells were transiently transfected with Cx43 cloned into a eukaryotic expression vector.

Introduction of functional connexin genes in cancer cells delays tumor growth in suspension or xenografts in nude mice, demonstrating the importance of connexin downregulation for tumor progression. *In vitro*, transfection of communication-deficient HeLa tumor cells with a Cx43-GFP construct resulted in expression, transport and assembly of Cx43 into functional gap junctions (Jordan et al., 1999).

In order to increase membrane localization of Cx43, to form gap junctions, and to reconstitute intercellular communication, Cx43 from human epidermal keratinocytes was cloned into a GFP expression vector (pEGFP-N1) and transiently overexpressed in communication-deficient HaCaT cells and SCL-1 tumor cells. In parallel, HeLa cells were used as technical control.

4.9.1. Construction of an expression vector for human Cx43

The Cx43 was tagged with an enhanced red-shifted mutant of green fluorescent protein (GFP) to construct a Cx43-EGFP chimera. The cloned Cx43 sequence is ~1100 bp in length and comprises the complete coding sequence (cds) of human Cx43 (nucleotide positions 208…1356 in Cx43 sequence, gene databank access Nr. NM000165) (Fig. 20, A).

The Cx43cds was amplified from cDNA of normal human epidermal keratinocytes by RT-PCR using specific primers to create an additional restriction site for *Xho*I at the 5’ end and for *BamH*I at the 3’ end of Cx43, respectively. Both, the PCR products and the vector pEGFP-N1 were digested with *Xho*I and *BamH*I, and in addition the vector was dephosphorylated with alkaline phosphatase. Upon ligation, Cx43cds was cloned in frame with EGFP, allowing the production of a fusion protein carrying EGFP at the C-terminus of Cx43 (B). In further investigations, this construct will be presented as Cx43-EGFP.

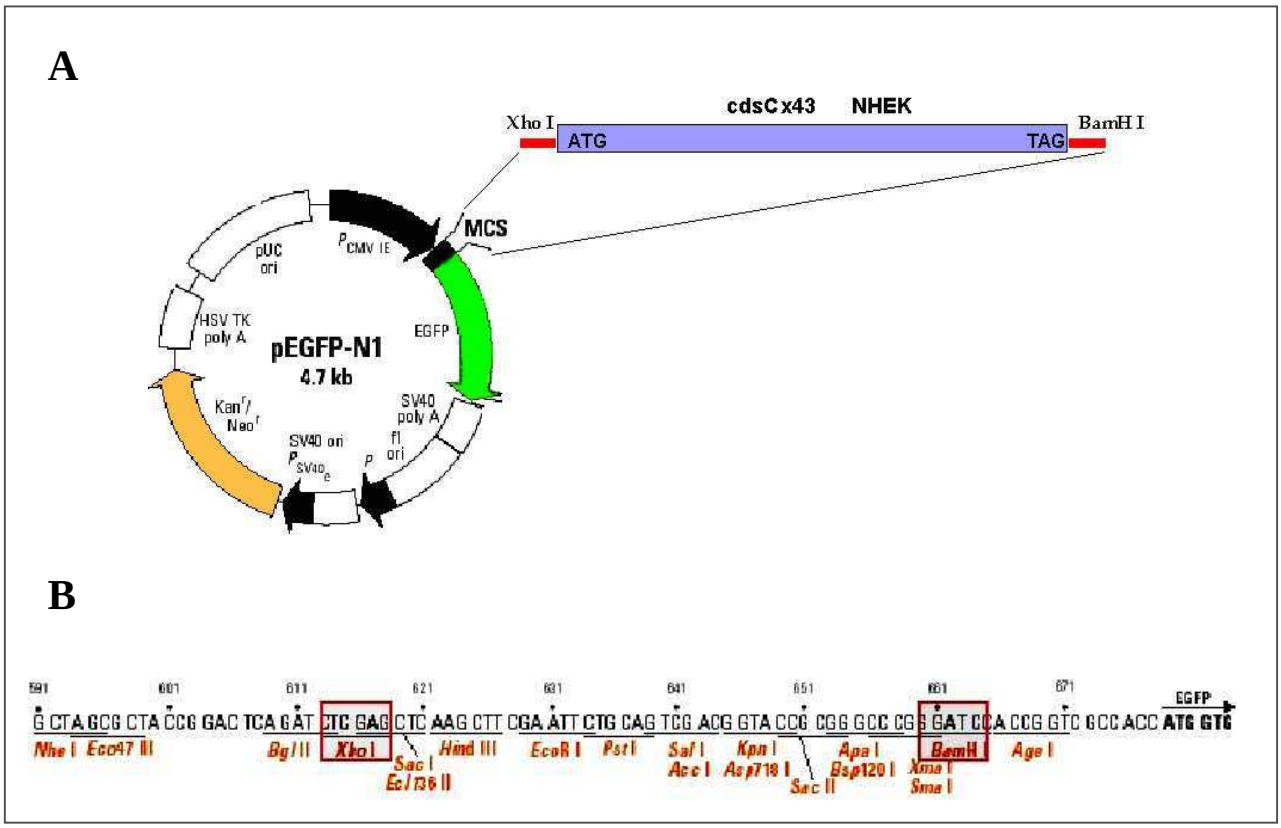

Fig. 20. Scheme of Cx43-EGFP expression vector

The complete coding sequence of Cx43, amplified from cDNA of normal human epidermal keratinocytes by RT-PCR with an additional restriction site for XhoI at the 5' end and for BamHI at the 3' end, was cloned in pEGFP-N1 expression vector (A). B shows the multiple cloning site (mcs) of pEGFP-N1 expression vector comprising XhoI and BamHI restriction sites.

Competent *E.coli* cells were transformed with the ligated Cx43-EGFP, and positive colonies were identified by digestion with *Xho*I/ *BamH*I (Fig. 21, lane 1) and *EcoR*I/ *Not*I (lane 2) restriction endonucleases, prior to separation on agarose gel.

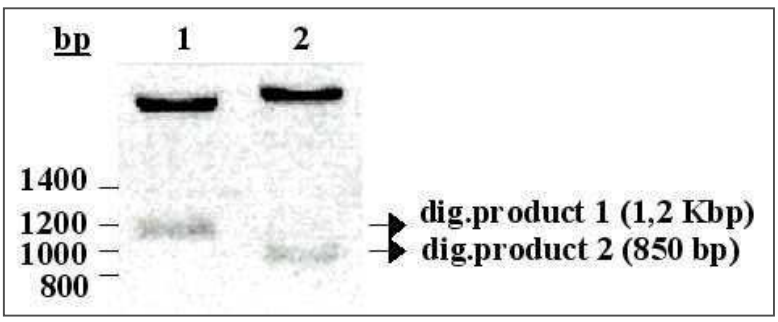

Fig. 21. Restriction analysis of DNA encoding Cx43-EGFP

Double digestion of pL DNA encoding for Cx43-EGFP was performed using two sets of restriction endonucleases. In lane 1, digestion product yielded after incubation with XhoI/BamHI was presented, while in lane 2 after incubation with EcoRI/NotI.

Restriction analysis confirmed the presence of the cloned sequence in vector, showing appropriate fragment sizes after gel electrophoresis. Digestion with *Xho*I/ *BamH*I (lane 1) yielded fragments of 4,7 Kbp and ~1,2 Kbp, while lane 2 shows fragment lengths of 5 Kbp and ~850 bp after digestion with *EcoR*I/ *Not*I, respectively. The sizes of restriction fragments correspond to the full size of the pL DNA for Cx43-EGFP of 5,9 Kbp.

Finally, the cDNA encoding the chimeric protein, Cx43-EGFP, was verified by sequencing, which confirmed that EGFP cDNA was cloned in frame with Cx43 cDNA (data not shown).

4.9.2. Immunodetection of Cx43-EGFP in transfected cells

HaCaT cells and SCL-1 tumor cells were transiently transfected by FuGENE6 transfection reagent with Cx43-EGFP. Furthermore, transfection of HeLa cells with Cx43-EGFP construct was used as control for overexpression and functional trafficking of Cx43 to the cell membrane (Fig. 22).

To confirm the overexpression of Cx43-EGFP fusion protein, Western blot analysis was performed (Fig. 23), using polyclonal antibodies raised against the C-terminus of Cx43 as well against a peptide corresponding to amino acids 3-17 of the Green Fluorescent Protein (GFP) from jellyfish *Aequorea Victoria*.

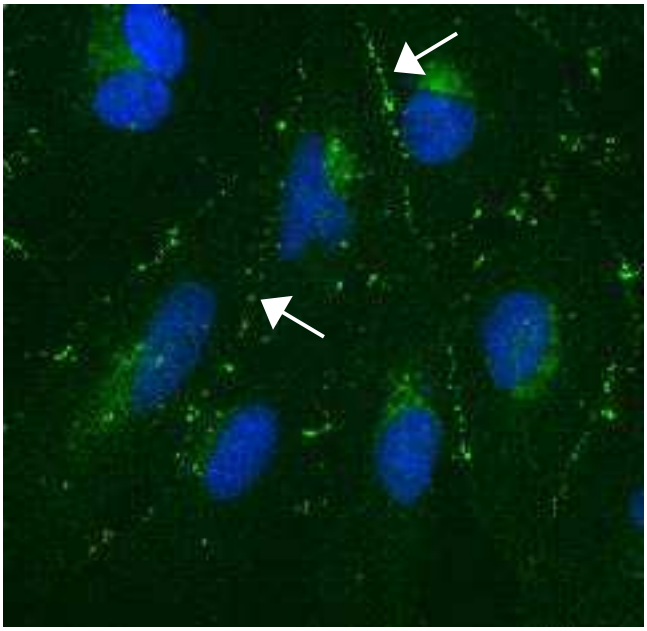

Fig. 22. Subcellular distribution of Cx43 in monolayer cultures of HeLa cells

HeLa cells were immunostained for Cx43. Green epifluorescence represents Cx43 protein. The arrows indicate presence of protein in the membrane. The blue staining (DAPI) reflects labeled nuclei.

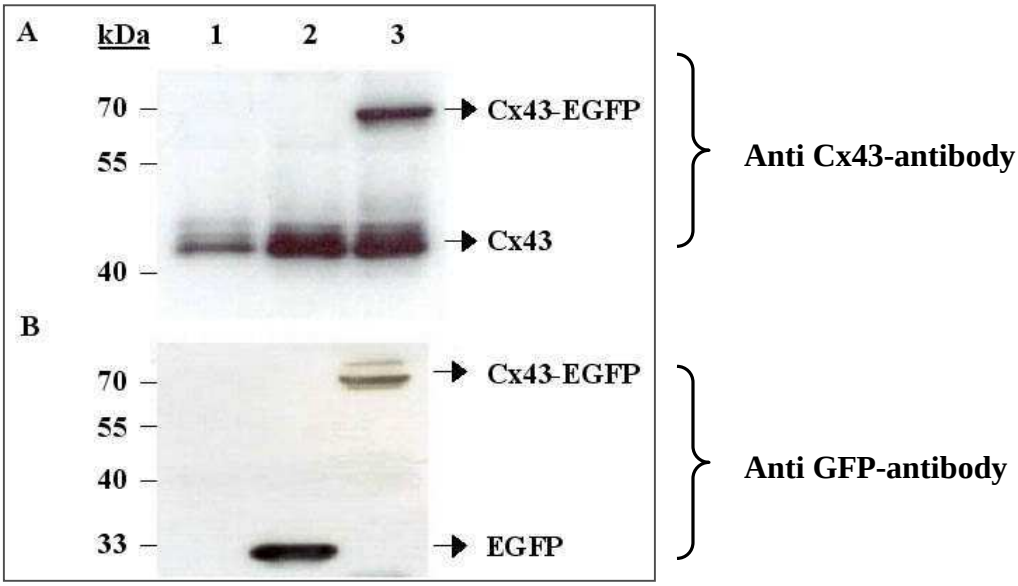

Fig. 23. Expression of Cx43-EGFP fusion protein in HeLa cells

Western blot analysis of cellular lysates from non-transfected HeLa cells (lane 1 in images A and B), HeLa cells transfected with wild type pEGFP-N1 vector (lane 2 in images A and B) and cellular lysates from HeLa cells that transiently express Cx43-EGFP (lane 3 in images A and B). Polyclonal anti-Cx43 antibody (image A) or polyclonal anti-GFP antibody (image B) was used. Experiments were performed in duplicates.

Lane 1 of image A of Fig. 23, demonstrates basal expression of Cx43 in HeLa cells, showing a three band pattern (P0, P1, P2) of Cx43 phosphorylation, which is identical to the pattern in cells expressing the GFP protein alone (A, lane 2). HeLa cells transiently overexpressing Cx43-EGFP (lane 3) were detected with anti-Cx43 antibody (A) and anti-GFP (B). Analysis revealed a major protein band of the fused protein at 70 kDa (B, lane 3). In contrast, HeLa cells, transfected with wild type pEGFP-N1 vector, expressed GFP protein with a molecular weight of 26 kDa (B, lane 2). Non-transfected HeLa cells were negative for GFP (B, lane 1).

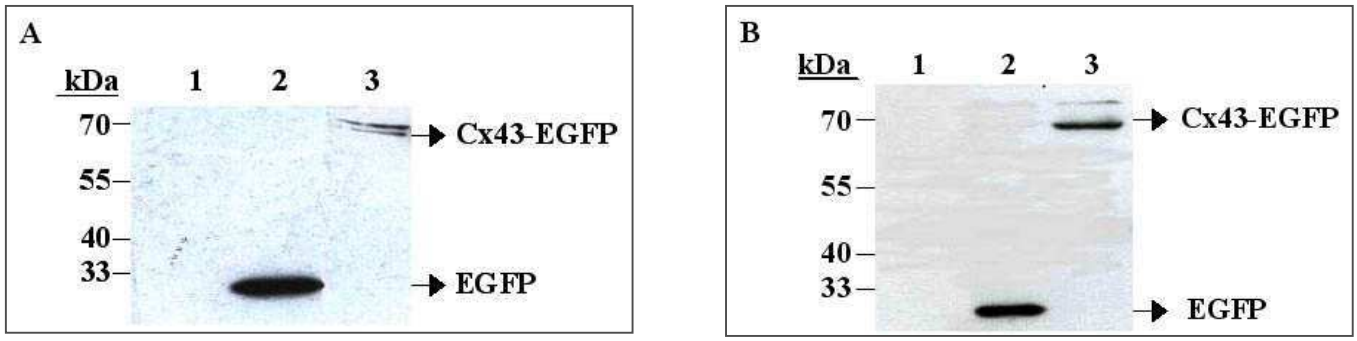

Fig. 24. Expression of Cx43-EGFP fusion protein in HaCaT (A) and SCL-1 cells (B)
Lysates from non-transfected cells (lane 1 in images A and B), cells transiently expressing GFP (lane 2 in images A and B) and cells transiently expressing Cx43-EGFP (lane 3 in images A and B) were probed with a polyclonal anti-GFP antibody in a representative immunoblot. Two independent experiments were performed.

Similar to HeLa cells, the Cx43-EGFP fusion protein in lysates from transfected HaCaT cells (Fig. 24, A) and SCL-1 tumor cells (B) was detected at 70 kDa with anti-GFP antibody (lanes 3). The cells transfected with cDNA encoding the GFP alone only display a 26 kDa band (lanes 2). Non-transfected HaCaT cells and SCL-1 tumor cells are negative for GFP (lanes 1).

The successful overexpression of tagged Cx43 made it available to detect Cx43 in tumor cells and to investigate its trafficking in living cells by fluorescence microscopy.

4.9.3. Localization of Cx43-EGFP in transfected cells

To examine whether the Cx43-EGFP chimera is properly transported to the plasma membrane and forms fluorescent cell-cell contacts, its localization was followed *in vivo* by fluorescent microscopy.

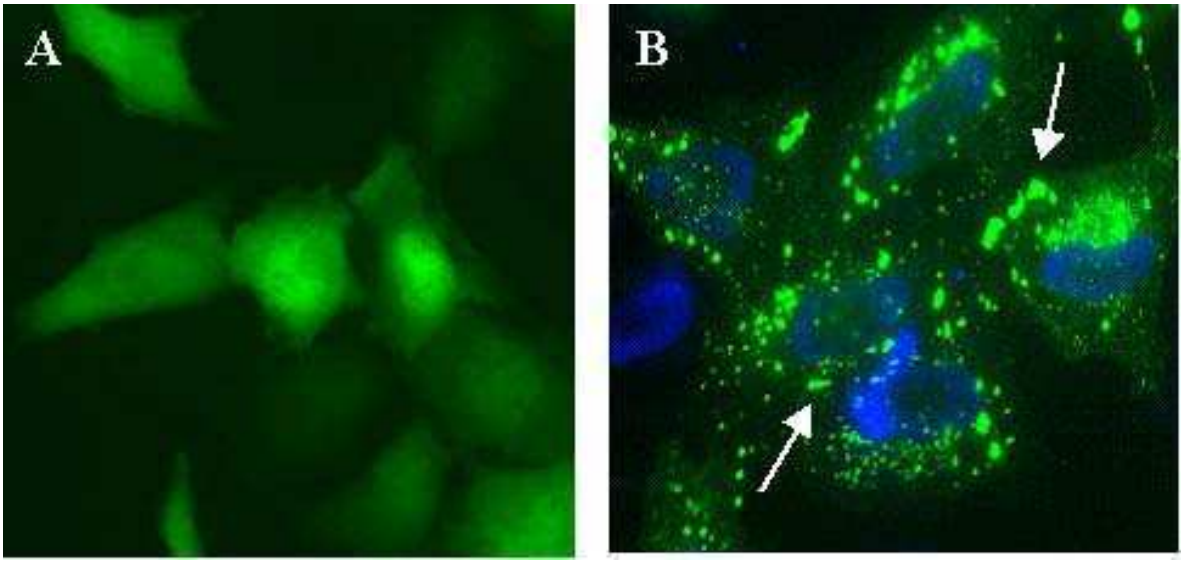

Fig. 25. Transient expression of Cx43-EGFP in HeLa cells
Imaging of living HeLa cells transiently expressing GFP alone (A) or Cx43-EGFP (B). Green dots represent Cx43-EGFP (B), while diffuse green staining represents GFP alone (A). The arrows indicate GJ plaques at the sites of cell-cell contacts. The blue staining (Hoehst) reflects labeled nuclei.

HeLa cells, transfected with Cx43-EGFP, showed strong punctual signals inside the cells and at sites of cell-cell contact, where both cells might contribute to GJ formation (Fig. 25, B). Control HeLa cells, expressing GFP alone, displayed no distinct localization pattern of this protein, as indicated by the wide spread staining of the cytoplasm and the nucleus (A). GFP alone was used as a technical control for efficient transfection procedure.

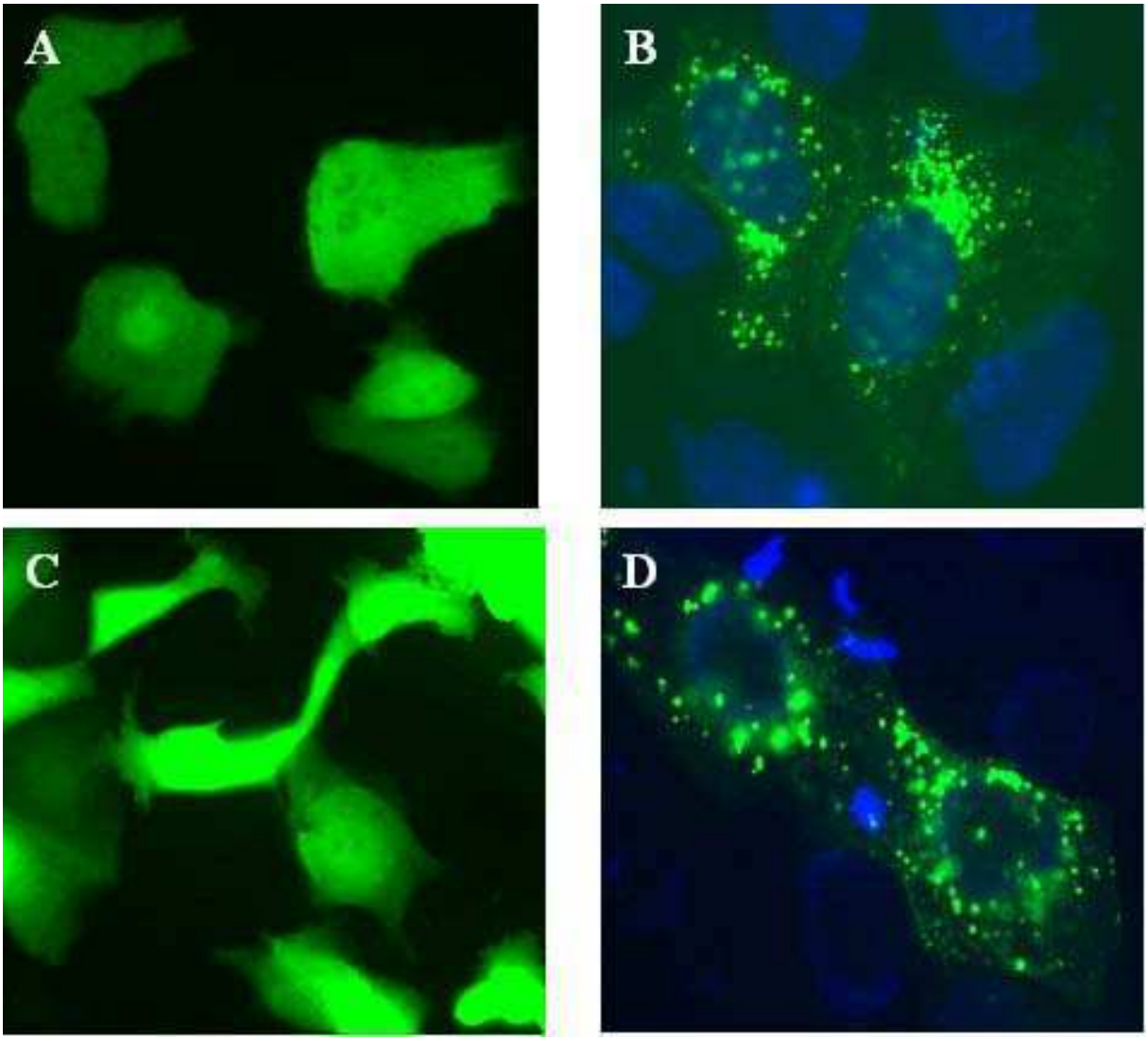

Fig. 26. Transient expression of Cx43-EGFP in living HaCaT and SCL-1 cells

A and C represent HaCaT and SCL-1 cells, transiently expressing GFP alone. HaCaT and SCL-1 cells expressing Cx43-EGFP are presented on B and D. Green dots represent Cx43-EGFP, while diffuse green staining represents GFP alone. The blue staining (Hoechst) reflects in vivo labeled nuclei.

In HaCaT cells and SCL-1 tumor cells transfected with Cx43-EGFP, live imaging showed the Cx43-EGFP chimera inside the cell, demonstrating no localization on the membrane. Adjacent HaCaT cells (Fig. 26, B), as well as SCL-1 (D) cells, show no Cx43-EGFP signal at the side of cell-cell contacts. Control cells, transfected with pEGFP vector alone, show staining throughout the cell, with no distinct pattern of localization (A, C).

Taken together, transformed keratinocyte-derived cells express normal non-mutated Cx43, which show subcellular localization around nucleus, although the trafficking machinery seems to be intact. As it was not possible to overcome the impaired transport of Cx43 towards cell membrane by overexpression of Cx43, other factors responsible for Cx43 posttranslational modifications and proper trafficking must be involved. As neither transcription nor trafficking seems to be the underlying reason for the impaired GJIC, (post)translational events on Cx43 were investigated in details below.

4.10. Cx43 phosphorylation in normal and tumor cells

Different phosphorylation states have been implicated in several stages of connexin lifecycle, such as trafficking, assembly/disassembly, and degradation. In order to increase the Cx43 expression and to 'trigger' Cx43 trafficking in HaCaT cells and SCL-1 tumor cells by modulation of the phosphorylation state of Cx43, the following approaches were applied.

4.10.1. Effect of cAMP levels on Cx43 trafficking in HaCaT cells and SCL-1 tumor cells

Agents that elevate intracellular cAMP levels have been shown to increase the amount of phosphorylated Cx43 and Cx43-mediated intercellular communication by elevated synthesis and/or increased trafficking of connexons to the cell membrane. The cyclic AMP-enhanced gap junctional assembly is mediated by protein kinase A (PKA) (Paulson et al., 2000; TenBroek et al., 2001). Forskolin is a cell-permeable diterpenoid isolated from *Coleus forskohlii*. Many of its biological effects are due to its activation of adenylyl cyclase, resulting in elevated intracellular cAMP concentrations. Therefore, forskolin was used as a model compound to investigate a possible link between cAMP-mediated changes in the phosphorylation pattern of Cx43 in HaCaT cells as well as in SCL-1 tumor cells, and its transport to the membrane.

After incubation of NHEK, HaCaT cells and SCL-1 tumor cells for 24h with forskolin, the phoshorylation status of Cx43 was analyzed. Immunoblot analysis of total cellular Cx43 demonstrated that Cx43 was efficiently phosphorylated by forskolin treatment of HaCaT, while NHEK showed higher phosphorylation. In SCL-1, no signal was seen (data not shown).

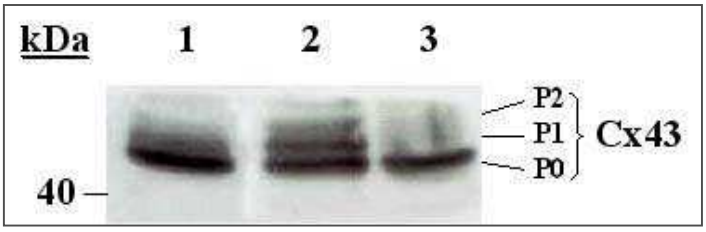

Fig. 27. Effect of forskolin on Cx43 phoshorylation pattern in NHEK
Cells were exposed to 15 µM forskolin for 24h and phosphorylation of Cx43 was analyzed by Western blotting, using polyclonal anti-Cx43 antibody. Lane 1: Cx43 phosphorylation pattern in non-treated cells; lane 2: forskolin +; lane 3: phosphatase treatment. Two independent experiments were performed.
P0, unphosphorylated form of Cx43; P1 and P2, phosphorylated Cx43

Comparing expression of Cx43 in control (non-treated) (Fig. 27, lane 1) and forskolin-treated NHEK (lane 2), a stronger Cx43 P1 (phosphorylated) band is observed, in addition to slight appearance of the Cx43 P2 form in treated cells. Dephosphorylation of proteins by phosphatase treatment demonstrated loss of phosphoforms of Cx43 protein (lane 3).

Following forskolin treatment, trafficking of Cx43 was expected to increase due to higher phosphorylation. After 24h incubation with forskolin, NHEK were fixed and Cx43 was immunochemically labeled. Localization of Cx43 was analyzed by epifluorescence. It revealed a correlation between phosphorylation and increased membrane localization of Cx43: image B on Figure 28, shows high amount of punctual staining on the membrane compared to rare membrane signals on image A.

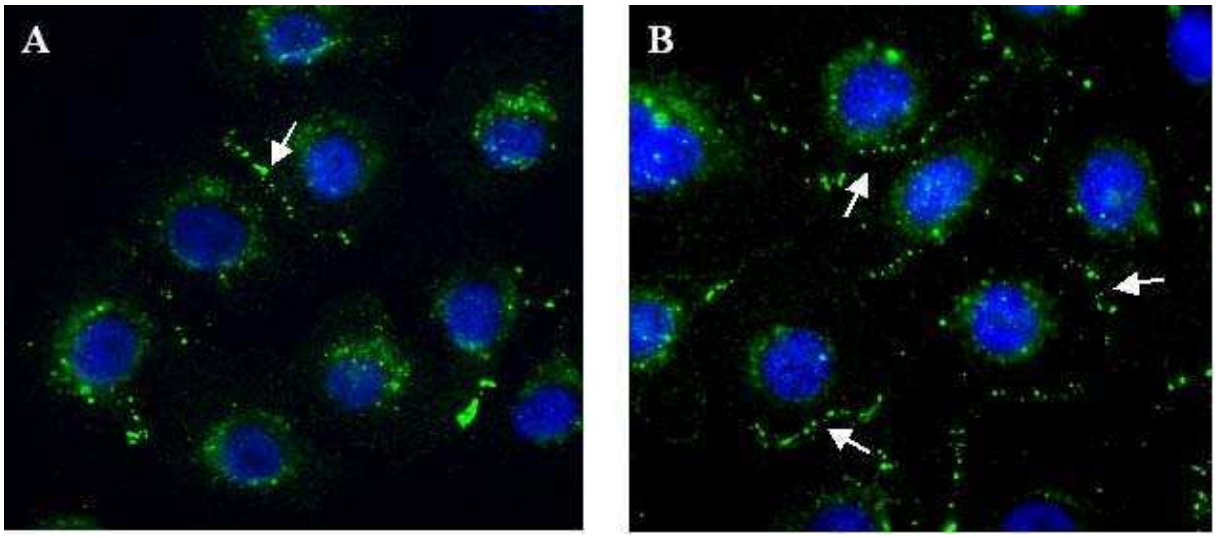

Fig. 28. Increased Cx43 trafficking in NHEK after forskolin treatment

NHEK were immunostained for Cx43 after 24h treatment with 15 µM forskolin, which results in increased membrane localization (B) compared with non-treated cells (A). Green dots represent Cx43. The arrows indicate protein on the membrane. The blue staining (DAPI) reflects labeled nuclei.

In non-treated HaCaT cells, Cx43 shows just the unphosphorylated P0 band (Fig. 29, A, lane 1), while in forskolin-treated cells there is a shift in the ratio of the different phosphorylated forms of Cx43, showing the P1 band (A, lane 2; B, lane 1). Following phosphatase treatment, this P1 co-migrates with Cx43 P0 (B, lane 2). However, in contrast to the demonstrated increase of Cx43 transport in control NHEK cells after forskolin treatment, epifluorescence did not show any change in Cx43 transport in HaCaT cells (data not shown).

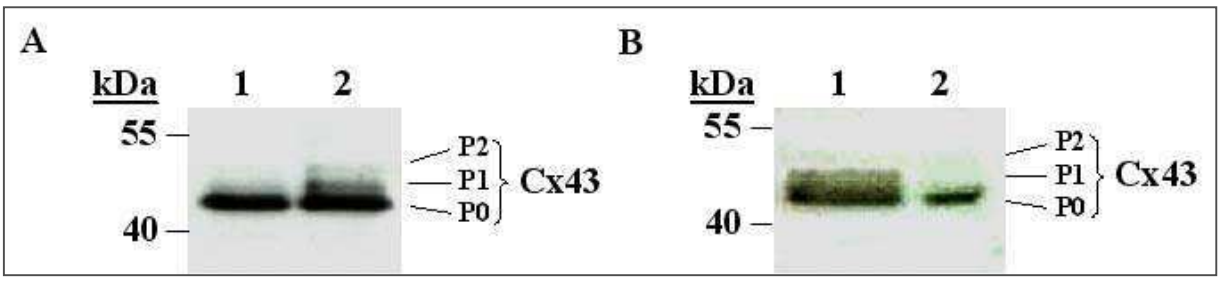

Fig. 29. Effect of forskolin on Cx43 phosphorylation pattern in HaCaT cells

After exposing HaCaT cells for 24h to 15 µM forskolin Western blot was performed. Expression of Cx43 in non-treated cells is represented in lane 1 (A), and effect of forskolin in lanes 2 (A) and 1 (B). To confirm the phosphorylated Cx43 protein, phosphatase treatment was performed (lane 3, B). Two independent experiments were performed.

P0, unphosphorylated form of Cx43; P1 and P2, phosphorylated Cx43

4.10.2. Effect of phosphatase inhibitor *okadaic acid* on Cx43 phosphorylation

Phosphatases could be involved in the trafficking, assembly/disassembly and degradation of connexins by modulation of their phosphorylation status. A co-localization of Cx43 with protein phosphatase type 1 and type 2A (PP1 and PP2A) was demonstrated in cells with markedly reduced GJIC. Inhibition of phosphatases with the specific inhibitor okadaic acid (OA) improved cell coupling (Ai and Pogwizd, 2005).

Herein, NHEK, HaCaT cells, and SCL-1 tumor cells were incubated for 6h with OA, prior to assessing the Cx43 phosphorylation pattern by immunoblotting.

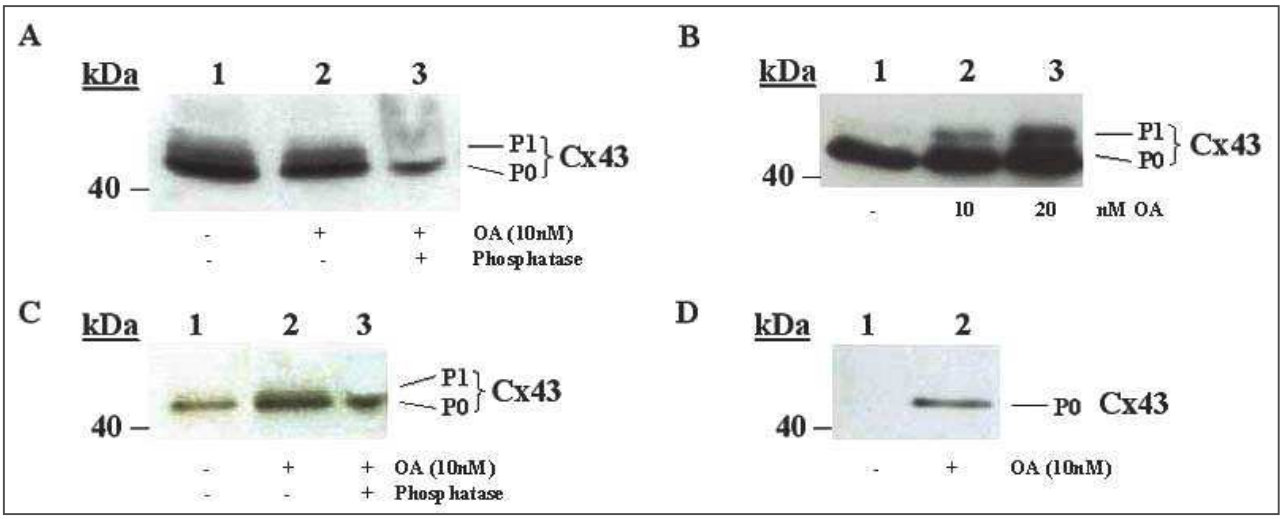

Fig. 30. Effect of okadaic acid (OA) on Cx43 phoshorylation in different cell types

NHEK (A), HaCaT cells (B, C) and SCL-1 tumor cells (D) were exposed for 6h to okadaic acid. Western blot analysis was performed, using polyclonal anti-Cx43 antibody. Pattern of Cx43 expression in non-treated cells (lanes 1). Pattern of Cx43 expression after treatment with OA (lanes 2). Phosphorylation of Cx43 was confirmed by phosphatase treatment (lanes 3 in A and C); lane 3B represents concentration-dependence in HaCaT cells. Two independent experiments were performed. P0, unphosphorylated form of Cx43; P1 and P2, phosphorylated Cx43

Lysates from untreated NHEK (Fig. 30, A, lane 1) and treated with 10 nM of OA (lane 2) show no significant difference in phosphorylation pattern of Cx43 expression. Following phosphatase treatment, the upper P1 band disappears and co-migrates with Cx43 P0 (lane 3). In HaCaT cells treated with 10 nM of OA (lanes 2 in B, C), a clear shift to P1 band of Cx43 is observed which is enhanced with a concentration of

20 nM OA (B, lane 3) compared to non-treated cells (lanes 1 in B, C). Dephosphorylation leads to the loss of P1 form (C, lane 3).
In SCL-1 cells, P0 band of Cx43 appeared after treatment with 10 nM of OA (D, lane 2), while untreated cells show no detectable expression (lane 1). It can be concluded from this observation that the protein is expressed, but it is not phosphorylated.
However, immunocytochemical labeling of Cx43 and analysis by fluorescent microscopy showed no change in transport of Cx43 to the cell membrane, neither in treated NHEK nor in HaCaT cells or SCL-1 tumor cells (data not shown). In addition, microinjection of Lucifer Yellow dye in treated HaCaT and SCL-1 single cells, revealed no change in GJIC (data not shown).

4.11. Inhibition of ERAD by *Epoxomicin* and its effect on Cx43 phoshorylation

Connexin turnover is demonstrated to be a target for up-regulation of intercellular communication. As misfolded proteins do not pass checkpoint control in ER, they are directed for ER associated degradation (ERAD) via proteasomes (Vanslyke and Musil 2003). As previous experiments revealed incomplete phosphorylation of Cx43 in HaCaT and SCL-1 cells, these proteins might be targeted for ERAD. In order to stabilize Cx43 for further transport to the membrane, proteasomal activity was inhibited by epoxomicin.
Epoxomicin is an irreversible proteasome inhibitor isolated from *Actinomycetes* species. It covalently binds to catalytic ß-subunits of the proteasome, inhibiting primarily chymotrypsin-like, but also trypsin-like activities of the proteasome.
In order to determine whether a lowered rate of Cx43 degradation could influence gap junction assembly and/or function, incubation with epoxomicin for 6h was assayed. Western blots were performed in order to investigate the change in Cx43 amount and/or its phosphorylation status.

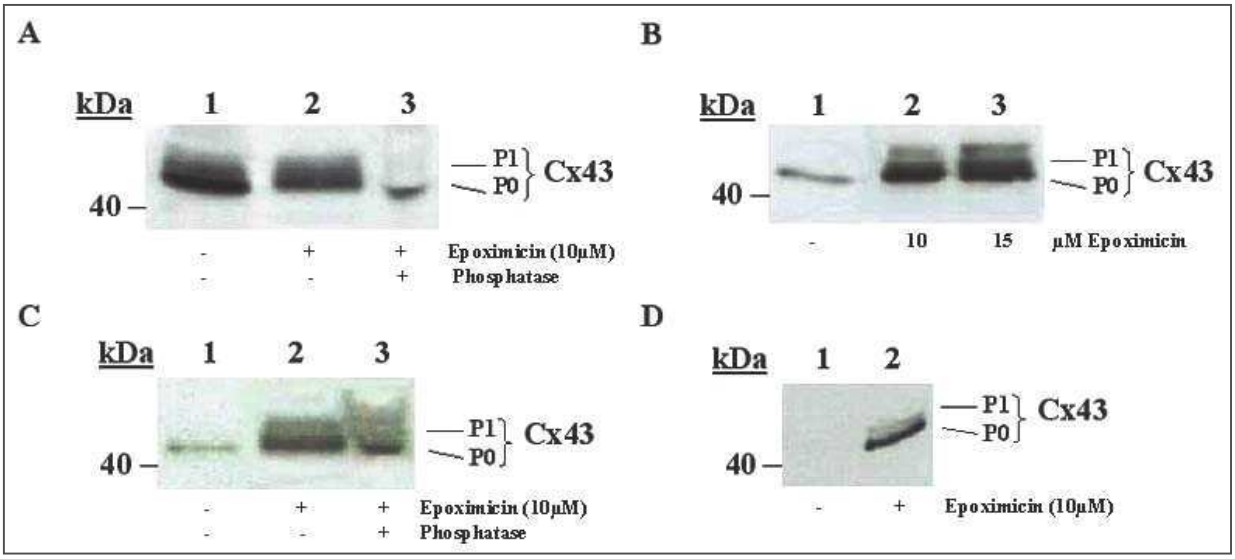

Fig. 31. Effect of epoxomicin on Cx43 turnover and phosphorylation

Immunodetection of Cx43 in NHEK (A), HaCaT (B, C) and SCL-1 (D) cells was performed using polyclonal anti-Cx43 antibody. Lanes 1 represents Cx43 expression pattern in non-treated cells. Epoxomicin effect on Cx43 expression is shown in lane 2 and phosphatase treatment was performed to confirm Cx43 phosphorylation (lanes 3 in A and C). Lane 3B represents concentration-dependence in HaCaT cells. Two independent experiments were performed.

P0, unphosphorylated form of Cx43; P1 and P2, phosphorylated Cx43

The Cx43 turnover was slightly decreased in NHEK cells treated with 10 µM of epoxomicin, as demonstrated by the higher amount of Cx43, detected as diffused band (Fig. 31, A, lane 2). This band is probably composed of a mixed 'population' of correctly and non-correctly modified Cx43 forms, representing different pre-phosphoforms of Cx43. Upon dephosphorylation with phosphatase the bands co-migrate as a discrete P0 band (A, lane 3).

In HaCaT cells and SCL-1 tumor cells, epoxomicin induced a shift to Cx43 P1 band (lanes 2 in B, D). The shift is even stronger when HaCaT cells were incubated with 15 µM of epoxomicin (lane 3 in B). This specific change in phosphorylation pattern was confirmed by dephosphorylation of the Cx43 protein (lane 3 in C).

Again, immunochemical labeling of Cx43 in HaCaT and SCL-1 cells did not show transport of Cx43 to the cell membrane (data not shown).

In HaCaT and SCL-1 cells, decrease of Cx43 turnover by inhibition of proteasomal degradation indicates changes in both protein amount and phosphorylation pattern of Cx43. In order to assess the possibility that the activity of the proteasomes is higher in these cells compared with the normal counterparts, measuring of the proteasomal

activity was performed. Cell lysates were co-incubated *in vitro* with fluorogenic precursor Suc-LLVY-AMC, which is a substrate for proteasome-dependent degradation and fluoresces after cleavege. Suc-LLVY-AMC is specifically cleaved by the rate-limiting chymotrypsin-like activity of the 20S proteasome (Rock et al., 1994). The increase of fluorescence, which can be measured with a spectrofluorometer, is proportional to enzymatic activity.

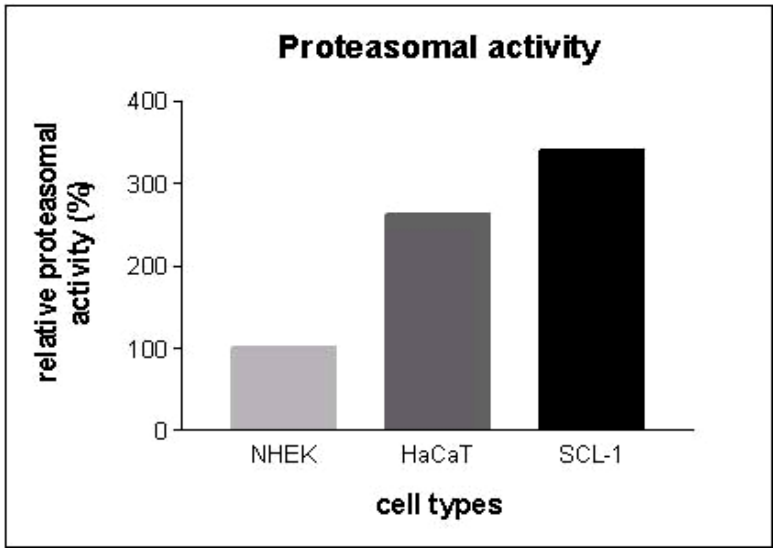

Fig. 32. Relative proteasomal activity
Increase of fluorescence measured after incubation of fluorogenic substrate with cell lysates; proteasomal activity in HaCaT and SCL-1 was calculated according to activity in NHEK, which was sat at 100%. Experiments were performed in duplicates.

Increase in fluorescence intensity in HaCaT and SCL-1 cell lysates was detected and compared to the lysate of normal keratinocytes (Fig. 32). This activity could be blocked almost completely by addition of proteasome-specific inhibitor lactacystin (data not shown).

5. Discussion

All cancers have been generally viewed as the result of a disruption of the homeostatic regulation of a cell's ability to respond appropriately to extracellular signals. Among these signals there are some, which trigger intracellular signalling and modulate gap junctional intercellular communication between the cells within a tissue. Normal homeostatic control of these three forms of cell communication (extracellular, intercellular and intracellular) determines whether the cell remains quiescent (G0), enters cell cycle, induces differentiation or starts apoptosis. During the evolutionary transition from a single cell to a multicellular organism, new genes accompanied new cellular functions, such as of cell proliferation and differentiation. Of these genes, the conexin codes for a membrane associated protein channels, the gap junctions, which allowed the passive transfer of ions and small molecular weight molecules between neighboring cells.

Most normal cells within solid tissues show functional gap junctional intercellular communication (GJIC). On the other hand, cancer cells of solid tissues have either dysfunctional homologous or heterologous GJIC (Klaunig et al., 1991; Carruba et al., 2002; Yamasaki et al., 1999). Therefore, among the many differences between a cancer cell and its normal parental cell, the carcinogenic process involves the transition from a GJIC-competent cell to GJIC-deficient cell (Trosko and Ruch, 1998).

Some characteristics are associated with all cancers (Borek et al., 1966; Abercrombie, 1979; Markert, 1968; Pierce, 1974; Potter, 1978; Fialkow, 1979; Greaves, 1986; Nowell, 1976; Till, 1982; Trosko et al., 1990, 1994). Overall, cancer is a disease of abnormal homeostasis mediated by defects in intra-, extra-, and intercellular forms of communication that disrupt the delicate balances between cellular proliferation, differentiation and apoptosis (Trosko and Ruch, 1998).

The size and number of gap junctions, the expression of connexin, and cell-cell coupling (GJIC) was studied in many neoplastic cells applying ultrastructural, biochemical, and immunological approaches and by introduction of fluorescent or radioactive tracers. The vast majority of neoplastic cells have fewer and smaller gap junctions, express less connexins, and have reduced GJIC compared to their non-

neoplastic counterparts (Loewenstein, 1981; Cesen-Cummings et al., 1998; Yamasaki, 1990).

In this study, the question for the molecular mechanisms underlying downregulation of GJIC in a squamous tumor cell line of human skin was addressed.
First, the communication level in tumor cells was examined and compared with normal dermal fibroblasts (HDF) and normal human epidermal keratinocytes (NHEK). Thereafter, transcription and translation of Cx43, the major connexin in skin cells was studied, followed by studies on the involvement proteins participating in gap junction assembly and transport. Finally, interesting results from overexpression experiments focused the investigations on posttranslational events.

As described earlier (Guo et al., 1992; Brissete et al., 1994; Stuhlmann et al., 2004), dermal fibroblasts as well as epidermal keratinocytes showed high level of communication. By contrast, the homologous GJIC in the immortalized keratinocyte cell line HaCaT and in the squamous cell line SCL-1, was completely abrogated. These results are in accordance with the hypothesis that the connexin protein appears to act as tumor suppressor, meaning that decoupling is associated with tumor progression (Mesnil, 2002). There are evidences suggesting that loss of GJIC correlates with the metastatic potential, as it was shown in rat mammary adenocarcinoma cells, human lung carcinoma and breast cancer (Zhang et al., 1998; Saunders et al., 2001).

Many growth inhibitors and anticancer agents increase connexin expression and GJIC in target cells (Ruch, 1994). Retinoids, carotenoids, green tea extract, certain flavonoids, dexamethasone, and cyclic AMP analogues and agonists inhibit neoplastic transformation and/or tumor cell growth and can block neoplastic transformation in some tissues. These agents also increase connexin expression and gap junction formation in target tissues (Ren et al., 1994; Rogers et al., 1990; Mehta et al., 1989; Zhang et al., 1992) or block the inhibitory effects of tumor promoters on GJIC (Ruch et al., 1989; Sigler et al., 1993; Chaumontet et al., 1994).

Carotenoids stimulate GJIC, by up-regulated expression of connexin in normal and preneoplastic cells (Bertram et al., 1995; Stahl et al., 1997). Incubation of primary human fibroblasts with the carotenoid canthaxanthin, resulted in a significant

increase in GJIC in contrast to HaCaT and SCL-1 cells, which did not reveal any change in communication. The molecular mechanism for up-regulation of GJIC in fibroblasts is still to be elucidated, suggesting a role of certain biologically active metabolites of carotenoids or RA receptor-dependent pathways, to be involved in increase of GJIC (Daubrawa et al., 2005). At present, treatment of preneoplastic cells, like oral leukoplakias, with carotenoids, showed up-regulation of Cx43 expression and GJIC, and consequently, delayed progression to malignancy (Garewal et al., 1995). Herein, the neoplastically transformed SCL-1 cells were unaffected by the carotenoid.

Interaction of tumor cells with the surrounding stroma, is of crucial importance for tumor survival, invasion and metastasis. Among the autocrine and paracrine acting factors involved in molecular processes of tumor–stroma interaction, transforming growth factor-ß1 (TGF-ß1), a 25 kDa homodimeric protein, plays a pivotal role. The bioactive TGF-ß1 results from dissociation of the latent inactive TGF-ß complex consisting of the non-covalently bound latency associated peptide (LAP) dimer to the active TGF-ß1 dimer which are secreted as LAP/TGF-ß1 complex by epithelial and mesenchymal cells (Govinden et al., 2003; Piek et al., 1999).

Recently, it was described (Stuhlmann et al., 2003; 2004) that the squamous cell carcinoma line SCL-1 significantly downregulates homologous GJIC of dermal fibroblasts by the effect of tumor-derived transforming growth factor TGF-ß1, emphazising the importance of cellular comunication processes. HaCaT and SCL-1 cells released a much higher amount of total and active TGF-ß1, compared to dermal fibroblasts and epidermal keratinocytes. This high amount of active TGF-b1 of tumor cells is responsible for downregulation of homologous GJIC of fibroblasts (Stuhlmann et al., 2004).

The effects of TGF-ß1 may be directed not only towards surrounding stromal cells, but also in autocrine manner (Liu et al., 2004).Therefore, a possible autocrine loop in the SCL-1 cells leading to impaired communication was checked. Treatment of HaCaT and SCL-1 cells with neutralizing TGF-ß1 antibody in order to improve GJIC of tumor cells, excluded autocrine effect of TGF-ß1 to be responsible for the impairment of GJIC. More possible, tumor-derived TGF-ß1 has a higher influence on

promoting invasion via interaction with stromal cells or on epithelial mesenchymal transition (EMT), as described elsewhere (De Wever et al., 2003).

The lack of GJIC among cancer cells is the consequence of either lack of expression or an aberrant localization of the connexin proteins. The lack of expression is often the consequence of a lack of transcription, which may be due to hypermethylation of the connexin (Yano et al., 2004; Hirai et al., 2003). In basal cell carcinoma and squamous cell carcinoma of human skin, the loss of GJIC is due to decreased expression of Cx43 and Cx26, or impossibility of translocation of connexons to the plasma membrane, as it has been shown in mouse skin carcinogenesis model (Tada et al., 1997). In this study, RT-PCR, Western blot analysis and immunostaining, indicated that the decrease in homologous GJIC of HaCaT and SCL-1 cells is not only due to down-regulation of Cx43 expression and changes in the phosphorylation state of Cx43 compared to normal cells, but rather due to the aberrant localization of Cx43 in the cytoplasm (Mesnil, 2002; Yamasaki et al., 1995).

While SCL-1 is a malignant cell line, HaCaT is an immortalized keratinocyte cell line, with no-tumorigenic potential (Boukamp, 2005). Lower Cx43 mRNA level and low amount of Cx43 protein in SCL-1 cells, compared to HaCaT cells, is presumed to be related with the higher metastatic potential of SCL-1 cells. Similar, Cx43 mRNA was not detected in a highly metastatic human lung carcinoma cell line (Zhang et al., 1998). This is also in accordance with similar observations in mouse skin, in which the decrease of Cx26 and Cx43 expression is related to the progression stages of the tumors (Kamibayashi et al., 1995). In addition, correlation was reported between the decrease of GJIC capacity and the progression of skin cancer (Klann et al., 1989; Budunova et al., 1996).

Even though it is not documented yet, a reason for the loss of GJIC and intracellular localization of connexin in tumor cells may be mutations in connexin genes. The only mutations in Cx43 gene, associated with cancer, are found in human colon sporadic adenocarcinomas and the expression of mutated Cx43 was restricted to the invasive structures of the tumors (Dubina et al., 2002). Mutations are reported on serine residues in the C-terminus of Cx43, which are associated with viscero-atrial heterotaxia, a severe heart malformation (Dasgupta et al., 2001). In the herein tested

squamous cell line SCL-1, a point mutation was found, leading to Valine-Alanine transition in the protein sequence. Considering biochemical properties of those amino acids, it is not to be assumed that this change has influence on Cx43 folding or its transport to the membrane as the loss of an aliphatic group has no influence on the structure of the resulting protein.

There are evidences for dominant negative effects of some connexins on gap junctional communication mediated by Cx43. In some seminoma tumors, expression of Cx33 is leading to Cx43 sequestration and down-regulation of Cx43 gap junctional coupling, by an interaction of Cx33 and the P0 form of Cx43 (Fiorini et al., 2004). Also, in certain skin disorders, associated with hearing impairment, some dominant Cx26 mutants, lowered wtCx26-mediated gap junctional communication (Rouan et al., 2001). Therefore, based on these data, we asked for a similar inhibiting effect of Cx43 pseudogene on Cx43 intracellular localization. For Cx43 a pseudogene was described (Willecke et al., 1990) which was shown to be transcribed in breast tumor cells, but not in normal cells (Kandouz et al., 2004). Recently, it was reported that a pseudogene could regulate the expression of its functional gene (Hirotsune et al., 2003), potentially acting through an antisense mechanism (Korneev et al., 1999). In the studied cells the ΨCx43 m RNA level was identical which excludes the possibility of a dominant-negative effect of that transcript or the pseudoprotein on wtCx43 translation or assembly into functional GJ. However, further investigations are necessary to elucidate association of Cx43 pseudogene with tumorigenesis.

Aberrant localization of the connexins in the cytoplasm was also suggested to be due to impairment of cell-cell recognition (Yamasaki et al., 1999). E-cadherin, a component of adherens junctions and the major transmembrane protein involved in the cell-cell recognition process of epithelial cells, often exhibits decreased expression and/or aberrant localization in carcinomas. Loss of E-cadherin expression was found in pancreatic cancer cells and is correlated with higher invasiveness (Pignatelli et *al*, 1994). On the other hand, transfection of E-cadherin cDNA into transformed invasive cells reversed the invasive phenotype (Frixen at al., 1991). Cadherin-deficient cell lines showed diminished gap junctional communication, which was up regulated by transfection of the appropriate cell adhesion molecules (Mége et al., 1988). It was also postulated that E-cadherin permits a correct addressing of

connexin to the cell membrane (Jongen et al., 1991). In addition, E-cadherin function is affected by mutations, hypermethylation (Nishimura et al., 2003) or by changes in expression and function of proteins involved in the cadherin-mediated signalling complex such as catenins and plakoglobin (Fukunaga et al., 2005).

Furthermore, E-cadherin expression was reduced in tissue sections from the epidermis with severe solar elastosis (Lyakhovitsky et al., 2004). Based on these data E-cadherin was examined and compared in normal keratinocytes, immortalized HaCaT line, and SCL-1 tumor cells.

HaCaT and SCL-1 cells showed significant E-cadherin expression and presence on the membrane. In HaCaT, higher expression of E-cadherin is to be expected, while those cells are not tumorigenic, although they lack GJIC. However, the presence of E-cadherin on the membrane of SCL-1 cells does not fit to the aggressive phenotype. In conclusion, HaCaT and SCL-1 cells, show E-cadherin expression, even though this expression is normally described to be prerequisite for GJIC.

Gain of expression of N-cadherin, another cell adhesion molecule, in tumor cells, is described to be associated with an increased invasive potential. Even if cells continue to express E-cadherin, the effect of expressed N-cadherin is dominant in promoting metastasis. This was demonstrated in MCF-7 breast cancer cell line, in which N-cadherin expression stimulated increase in cell migration, invasive capacity and MMP-9 production (Hazan et al., 2000). In addition, siRNA studies, showed that correct gap junction formation, requires intracellular coassembly with N-cadherin (Wei et al., 2004). As normal keratinocytes do not express N-cadherin, neither in low nor in high calcium conditions, but do transport Cx43 to the membrane and exhibit GJIC, it could be assumed that the coassembly is not necessary in those cells. However, HaCaT and SCL-1 cells do express N-cadherin, which is localized - in contrast to Cx43 - on the membrane. This rather reflects an increase in their invasive potential, as described earlier, for stromal and endothelial cells, which increased migration correlates with N-cadherin expression. Here, the expression of N-cadherin in HaCaT and SCL-1 cells is not related to transport of assembled connexons to the membrane.

Although there is no obvious connection between ß-catenin and lack of GJIC in tumor cells, the role of ß-catenin in tumor invasion, is interesting. In different human cancer cell lines, mutations or phosphorylation of catenin proteins have been associated with disruption of the cadherin-catenin complex (Behrens, 1993; Oyama et al., 1994). In addition to its well-defined role in regulating cell-cell adhesion via interactions with E-cadherin and other cadherins, ß-catenin has a critical role in the highly conserved Wnt signaling pathway (Cadigan et al., 1997). Cx43 was identified as a functional target for Wnt signaling (Van der Heyden et al., 1998). It was demonstrated that stable overexpression of Wnt-1, increases mRNA and protein level of Cx43 and enhances GJIC. Wnt exerts some of its downstream effects via ß-catenin-dependent regulation of transcription. A cytoplasmic localization of ß-catenin is the prerequisite. HaCaT and SCL-1 cells show expression of ß-catenin, which is present adjacent to the membrane. No free intracellular pool is demonstrated, therefore dealing rather with its role as adhesion molecule, and not to be involved in direct regulation of the Cx43 mRNA level.

The ß-catenin pool that functions in Wnt signaling is regulated in part by a multiprotein complex, consisting of the adenomatous polyposis coli (APC) tumor suppressor, AXIN, and glycogen synthase kinase 3ß (GSK3ß) proteins (Zhai et al., 2002). In the absence of Wnt signals, ß-catenin is bound by APC and then phosphorylated by GSK3ß, recognized and ubiquitinated by a multiprotein complex and degraded by the proteasome. Wnt ligands, after their binding to a Frizzled-LRP transmembrane receptor complex, activate a pathway that inhibits GSK3ß activity, with resultant stabilization of ß-catenin. Stabilization of ß-catenin leads, in turn, to its enhanced interaction with members of the T-cell factor (TCF) family of transcription factors.

Therefore, deregulation of ß-catenin leads to constitutive formation of ß-catenin-TCF complexes and altered expression of TCF-regulated target genes. The proteins encoded by these TCF-regulated genes presumably play important roles in effecting neoplastic transformation. Proposed ß-catenin/TCF target genes in cancer cells include well-established oncogenes, such as c-*myc* and *CCND1* (*Cyclin D1*), as well as *MMP-7* (*matrix metalloproteinase 7/matrilysin*), *PPAR*-δ (*peroxisome proliferator-activated receptor delta*), *CX43* (*connexin 43*), and *gastrin* genes (Zhai et al., 2002).

As the studied adhesion molecules, which normally are linked to correct gap junction formation, were found in GJIC-deficient HaCaT and SCL-1 cells, other mechanisms seem to be responsible for the intracellular localization of Cx43.

Subcellular fractionation, immunoprecipitation and immuno-localization with antibodies directed against organelle marker proteins demonstrated that Cx polypeptides follow the general intracellular transport route, referred to as the secretory pathway (Rothman et al., 1996; Pfeffer et al., 1987). Multicolour time-lapse microscopy studies on the delivery of connexons assembled from GFP-tagged Cx43 in transfected HeLa cells showed that connexons travel in vesicles along microtubules from the Golgi to the plasma membrane (Lauf et al., 2002). It was already shown that Cx43 interacts directly with microtubules via its C-terminal tail, as demonstrated in rat liver epithelial T51B cells, human fibroblasts, MDCK, COS7, A431 and HEK293 cells (Giepmans et al., 2001). In order to examine disrupted microtubules to be responsible for impaired transport of Cx43 to the membrane, cells were stained for α-tubulin, a subunit of functional microtubules. HaCaT and SCL-1 cells showed similar to identical organization of α-tubulin, as the normal control keratinocytes. Its distribution throughout the cell indicates no disruption in polymerization of tubulin. Therefore, intact microtubules are not necessary for the regulation of Cx43 transport and GJIC. This might be in accordance with similar observation in Rat-1 cells, in which treatment of the cells with the microtubule-disrupting agent nocodazol, did not significantly alter functional cell-cell coupling (Giepmans et al., 2001). On the other hand, Cx26 and some other connexins can also traffic in a microtubule-independent way (Martin et al., 2001). Membranes of the rough ER can be located very close to the plasma membrane and therefore, connexons assembled in ER might go directly to PM. This observation might explain the delivery of connexons even when microtubules and Golgi membranes have been disrupted.

There are also some indications that intact actin filaments could be involved in delivery of connexins to the membrane, as showed for Cx26 (Thomas et al., 2001). Irradiation of normal keratinocytes with UVA or treatment with TPA induced loss of direct cell-to-cell communication. This loss was partially due to translocation of Cx43 from the membrane to the cytoplasm. Both treatments induced changes in actin

cytoskeleton organization. Irradiated keratinocytes showed completely disorganized actin cytoskeleton, while TPA induced reorganization of actin in an intense and thin network at the cell borders (Provost et al., 2003).

Phalloidin labeling of actin in normal keratinocytes showed cortical actin filament (CAF) network, if the cells were maintained under low calcium conditions. Upon differentiation, when Cx43 is also intracellulary localized or even not expressed (as described in Brissette et al., 1994), actin is almost completely organized in a cortical actin filament (CAF) network and only a few cells display stress fibers. The majority of HaCaT cells show stress fibers, while SCL-1 cells show CAF. These data suggest that the actin network is not responsible for downregulation of GJIC in transformed cells.

Connexin gene expression was enhanced in malignant cell lines by transfection of connexin cDNAs (Mehta et al., 1991, Zhu et al., 1991; Eghbali et al., 1991; Naus et al., 1992; Mesnil et al., 1995; Hirschi et al., 1996; Ruch et al., 1998). In these "re-communicating" neoplastic cells, growth rates *in vitro* and/or tumor formation were highly reduced and these effects often correlated with the re-established GJIC. In some cases, the connexin-transfected cells also expressed altered levels of cell cycle regulatory proteins (Masuda et al., 1995) or more differentiated functions (Hirschi et al., 1996). In another study (Naus et al., 1992), the connexin-transfected cells secreted a soluble, peptide growth inhibitor. In order to find out more about trafficking of Cx43 to the membrane, further investigations focused on overexpression of exogenous Cx43 in tumor cells.

We engineered and expressed a Cx43-GFP chimera, which exhibited properties and characteristics of wild-type Cx43. It was demonstrated by Jordan et al. (1999), that transfection of Cx43-GFP into communication-competent normal rat kidney cells, Cx43-negative MDCK cells, communication-deficient Neuro2A cells or HeLa cells, resulted in the expression of the fused protein with the predicted size as well as transport and assembly into functional gap junction.

As control for overexpression and functional trafficking of Cx43-GFP, HeLa cells were used. This HeLa clone showed endogenous Cx43 expression and membrane localization, but very low intercellular communication. Even though, Cx43

phosphorylation pattern displays three bands, the low communication could be due to some regulatory changes in opening and closing of the gap junctional channel, process which is still not completely explained. The intact fused protein migrated as a major protein band at 70 kDa, detected using antibodies for both Cx43 and GFP protein. Moreover, the transient overexpression in HeLa cells revealed transport of Cx43-GFP to the membrane and forming of gap junctional plaques. Introduction of cDNA encoding Cx43-GFP into HaCaT and SCL-1 cells, demonstrated similar findings. The fused protein was expressed, as a 70 kDa protein band. However, in vivo imaging of transfected cells, showed no transport towards the membrane. The fused protein was retained inside both cell types. This finding is in contradiction with earlier published experimental data showing increase in GJIC by overexpression of exogenously introduced Cx (Jordan et al., 1999). That directed us to address the question of whether post-translational events on Cx43 might be involved in the impaired transport of Cx43 in HaCaT and SCL-1 cells.

Phosphorylation has been implicated in several stages of connexin lifecycle, such as trafficking, assembly/disassembly, and degradation, as well as in the gating of hemichannels or intact gap junction channels. Many of the connexins contain consensus phosphorylation sequences, recognized by protein kinases and phosphatases. In that regard, many connexins (Cx31, 32, 37, 40, 43, 45, 46, 50 and 56) can be detected as phosphoproteins by either a shift in their electrophoretic mobility or direct incorporation of ^{32}P (Lampe and Lau, 2000; Saez et al., 1998). The C-terminal region of the connexin proteins appears to be the primary target that becomes phosphorylated. No reports of phosphorylation of the N-terminal region of connexins have been presented. Cx26 is the only connexin, which is not phosphorylated (Traub et al., 1989) which may be due to the short C-terminus. As Cx26 forms functional channels, connexin phosphorylation clearly is not necessary for the formation of gap junction channels. Furthermore, truncated Cx43 mutants lacking a part of the C-terminus can nevertheless form functional channels, but they exhibit different permeability and electrophysiological properties than those formed by wild-type Cx43 (Fishman et al., 1991).

Cx43 demonstrates multiple electrophoretic isoforms when analyzed by SDS–PAGE, including a faster migrating, non-phosphorylated (P0 or NP) form, and at least two slower migrating forms, commonly termed P1 and P2. P1 and P2 bands co-migrate

with NP following alkaline phosphatase treatment, suggesting that phosphorylation is the primary covalent modification (Musil et al., 1990). Phosphoamino acid analysis indicates that the majority of the phosphorylation events occur on serine residues (Lampe et al., 1998; Musil et al., 1990; Warn-Cramer et al., 1996), although tyrosine phosphorylation was detected in the presence of activated pp60src kinase (Swenson et al, 1990). Pulse-chase studies demonstrated that Cx43 phosphorylation may occur prior to reaching the plasma membrane (Crow et al., 1990; Laird et al., 1995).

Agents that elevate intracellular cAMP have been shown to increase Cx43 phosphorylation and Cx43-mediated communication (Darrow et al., 1996), the size and number of GJs (Atkinson et al., 1995), and the assembly of new GJs (Paulson et al., 2000). Such enhancement has been shown to result from increased synthesis (Mehta et al., 1992) and/or the increased trafficking of connexons to the plasma membrane (Burghardt et al., 1995; Holm et al., 1999; Paulson et al., 2000). Cyclic AMP-enhanced GJ assembly is mediated by protein kinase A (PKA) (Paulson et al., 2000), and microinjected PKA catalytic subunit has rapid positive effects on GJ communication (Britz-Cunningham et al., 1995; Godwin et al., 1993). Serine residue at position 364 (S364) is a major phosphorylation site in cellular Cx43 and phosphorylation of this site appears to be critical for cAMP/PKA-enhanced GJ assembly (TenBroek, et al., 2001). There is significant biological interest associated with S364. S364 resides in the first of a tandem RXSSR repeat found from R362–R374. A serine to proline conversion at S364 (S364P) was first identified as a mutation in a subset of patients with visceral atrial heterotaxia, and transfected cells expressing the S364P mutant Cx43 displayed altered gap junctional properties in response to PKC or PKA activity (Britz-Cunningham et al., 1995). In addition, protein kinase A has been implicated as a positive modulator of trafficking and secretion in different systems, including renal epithelial cells (Valenti et al., 1998), pancreatic acinar cells (Delisle and Howell, 1995) and MDCK cells (Brignoni et al., 1995; Hansen and Casanova, 1994).

As increase in the cAMP concentration in the studied cells was achieved by incubation with cell-permeable forskolin. The biological effect of forskolin is due to its activation of adenylyl cyclase and the resulting increase in intracellular cAMP. Normal keratinocytes, HaCaT and SCL-1 cells were treated with forskolin, and afterwards, phosphorylation pattern and immunolocalization of Cx43, were assessed.

The elevation of intracellular cAMP changed the phosphorylation status of Cx43 in NHEK and HaCaT, as indicated by altered mobility of Cx43, while no band was detected in SCL-1 cells. However, the changes in the phosphorylation pattern did not result in an increase in GJIC of HaCaT and SCL-1 cells. Even a weak P2 band of Cx43 appeared in normal keratinocytes, while a shift from P0 to P1 was demonstrated for HaCaT cells.

Given the large number of phosphorylation sites on Cx43, a distinct role for phosphoprotein phosphatases (PP) can be assumed. In nonischemic heart failure, an increased co-localization of PP2A with Cx43 was observed, together with enhanced levels of Cx43 P0 form and low GJIC. Okadaic acid modulated Cx43 phosphorylation and significantly improved intracellular communication (Ai and Pogwizd, 2005). A transgenic mouse model with cardiac-specific expression of an active form of calcineurin (PP2B) showed reduced Cx43 expression and phosphorylation, which correlated with a reduction in redistribution of Cx43 from the intercalated disc region to the long axis of the plasma membrane (Chu et al., 2002). These data implied a role for PP2B-sensitive phosphorylation sites in Cx43 localization and stability. However, in many untreated cell types, okadaic acid had little effect on gap junctional communication (Berthoud et al., 1992; Guan et al., 1996; Husoy et al., 1993; Lau et al., 1992; Saez et al., 1993).

Treatment of normal keratinocytes with okadaic acid (OA) had almost no effect on Cx43 mobility in SDS-PAGE, while the phosphorylation pattern of HaCaT and SCL-1 cells was altered. A higher amount of the P1 band was detected in HaCaT cells, but the Cx43 protein remained intracellulary. SCL-1 cells exhibited Cx43 expression, which was detected as the unphosphorylated P0 form of Cx43. Again, an increase in GJIC was not observed.

Okadaic acid affected gap junctional communication in several cell types, which were stimulated by various agents. Okadaic acid counteracted the epidermal growth factor (EGF)-mediated downregulation of GJIC in rat liver epithelial cells (Lau et al., 1992). Likewise, okadaic acid blocked the disruption of gap junctional communication and the dephosphorylation of Cx43 stimulated by 18-glycyrrhetinic acid (Guan et al., 1996). In a similar manner, inhibitors of PP2B delayed the recovery of gap junctional

communication and the loss of highly phosphorylated forms of Cx43, which normally occurred following removal of TPA (Cruciani et al., 1999). Thus, these inhibitor studies suggest that phosphatases play a role in modulation of direct cell-to-cell communication. In this study, phosphatase inhibitor OA did not affect intercellular communication.

It is described that lowering of connexin degradation with proteasome inhibitors is associated with an increase in gap junction assembly and intercellular dye transfer in cells, inefficient in both processes under basal conditions (Musil et al., 2000).

Because connexins are integral membrane proteins, their half-lives were expected to be long (>20 h). However, many experiments have demonstrated that connexins have relatively short half-lives (1,5-4h). The short half-life of connexins was used to argue that the degree of intercellular communication between cells is regulated by changes in synthesis or degradation rates. Three pathways for their degradation have been proposed: (1) misfolded/abnormally oligomerized connexins are retrogradely translocated and degraded by the proteasome through endoplasmic reticulum-associated degradation (ERAD), (2) connexins (as monomers or oligomers) may traffic directly from an early secretory compartment to the lysosome for degradation without reaching the plasma membrane, (3) connexins within gap junction plaques are degraded by the lysosome after endocytotic internalization.

Referring to the first pathway of connexin degradation, there are evidences suggesting that 40% or more of newly synthesized wild-type connexin 43 (Cx43) and connexin 32, and up to 100% of mutant forms of Cx32, are rapidly degraded in the cell types examined even if their exit from the ER is blocked (VanSlyke et al., 2000). This ER-associated turnover is sensitive to chemical inhibitors of the proteasome, thereby characterizing connexins as substrates for ERAD. It is likely, but has not yet been definitively established, that degradation of connexins at the ER is a consequence of slow and/or inefficient folding (VanSlyke and Musil, 2003).

The investigated cells were treated with epoxomicin, potent and highly specific, irreversible inhibitor of the proteasome, which has no effect on the lysosome (Marques et al., 2004). The amount of Cx43 was significantly elevated in epoxomicin treated HaCaT and SCL-1 cells, compared with untreated control. In addition,

epoxomicin induced a shift in phosphorylation of Cx43, from P0 to phoshorylated P1 form. However, GJIC was not affected in HaCaT and SCL-1 cells by this treatment.
In accordance with those findings, the treatment of CHO cells with proteasomal inhibitors induced a dramatic increase in the amount of Cx43, but in these cells an increase in intercellular dye transfer was detected as well (Musil and VanSlyke, 2000). In the communication-deficient breast cancer line MDA-MB-231, treatment with the proteasomal inhibitor lactacystin, resulted in a marked increase in phosphorylated Cx43 and this change corresponded with an increase in “oversized” gap junction plaques (Qin et al., 2003).

In contrast, there are also observations that increased phosphorylation of Cx43 in rat liver cells with EGF (Leithe et al., 2004) or in response to TPA (Lampe, 1994), can destabilize the protein and target it for degradation, decreasing GJIC.

Although proteasome primary function is to degrade abnormal and oxidatively damaged proteins that have been flagged by the ubiquitin conjugation system, proteasomes play a central role in a broad range of cellular pathways such as apoptosis, cell cycle, cell differentiation, DNA repair and degradation of many important rate-limiting enzymes involved in metabolic pathways (Ciechanover et al., 1998; Davies, 2001; Adams, 2003). High proteasome cell level is observed in immature stages of cell differentiation and neoplastic processes (Kumatori et al., 1990; Henry et al., 1996; Bureau et al., 1997). Proteasome expression has been demonstrated in the skin (Suga et al., 1993) and its expression and activity decrease with age together with a modification in subunit composition, this being correlated with tissue accumulation of oxidatively modified and ubiquitinated proteins (Bulteau et al., 2000; Petropoulos et al., 2000). Such an accumulation of oxidatively modified proteins and impairment of proteasome function can also result from ultraviolet (UV) A and UVB irradiation of normal human keratinocytes, and this raises the question of a putative role for proteasomes in photoageing and photocarcinogenesis.

Proteasomal activity was measured in normal keratinocytes, HaCaT and SCL-1 cells, in order to find out whether its higher activity could be involved in enhanced degradation of Cx43. It was shown, that proteasomal activity in HaCaT and SCL-1 cells is 3-4x fold higher compared with normal keratinocytes. This finding

corresponds with the measurement of high proteasome amounts among patients with malignant melanoma (Stoebner et al., 2005).

6. Conclusion

The immortalized keratinocyte cell line HaCaT, as well as the tumorigenic squamous cel line SCL-1 have completely abrogated gap junctional intercellular communication. Expression of Cx43 in HaCaT and SCL-1 cells is similar, meaning that the mRNA level as well as protein amount is low.

Proteins involved in cell-cell recognition show similar to identical expression in non-tumorigenic and tumorigenic cells, as well as in the normal human epidermal keratinocytes. However, transformed cells gained expression of N-cadherin, known to be be marker for epithelial mesenchymal transition (EMT). Cytoskeletal network, having its role in the trafficking route of proteins, also seems to look intact.

Introduction of exogenous Cx43 did not overcome the impaired transport of Cx43 into the membrane, neither in HaCaT nor in SCL-1 cells.

However, further investigations brought us a step closer in understanding possible mechanisms underlying the loss of GJIC. For connexin proteins, which are posttranslationally modified by phosphorylation, the action of kinases is counteracted and balanced by protein phosphatases. This work showed that it is possible to modulate phosphorylation pattern of Cx43 in transformed cells, although this did not recover GJIC. This indicates that appropriate phosphorylation/dephosphorylation, involved in correct folding, assembly and trafficking of Cx43, is a prerequisite for functional gap junctions. In that context, inhibition of proteasomal degradation (ERAD) in transformed cells revealed changes in phosphorylation pattern of Cx43, indicating that inappropriate phosphorylation of Cx43 in transformed cells may be responsible for their GJIC impairment.

In addition, activity of proteasome was demonstrated to be significantly higher compared to normal cells.

To summarize, the interpretation of the data of this study indicates that combination of impaired expression and inappropriate phosphorylation as well as enhanced proteasomal activity in tumor cells, is responsible for the loss of homologous GJIC in these cells.

Summary

Functional gap junctions (GJ) composed of connexin subunits, are specialized contacts between cells allowing the passive transfer of ions and small molecular weight molecules, in order to coordinate cellular homeostasis.

The carcinogenic process involves the transition from a normal, junctional intercellular communication (GJIC)-competent cell to one, which is defective in GJIC. The ability of cells to form functional GJ is not only dependent on connexin gene expression, but also relies on cell-cell adhesion, GJ assembly/disassembly and connexin stability.

Gap junctions in skin cells are mainly composed of the connexin Cx43. In skin derived tumor cells, GJIC was completely abrogated. The main reason for this loss of GJIC in tumor cells was not the low expression of Cx43, but rather the intracellular localization of the protein and/or its phosphorylation status.

Several approaches were used to investigate the possible implications of sequestration of Cx43 inside the cell and of its impaired transport to the membrane. Proteins of the cell-cell recognition apparatus, cadherins and ß-catenin, displayed appropriate expression and localization as well as the proteins involved in cytoskeletal organization, tubulin and actin. This indicated that the impaired transport of Cx43 was not due to the modulation of those mechanisms, which are known to be involved in transport of connexins and forming of gap junctions. Introduction of exogenous Cx43 by transient overexpression, failed to overcome the impaired transport.

Phosphorylation has been implicated in several stages of connexin life cycle, such as trafficking, assembly/disassembly, and degradation, as well as in the gating of hemichannels or intact gap junction channels.

Modulation of the activity of protein kinase A, a kinase known to be involved in enhanced transport of Cx43, exhibited changes in the phosphorylation pattern of Cx43 in tumor cells, but neither the transport of the protein nor GJIC increased. Similarly, modulation of phosphatase activity did not influence Cx43 transport and GJIC.

Endoplasmatic reticulum associated degradation (ERAD) via proteasomes was investigated in context of inappropriate Cx43 phosphorylation. Inhibition of proteasomal degradation resulted in higher amounts of Cx43 and the appearance of

different phosphorylation states in HaCaT and SCL-1 cells. However, the transport to the membrane, as well as GJIC did not increase.

Taken together, a combination of impaired expression and inappropriate phosphorylation of Cx43, together with enhanced proteasomal activity, seem to be the reason for loss of homologous and heterologous GJIC in tumor cells.

References

Introduction

Alessandro R, Kohn EC.
Signal transduction targets in invasion.
Clin Exp Metastasis. 2002;19(3):265-73.]

Barker RJ, Price RL, Gourdie RG.
Increased association of ZO-1 with connexin43 during remodeling of cardiac gap junctions.
Circ Res. 2002 Feb 22;90(3):317-24.

Barker RJ, Price RL, Gourdie RG.
Increased co-localization of connexin43 and ZO-1 in dissociated adult myocytes.
Cell Commun Adhes. 2001;8(4-6):205-8.

Bennett MV, Contreras JE, Bukauskas FF, Saez JC.
New roles for astrocytes: gap junction hemichannels have something to communicate.
Trends Neurosci. 2003 Nov;26(11):610-7.

Bergoffen J, Scherer SS, Wang S, Scott MO, Bone LJ, Paul DL, Chen K, Lensch MW, Chance PF, Fischbeck KH.
Connexin mutations in X-linked Charcot-Marie-Tooth disease.
Science. 1993 Dec 24;262(5142):2039-42.

Bernstein SC, Lim KK, Brodland DG, Heidelberg KA.
The many faces of squamous cell carcinoma.
Dermatol Surg. 1996 Mar;22(3):243-54.

Boukamp P.
UV-induced skin cancer: similarities--variations.
J Dtsch Dermatol Ges. 2005 Jul;3(7):493-503.

Brash DE, Ziegler A, Jonason AS, Simon JA, Kunala S, Leffell DJ.
Sunlight and sunburn in human skin cancer: p53, apoptosis, and tumor promotion.
J Investig Dermatol Symp Proc. 1996 Apr;1(2):136-42.

Brenneisen P, Sies H, Scharffetter-Kochanek K.
Ultraviolet-B irradiation and matrix metalloproteinases: from induction via signaling to initial events.
Ann N Y Acad Sci. 2002 Nov;973:31-43

Bruzzone R, White TW, Paul DL.
Connections with connexins: the molecular basis of direct intercellular signaling.
Eur J Biochem. 1996 May 15;238(1):1-27.

Budunova IV, Williams GM.
Cell culture assays for chemicals with tumor-promoting or tumor-inhibiting activity based on the modulation of intercellular communication.
Cell Biol Toxicol. 1994 Apr;10(2):71-116.

Budunova IV, Mittelman LA, Miloszewska J.
Role of protein kinase C in the regulation of gap junctional communication.
Teratog Carcinog Mutagen. 1994;14(6):259-70.

Budunova IV, Williams GM, Spray DC.
Effect of tumor promoting stimuli on gap junction permeability and connexin43 expression in ARL18 rat liver cell line.
Arch Toxicol. 1993;67(8):565-72.

Bukauskas FF, Elfgang C, Willecke K, Weingart R.
Heterotypic gap junction channels (connexin26-connexin32) violate the paradigm of unitary conductance.
Pflugers Arch. 1995 Apr;429(6):870-2.

Burgeson RE, Christiano AM.
The dermal-epidermal junction.
Curr Opin Cell Biol. 1997 Oct;9(5):651-8.

Carystinos GD, Kandouz M, Alaoui-Jamali MA, Batist G.
Unexpected induction of the human connexin 43 promoter by the ras signalling pathway is mediated by a novel putative promoter sequence.
Mol Pharmacol. 2003 Apr;63(4):821-31.

Cesen-Cummings K, Fernstrom MJ, Malkinson AM, Ruch RJ.
Frequent reduction of gap junctional intercellular communication and connexin43 expression in human and mouse lung carcinoma cells.
Carcinogenesis. 1998 Jan;19(1):61-7.

Chan LS.
Human skin basement membrane in health and in autoimmune diseases.
Front Biosci. 1997 Jul 15;2:d343-52.

Chaumontet C, Bex V, Gaillard-Sanchez I, Seillan-Heberden C, Suschetet M, Martel P.
Apigenin and tangeretin enhance gap junctional intercellular communication in rat liver epithelial cells.
Carcinogenesis. 1994 Oct;15(10):2325-30.

Clark EA, Brugge JS.
Integrins and signal transduction pathways: the road taken.
Science. 1995 Apr 14;268(5208):233-9.

Cleaver JE, Crowley E.
UV damage, DNA repair and skin carcinogenesis.
Front Biosci. 2002 Apr 1;7:d1024-43.

Cooper CD, Lampe PD.
Casein kinase 1 regulates connexin-43 gap junction assembly.
J Biol Chem. 2002 Nov 22;277(47):44962-8. Epub 2002 Sep 20.

Cruciani V, Mikalsen SO.
Connexins, gap junctional intercellular communication and kinases.
Biol Cell. 2002 Nov;94(7-8):433-43.

Das Sarma J, Meyer RA, Wang F, Abraham V, Lo CW, Koval M.
Multimeric connexin interactions prior to the trans-Golgi network.
J Cell Sci. 2001 Nov;114(Pt 22):4013-24.

de Gruijl FR.
Photocarcinogenesis: UVA vs UVB.
Methods Enzymol. 2000;319:359-66.

De Sousa PA, Valdimarsson G, Nicholson BJ, Kidder GM.
Connexin trafficking and the control of gap junction assembly in mouse preimplantation embryos.
Development. 1993 Apr;117(4):1355-67.

Ebihara L.
New roles for connexons.
News Physiol Sci. 2003 Jun;18:100-3.

Ellenrieder V, Adler G, Gress TM.
Invasion and metastasis in pancreatic cancer.
Ann Oncol. 1999;10 Suppl 4:46-50.

Ellgaard L, Helenius A.
Quality control in the endoplasmic reticulum.
Nat Rev Mol Cell Biol. 2003 Mar;4(3):181-91.

Evans WH, Ahmad S, Diez J, George CH, Kendall JM, Martin PE.
Trafficking pathways leading to the formation of gap junctions.
Novartis Found Symp. 1999;219:44-54; discussion 54-9

Falk MM, Gilula NB.
Connexin membrane protein biosynthesis is influenced by polypeptide positioning within the translocon and signal peptidase access.
J Biol Chem. 1998 Apr 3;273(14):7856-64.

Falk MM, Kumar NM, Gilula NB.
Membrane insertion of gap junction connexins: polytopic channel forming membrane proteins.
J Cell Biol. 1994 Oct;127(2):343-55.

Forge A, Becker D, Casalotti S, Edwards J, Marziano N, Nevill G.
Gap junctions in the inner ear: comparison of distribution patterns in different vertebrates and assessement of connexin composition in mammals.
J Comp Neurol. 2003 Dec 8;467(2):207-31.

Ghoshroy S, Goodenough DA, Sosinsky GE.
Preparation, characterization, and structure of half gap junctional layers split with urea and EGTA.
J Membr Biol. 1995 Jul;146(1):15-28.

Goodenough DA, Musil LS.
Gap junctions and tissue business: problems and strategies for developing specific functional reagents.
J Cell Sci Suppl. 1993;17:133-8.

Goodenough DA, Gilula NB.
The splitting of hepatocyte gap junctions and zonulae occludentes with hypertonic disaccharides.
J Cell Biol. 1974 Jun;61(3):575-90.

Gorlich D, Rapoport TA.
Protein translocation into proteoliposomes reconstituted from purified components of the endoplasmic reticulum membrane.
Cell. 1993 Nov 19;75(4):615-30.

Grifa A, Wagner CA, D'Ambrosio L, Melchionda S, Bernardi F, Lopez-Bigas N, Rabionet R, Arbones M, Monica MD, Estivill X, Zelante L, Lang F, Gasparini P.
Mutations in GJB6 cause nonsyndromic autosomal dominant deafness at DFNA3 locus.
Nat Genet. 1999 Sep;23(1):16-8.

Herve JC, Sarrouilhe D.
Modulation of junctional communication by phosphorylation: protein phosphatases, the missing link in the chain.
Biol Cell. 2002 Nov;94(7-8):423-32.

High S, Dobberstein B.
The signal sequence interacts with the methionine-rich domain of the 54-kD protein of signal recognition particle.
J Cell Biol. 1991 Apr;113(2):229-33.

High S, Gorlich D, Wiedmann M, Rapoport TA, Dobberstein B.
The identification of proteins in the proximity of signal-anchor sequences during their targeting to and insertion into the membrane of the ER.
J Cell Biol. 1991 Apr;113(1):35-44.

High S, Flint N, Dobberstein B.
Requirements for the membrane insertion of signal-anchor type proteins.
J Cell Biol. 1991 Apr;113(1):25-34.

Huang XD, Horackova M, Pressler ML.
Changes in the expression and distribution of connexin 43 in isolated cultured adult guinea pig cardiomyocytes.
Exp Cell Res. 1996 Nov 1;228(2):254-61.

Hurtley SM, Helenius A.
Protein oligomerization in the endoplasmic reticulum.
Annu Rev Cell Biol. 1989;5:277-307.

Hussein MR.
Ultraviolet radiation and skin cancer: molecular mechanisms.
J Cutan Pathol. 2005 Mar;32(3):191-205.

Hussein MR, Haemel AK, Wood GS.
p53-related pathways and the molecular pathogenesis of melanoma.
Eur J Cancer Prev. 2003 Apr;12(2):93-100.

Johansson N, Ahonen M, Kahari VM.
Matrix metalloproteinases in tumor invasion.
Cell Mol Life Sci. 2000 Jan 20;57(1):5-15.

Jongen WM, Fitzgerald DJ, Asamoto M, Piccoli C, Slaga TJ, Gros D, Takeichi M, Yamasaki H.
Regulation of connexin 43-mediated gap junctional intercellular communication by Ca2+ in mouse epidermal cells is controlled by E-cadherin.
J Cell Biol. 1991 Aug;114(3):545-55.

Jordan K, Chodock R, Hand AR, Laird DW.
The origin of annular junctions: a mechanism of gap junction internalization.
J Cell Sci. 2001 Feb;114(Pt 4):763-73.

Kalies KU, Gorlich D, Rapoport TA.
Binding of ribosomes to the rough endoplasmic reticulum mediated by the Sec61p-complex.
J Cell Biol. 1994 Aug;126(4):925-34.

Kalimi GH, Lo CW.
Communication compartments in the gastrulating mouse embryo.
J Cell Biol. 1988 Jul;107(1):241-55.

Kanemitsu MY, Lau AF.
Epidermal growth factor stimulates the disruption of gap junctional communication and connexin43 phosphorylation independent of 12-0-tetradecanoylphorbol 13 acetate-sensitive protein kinase C: the possible involvement of mitogen-activated protein kinase.
Mol Biol Cell. 1993 Aug;4(8):837-48.

Kelsell DP, Dunlop J, Stevens HP, Lench NJ, Liang JN, Parry G, Mueller RF, Leigh IM.
Connexin 26 mutations in hereditary non-syndromic sensorineural deafness.
Nature. 1997 May 1;387(6628):80-3.

Kerkela E, Saarialho-Kere U.
Matrix metalloproteinases in tumor progression: focus on basal and squamous cell skin cancer.
Exp Dermatol. 2003 Apr;12(2):109-25.

Klaunig JE, Ruch RJ, Weghorst CM.
Comparative effects of phenobarbital, DDT, and lindane on mouse hepatocyte gap junctional intercellular communication.
Toxicol Appl Pharmacol. 1990 Mar 1;102(3):553-63.

Laird DW.
The life cycle of a connexin: gap junction formation, removal, and degradation.
J Bioenerg Biomembr. 1996 Aug;28(4):311-8.

Laird DW, Castillo M, Kasprzak L.
Gap junction turnover, intracellular trafficking, and phosphorylation of connexin43 in brefeldin A-treated rat mammary tumor cells.
J Cell Biol. 1995 Dec;131(5):1193-203.

Lampe PD.
Analyzing phorbol ester effects on gap junctional communication: a dramatic inhibition of assembly.
J Cell Biol. 1994 Dec;127(6 Pt 2):1895-905.

Larsen WJ, Hai-Nan.
Origin and fate of cytoplasmic gap junctional vesicles in rabbit granulosa cells.
Tissue Cell. 1978;10(3):585-98.

Lauf U, Giepmans BN, Lopez P, Braconnot S, Chen SC, Falk MM.
Dynamic trafficking and delivery of connexons to the plasma membrane and accretion to gap junctions in living cells.
Proc Natl Acad Sci U S A. 2002 Aug 6;99(16):10446-51. Epub 2002 Jul 29.

Lawrence TS, Beers WH, Gilula NB.
Transmission of hormonal stimulation by cell-to-cell communication.
Nature. 1978 Apr 6;272(5653):501-6.

Ling G, Ahmadian A, Persson A, Unden AB, Afink G, Williams C, Uhlen M, Toftgard R, Lundeberg J, Ponten F.
PATCHED and p53 gene alterations in sporadic and hereditary basal cell cancer.
Oncogene. 2001 Nov 22;20(53):7770-8.

Liu XZ, Xia XJ, Xu LR, Pandya A, Liang CY, Blanton SH, Brown SD, Steel KP,
Nance WE.
Mutations in connexin31 underlie recessive as well as dominant non-syndromic hearing loss.
Hum Mol Genet. 2000 Jan 1;9(1):63-7.

Loewenstein WR.
Cell-to-cell communication and the control of growth.
Am Rev Respir Dis. 1990 Dec;142(6 Pt 2):S48-53.

Loewenstein WR.
Junctional intercellular communication: the cell-to-cell membrane channel.
Physiol Rev. 1981 Oct;61(4):829-913.

Loewenstein WR.
Junctional intercellular communication and the control of growth.
Biochim Biophys Acta. 1979 Feb 4;560(1):1-65.

Loewenstein WR, Kanno Y.
Intercellular communication and the control of tissue growth: lack of communication between cancer cells.
Nature. 1966 Mar 19;209(29):1248-9.

Malewicz B, Kumar VV, Johnson RG, Baumann WJ.
Lipids in gap junction assembly and function.
Lipids. 1990 Aug;25(8):419-27.

McNutt NS, Weinstein RS.
The ultrastructure of the nexus. A correlated thin-section and freeze-cleave study.
J Cell Biol. 1970 Dec;47(3):666-88.

Mehta PP, Bertram JS, Loewenstein WR.
The actions of retinoids on cellular growth correlate with their actions on gap junctional communication.
J Cell Biol. 1989 Mar;108(3):1053-65.

Mograbi B, Corcelle E, Defamie N, Samson M, Nebout M, Segretain D, Fenichel P, Pointis G.
Aberrant Connexin 43 endocytosis by the carcinogen lindane involves activation of the ERK/mitogen-activated protein kinase pathway.
Carcinogenesis. 2003 Aug;24(8):1415-23. Epub 2003 Jun 5.

Mothes W, Heinrich SU, Graf R, Nilsson I, von Heijne G, Brunner J, Rapoport TA.
Molecular mechanism of membrane protein integration into the endoplasmic reticulum.
Cell. 1997 May 16;89(4):523-33.

Musil LS, Goodenough DA.
Multisubunit assembly of an integral plasma membrane channel protein, gap junction connexin43, occurs after exit from the ER.
Cell. 1993 Sep 24;74(6):1065-77.

Musil LS, Cunningham BA, Edelman GM, Goodenough DA.
Differential phosphorylation of the gap junction protein connexin43 in junctional communication-competent and -deficient cell lines.
J Cell Biol. 1990 Nov;111(5 Pt 1):2077-88.

Musil LS, Beyer EC, Goodenough DA.
Expression of the gap junction protein connexin43 in embryonic chick lens: molecular cloning, ultrastructural localization, and post-translational phosphorylation.
J Membr Biol. 1990 Jun;116(2):163-75.

Nguyen TA, Boyle DL, Wagner LM, Shinohara T, Takemoto DJ.
LEDGF activation of PKC gamma and gap junction disassembly in lens epithelial cells.
Exp Eye Res. 2003 May;76(5):565-72.

Parkinson EK.
Epidermal keratinocyte stem cells: their maintenance and regulation.
Semin Cell Biol. 1992 Dec;3(6):435-44

Pfeffer SR, Rothman JE.
Biosynthetic protein transport and sorting by the endoplasmic reticulum and Golgi.
Annu Rev Biochem. 1987;56:829-52

Popp S, Waltering S, Herbst C, Moll I, Boukamp P.
UV-B-type mutations and chromosomal imbalances indicate common pathways for the development of Merkel and skin squamous cell carcinomas.
Int J Cancer. 2002 May 20;99(3):352-60.

Potten CS, Hendry JH.
Letter: Clonogenic cells and stem cells in epidermis.
Int J Radiat Biol Relat Stud Phys Chem Med. 1973 Nov;24(5):537-40.

Qin H, Shao Q, Igdoura SA, Alaoui-Jamali MA, Laird DW.
Lysosomal and proteasomal degradation play distinct roles in the life cycle of Cx43 in gap junctional intercellular communication-deficient and –competent breast tumor cells.
J Biol Chem. 2003 Aug 8;278(32):30005-14. Epub 2003 May 26.

Qin H, Shao Q, Belliveau DJ, Laird DW.
Aggregated DsRed-tagged Cx43 and over-expressed Cx43 are targeted to lysosomes in human breast cancer cells.
Cell Commun Adhes. 2001;8(4-6):433-9.

Rebel H, Mosnier LO, Berg RJ, Westerman-de Vries A, van Steeg H, van Kranen HJ, de Gruijl FR.
Early p53-positive foci as indicators of tumor risk in ultraviolet-exposed hairless mice: kinetics of induction, effects of DNA repair deficiency, and p53 heterozygosity.
Cancer Res. 2001 Feb 1;61(3):977-83.

Ren P, de Feijter AW, Paul DL, Ruch RJ.
Enhancement of liver cell gap junction protein expression by glucocorticoids.
Carcinogenesis. 1994 Sep;15(9):1807-13.

Richard G.
Connexins: a connection with the skin.
Exp Dermatol. 2000 Apr;9(2):77-96.

Richard G, Brown N, Smith LE, Terrinoni A, Melino G, Mackie RM, Bale SJ, Uitto J.
The spectrum of mutations in erythrokeratodermias--novel and de novo mutations in GJB3.
Hum Genet. 2000 Mar;106(3):321-9.

Richard G, White TW, Smith LE, Bailey RA, Compton JG, Paul DL, Bale SJ.
Functional defects of Cx26 resulting from a heterozygous missense mutation in a family with dominant deaf-mutism and palmoplantar keratoderma.
Hum Genet. 1998 Oct;103(4):393-9.

Rogers M, Berestecky JM, Hossain MZ, Guo HM, Kadle R, Nicholson BJ, Bertram JS.
Retinoid-enhanced gap junctional communication is achieved by increased levels of connexin 43 mRNA and protein.
Mol Carcinog. 1990;3(6):335-43.

Rothman JE, Wieland FT.
Protein sorting by transport vesicles.
Science. 1996 Apr 12;272(5259):227-34.

Rothman JE, Orci L.
Budding vesicles in living cells.
Sci Am. 1996 Mar;274(3):70-5

Rothman JE.
The protein machinery of vesicle budding and fusion.
Protein Sci. 1996 Feb;5(2):185-94.

Ruch RJ.
The role of gap junctional intercellular communication in neoplasia.
Ann Clin Lab Sci. 1994 May-Jun;24(3):216-31.

Ruch RJ, Cheng SJ, Klaunig JE.
Prevention of cytotoxicity and inhibition of intercellular communication by antioxidant catechins isolated from Chinese green tea.
Carcinogenesis. 1989 Jun;10(6):1003-8.

Salomon D, Masgrau E, Vischer S, Ullrich S, Dupont E, Sappino P, Saurat JH, Meda P.
Topography of mammalian connexins in human skin.
J Invest Dermatol. 1994 Aug;103(2):240-7.

Scharffetter-Kochanek K, Brenneisen P, Wenk J, Herrmann G, Ma W, Kuhr L, Meewes C, Wlaschek M.
Photoaging of the skin from phenotype to mechanisms.
Exp Gerontol. 2000 May;35(3):307-16.

Scharffetter-Kochanek K, Wlaschek M, Brenneisen P, Schauen M, Blaudschun R, Wenk J.
UV-induced reactive oxygen species in photocarcinogenesis and photoaging.
Biol Chem. 1997 Nov;378(11):1247-57.

Schubert AL, Schubert W, Spray DC, Lisanti MP.
Connexin family members target to lipid raft domains and interact with caveolin-1.
Biochemistry. 2002 May 7;41(18):5754-64.

Schwartz MA.
Signaling by integrins: implications for tumorigenesis.
Cancer Res. 1993 Apr 1;53(7):1503-6.

Severs NJ.
Cardiovascular disease.
Novartis Found Symp. 1999;219:188-206; discussion 206-11.

Shiokawa-Sawada M, Mano H, Hanada K, Kakudo S, Kameda T, Miyazawa K, Nakamaru Y, Yuasa T, Mori Y, Kumegawa M, Hakeda Y.
Down-regulation of gap junctional intercellular communication between osteoblastic MC3T3-E1 cells by basic fibroblast growth factor and a phorbol ester (12-O-tetradecanoylphorbol-13-acetate).
J Bone Miner Res. 1997 Aug;12(8):1165-73.

Sigler K, Ruch RJ.
Enhancement of gap junctional intercellular communication in tumor promoter-treated cells by components of green tea.
Cancer Lett. 1993 Apr 15;69(1):15-9.

Simons K, Ehehalt R.
Cholesterol, lipid rafts, and disease.
J Clin Invest. 2002 Sep;110(5):597-603.

Solan JL, Lampe PD.
Connexin phosphorylation as a regulatory event linked to gap junction channel assembly.
Biochim Biophys Acta. 2005 Jun 10;1711(2):154-63. Epub 2004 Oct 12.

Sosinsky G.
Mixing of connexins in gap junction membrane channels.
Proc Natl Acad Sci U S A. 1995 Sep 26;92(20):9210-4.

Spray DC.
Gap junction proteins: where they live and how they die.
Circ Res. 1998 Sep 21;83(6):679-81.

Stahl W, von Laar J, Martin HD, Emmerich T, Sies H.
Stimulation of gap junctional communication: comparison of acyclo-retinoic acid and lycopene.
Arch Biochem Biophys. 2000 Jan 1;373(1):271-4.

Stuhlmann D, Steinbrenner H, Wendlandt B, Mitic D, Sies H, Brenneisen P.
Paracrine effect of TGF-beta1 on downregulation of gap junctional intercellular communication between human dermal fibroblasts.
Biochem Biophys Res Commun. 2004 Jun 25;319(2):321-6.

Stuhlmann D, Ale-Agha N, Reinehr R, Steinbrenner H, Ramos MC, Sies H, Brenneisen P.
Modulation of homologous gap junctional intercellular communication of human dermal fibroblasts via a paracrine factor(s) generated by squamous tumor cells.
Carcinogenesis. 2003 Nov;24(11):1737-48. Epub 2003 Aug 29.

Teicher VB, Kucharski N, Martin HD, van der Saag P, Sies H, Stahl W.
Biological activities of Apo-canthaxanthinoic acids related to gap junctional communication.
Arch Biochem Biophys. 1999 May 1;365(1):150-5.

Thomas MA, Zosso N, Scerri I, Demaurex N, Chanson M, Staub O.
A tyrosine-based sorting signal is involved in connexin43 stability and gap junction turnover.
J Cell Sci. 2003 Jun 1;116(Pt 11):2213-22.

Timpl R, Fujiwara S, Dziadek M, Aumailley M, Weber S, Engel J.
Laminin, proteoglycan, nidogen and collagen IV: structural models and molecular interactions.
Ciba Found Symp. 1984;108:25-43.

Trosko JE, Ruch RJ.
Cell-cell communication in carcinogenesis.
Front Biosci. 1998 Feb 15;3:d208-36

Trosko JE, Chang CC, Madhukar BV, Klaunig JE.
Chemical, oncogene and growth factor inhibition gap junctional intercellular communication: an integrative hypothesis of carcinogenesis.
Pathobiology. 1990;58(5):265-78.

Trosko JE, Jone C, Chang CC.
Inhibition of gap junctional-mediated intercellular communication in vitro by aldrin, dieldrin, and toxaphene: a possible cellular mechanism for their tumor-promoting and neurotoxic effects.
Mol Toxicol. 1987 Jan-Mar;1(1):83-93.

VanSlyke JK, Deschenes SM, Musil LS.
Intracellular transport, assembly, and degradation of wild-type and disease-linked mutant gap junction proteins.
Mol Biol Cell. 2000 Jun;11(6):1933-46.

Weinberg R.
Tumor suppressor genes.
Neuron. 1993 Aug;11(2):191-6.

Weinstein RS, Pauli BU.
Cell junctions and the biological behaviour of cancer.
Ciba Found Symp. 1987;125:240-60.

Wheelock MJ, Knudsen KA.
Cadherins and associated proteins.
In Vivo. 1991 Sep-Oct;5(5):505-13.

White TW, Paul DL, Goodenough DA, Bruzzone R.
Functional analysis of selective interactions among rodent connexins.
Mol Biol Cell. 1995 Apr;6(4):459-70.

Willecke K, Eiberger J, Degen J, Eckardt D, Romualdi A, Guldenagel M, Deutsch U, Sohl G.
Structural and functional diversity of connexin genes in the mouse and human genome.
Biol Chem. 2002 May;383(5):725-37.

Wiszniewski L, Limat A, Saurat JH, Meda P, Salomon D.
Differential expression of connexins during stratification of human keratinocytes.
J Invest Dermatol. 2000 Aug;115(2):278-85.

Wu JC, Tsai RY, Chung TH.
Role of catenins in the development of gap junctions in rat cardiomyocytes.
J Cell Biochem. 2003 Mar 1;88(4):823-35.

Yamasaki H.
Gap junctional intercellular communication and carcinogenesis.
Carcinogenesis. 1990 Jul;11(7):1051-8.

Yurchenco PD, Cheng YS, Colognato H.
Laminin forms an independent network in basement membranes.
J Cell Biol. 1992 Jun;117(5):1119-33. Erratum in: J Cell Biol 1992 Jun;118(2):493.

Yurchenco PD, Furthmayr H.
Self-assembly of basement membrane collagen.
Biochemistry. 1984 Apr 10;23(8):1839-50.

Zerial M, Melancon P, Schneider C, Garoff H.
The transmembrane segment of the human transferrin receptor functions as a signal peptide.
EMBO J. 1986 Jul;5(7):1543-50.

Zhang LX, Cooney RV, Bertram JS.
Carotenoids up-regulate connexin43 gene expression independent of their provitamin A or antioxidant properties.
Cancer Res. 1992 Oct 15;52(20):5707-12.

Results, Discussion

Abercrombie M.
Contact inhibition and malignancy.
Nature. 1979 Sep 27;281(5729):259-62.

Adams J.
The proteasome: structure, function, and role in the cell.
Cancer Treat Rev. 2003 May;29 Suppl 1:3-9.

Ai X, Pogwizd SM.
Connexin 43 downregulation and dephosphorylation in nonischemic heart failure is associated with enhanced colocalized protein phosphatase type 2A.
Circ Res. 2005 Jan 7;96(1):54-63. Epub 2004 Dec 2.

Atkinson MM, Lampe PD, Lin HH, Kollander R, Li XR, Kiang DT.
Cyclic AMP modifies the cellular distribution of connexin43 and induces a persistent increase in the junctional permeability of mouse mammary tumor cells.
J Cell Sci. 1995 Sep;108 (Pt 9):3079-90.

Behrens J.
The role of cell adhesion molecules in cancer invasion and metastasis.
Breast Cancer Res Treat. 1993;24(3):175-84.

Berthoud VM, Ledbetter ML, Hertzberg EL, Saez JC.
Connexin43 in MDCK cells: regulation by a tumor-promoting phorbol ester and Ca2+.
Eur J Cell Biol. 1992 Feb;57(1):40-50.

Bertram JS.
Dietary carotenoids, connexins and cancer: what is the connection?
Biochem Soc Trans. 2004 Dec;32(Pt 6):985-9.

Bertram JS, Bortkiewicz H.
Dietary carotenoids inhibit neoplastic transformation and modulate gene expression in mouse and human cells.
Am J Clin Nutr. 1995 Dec;62(6 Suppl):1327S-1336S.

Borek C, Sachs L.
THE DIFFERENCE IN CONTACT INHIBITION OF CELL REPLICATION BETWEEN NORMAL CELLS AND CELLS TRANSFORMED BY DIFFERENT CARCINOGENS.
Proc Natl Acad Sci U S A. 1966 Dec;56(6):1705-1711.

Boukamp P.
Non-melanoma skin cancer: what drives tumor development and progression?
Carcinogenesis. 2005 Oct;26(10):1657-67. Epub 2005 May 19

Boukamp P.
UV-induced skin cancer: similarities--variations.
J Dtsch Dermatol Ges. 2005 Jul;3(7):493-503.

Boukamp P, Petrussevska RT, Breitkreutz D, Hornung J, Markham A, Fusenig NE.
Normal keratinization in a spontaneously immortalized aneuploid human keratinocyte cell line.
J Cell Biol. 1988 Mar;106(3):761-71.

Brignoni M, Pignataro OP, Rodriguez ML, Alvarez A, Vega-Salas DE, Rodriguez-Boulan E, Salas PJ.
Cyclic AMP modulates the rate of 'constitutive' exocytosis of apical membrane proteins in Madin-Darby canine kidney cells.
J Cell Sci. 1995 May;108 (Pt 5):1931-43.

Brissette JL, Kumar NM, Gilula NB, Hall JE, Dotto GP.
Switch in gap junction protein expression is associated with selective changes in junctional permeability during keratinocyte differentiation.
Proc Natl Acad Sci U S A. 1994 Jul 5;91(14):6453-7.

Britz-Cunningham SH, Shah MM, Zuppan CW, Fletcher WH.
Mutations of the Connexin43 gap-junction gene in patients with heart malformations and defects of laterality.
N Engl J Med. 1995 May 18;332(20):1323-9.

Budunova IV, Carbajal S, Viaje A, Slaga TJ.
Connexin expression in epidermal cell lines from SENCAR mouse skin tumors.
Mol Carcinog. 1996 Mar;15(3):190-201.

Bulteau AL, Petropoulos I, Friguet B.
Age-related alterations of proteasome structure and function in aging epidermis.
Exp Gerontol. 2000 Sep;35(6-7):767-77.

Bureau JP, Henry L, Baz A, Scherrer K, Chateau MT.
Prosomes (proteasomes) changes during differentiation are related to the type of inducer.
Mol Biol Rep. 1997 Mar;24(1-2):57-62.

Burghardt RC, Barhoumi R, Sewall TC, Bowen JA.
Cyclic AMP induces rapid increases in gap junction permeability and changes in the cellular distribution of connexin43.
J Membr Biol. 1995 Dec;148(3):243-53.

Cadigan KM, Nusse R.
Wnt signaling: a common theme in animal development.
Genes Dev. 1997 Dec 15;11(24):3286-305.

Carruba G, Webber MM, Quader ST, Amoroso M, Cocciadiferro L, Saladino F, Trosko JE, Castagnetta LA.
Regulation of cell-to-cell communication in non-tumorigenic and malignant human prostate epithelial cells.
Prostate. 2002 Feb 1;50(2):73-82.

Cesen-Cummings K, Fernstrom MJ, Malkinson AM, Ruch RJ.
Frequent reduction of gap junctional intercellular communication and connexin43 expression in human and mouse lung carcinoma cells.
Carcinogenesis. 1998 Jan;19(1):61-7.

Chaumontet C, Bex V, Gaillard-Sanchez I, Seillan-Heberden C, Suschetet M, Martel P.
Apigenin and tangeretin enhance gap junctional intercellular communication in rat liver epithelial cells.
Carcinogenesis. 1994 Oct;15(10):2325-30.

Chu G, Carr AN, Young KB, Lester JW, Yatani A, Sanbe A, Colbert MC, Schwartz SM, Frank KF, Lampe PD, Robbins J, Molkentin JD, Kranias EG.
Enhanced myocyte contractility and Ca2+ handling in a calcineurin transgenic model of heart failure.
Cardiovasc Res. 2002 Apr;54(1):105-16.

Ciechanover A.
The ubiquitin-proteasome pathway: on protein death and cell life.
EMBO J. 1998 Dec 15;17(24):7151-60.

Ciechanover A, Schwartz AL.
The ubiquitin-proteasome pathway: the complexity and myriad functions of proteins death.
Proc Natl Acad Sci U S A. 1998 Mar 17;95(6):2727-30.

Coux O, Tanaka K, Goldberg AL.
Structure and functions of the 20S and 26S proteasomes.
Annu Rev Biochem. 1996;65:801-47

Cruciani V, Kaalhus O, Mikalsen SO.
Phosphatases involved in modulation of gap junctional intercellular communication and dephosphorylation of connexin43 in hamster fibroblasts: 2B or not 2B?
Exp Cell Res. 1999 Nov 1;252(2):449-63.

Darrow BJ, Fast VG, Kleber AG, Beyer EC, Saffitz JE.
Functional and structural assessment of intercellular communication. Increased conduction velocity and enhanced connexin expression in dibutyryl cAMP-treated cultured cardiac myocytes.
Circ Res. 1996 Aug;79(2):174-83.

Dasgupta C, Martinez AM, Zuppan CW, Shah MM, Bailey LL, Fletcher WH.
Identification of connexin43 (alpha1) gap junction gene mutations in patients with hypoplastic left heart syndrome by denaturing gradient gel electrophoresis (DGGE).
Mutat Res. 2001 Aug 8;479(1-2):173-86.

Daubrawa F, Sies H, Stahl W.
Astaxanthin diminishes gap junctional intercellular communication in primary human fibroblasts.
J Nutr. 2005 Nov;135(11):2507-11.

Davies KJ.
Degradation of oxidized proteins by the 20S proteasome.
Biochimie. 2001 Mar-Apr;83(3-4):301-10

De Lisle RC, Howell GW.
Evidence of heterotrimeric G-protein involvement in regulated exocytosis from permeabilized pancreatic acini.
Pancreas. 1995 May;10(4):374-81.

De Wever O, Mareel M.
Role of tissue stroma in cancer cell invasion.
J Pathol. 2003 Jul;200(4):429-47

Dubina MV, Iatckii NA, Popov DE, Vasil'ev SV, Krutovskikh VA.
Connexin 43, but not connexin 32, is mutated at advanced stages of human sporadic colon cancer.
Oncogene. 2002 Jul 25;21(32):4992-6.

Eghbali B, Kessler JA, Reid LM, Roy C, Spray DC.
Involvement of gap junctions in tumorigenesis: transfection of tumor cells with connexin 32 cDNA retards growth in vivo.
Proc Natl Acad Sci U S A. 1991 Dec 1;88(23):10701-5.

Fialkow PJ.
Clonal origin of human tumors.
Annu Rev Med. 1979;30:135-43.

Fiorini C, Mograbi B, Cronier L, Bourget I, Decrouy X, Nebout M, Ferrua B, Malassine A, Samson M, Fenichel P, Segretain D, Pointis G.
Dominant negative effect of connexin33 on gap junctional communication is mediated by connexin43 sequestration.
J Cell Sci. 2004 Sep 15;117(Pt 20):4665-72. Epub 2004 Aug 25.

Fishman GI, Moreno AP, Spray DC, Leinwand LA.
Functional analysis of human cardiac gap junction channel mutants.
Proc Natl Acad Sci U S A. 1991 May 1;88(9):3525-9.

Fleischmajer R, Perlish JS, Krieg T, Timpl R.
Variability in collagen and fibronectin synthesis by scleroderma fibroblasts in primary culture.
J Invest Dermatol. 1981 May;76(5):400-3.

Frixen UH, Behrens J, Sachs M, Eberle G, Voss B, Warda A, Lochner D, Birchmeier W.
E-cadherin-mediated cell-cell adhesion prevents invasiveness of human carcinoma cells.
J Cell Biol. 1991 Apr;113(1):173-85.

Fukunaga Y, Liu H, Shimizu M, Komiya S, Kawasuji M, Nagafuchi A.
Defining the roles of beta-catenin and plakoglobin in cell-cell adhesion: isolation of beta-catenin/plakoglobin-deficient F9 cells.
Cell Struct Funct. 2005;30(2):25-34.

Garewal HS, Schantz S.
Emerging role of beta-carotene and antioxidant nutrients in prevention of oral cancer.
Arch Otolaryngol Head Neck Surg. 1995 Feb;121(2):141-4

Giepmans BN, Verlaan I, Hengeveld T, Janssen H, Calafat J, Falk MM, Moolenaar WH.
Gap junction protein connexin-43 interacts directly with microtubules.
Curr Biol. 2001 Sep 4;11(17):1364-8.

Giepmans BN, Verlaan I, Moolenaar WH.
Connexin-43 interactions with ZO-1 and alpha- and beta-tubulin.
Cell Commun Adhes. 2001;8(4-6):219-23.

Glade CP, Seegers BA, Meulen EF, van Hooijdonk CA, van Erp PE, van de Kerkhof PC.
Multiparameter flow cytometric characterization of epidermal cell suspensions prepared from normal and hyperproliferative human skin using an optimised thermolysin-trypsin protocol.
Arch Dermatol Res. 1996 Apr;288(4):203-10.

Godwin AJ, Green LM, Walsh MP, McDonald JR, Walsh DA, Fletcher WH.
In situ regulation of cell-cell communication by the cAMP-dependent protein kinase and protein kinase C.
Mol Cell Biochem. 1993 Nov;127-128:293-307.

Govinden R, Bhoola KD.
Genealogy, expression, and cellular function of transforming growth factor-beta.
Pharmacol Ther. 2003 May;98(2):257-65.

Greaves MF.
Differentiation-linked leukemogenesis in lymphocytes.
Science. 1986 Nov 7;234(4777):697-704.

Guan X, Wilson S, Schlender KK, Ruch RJ.
Gap-junction disassembly and connexin 43 dephosphorylation induced by 18 beta-glycyrrhetinic acid.
Mol Carcinog. 1996 Jul;16(3):157-64.

Guo H, Acevedo P, Parsa FD, Bertram JS.
Gap-junctional protein connexin 43 is expressed in dermis and epidermis of human skin: differential modulation by retinoids.
J Invest Dermatol. 1992 Oct;99(4):460-7.

Hansen SH, Casanova JE.
Gs alpha stimulates transcytosis and apical secretion in MDCK cells through cAMP and protein kinase A.
J Cell Biol. 1994 Aug;126(3):677-87.

Hazan RB, Phillips GR, Qiao RF, Norton L, Aaronson SA.
Exogenous expression of N-cadherin in breast cancer cells induces cell migration, invasion, and metastasis.
J Cell Biol. 2000 Feb 21;148(4):779-90. Erratum in: J Cell Biol 2000 Apr 3;149(1):following 236.

Henry L, Baz A, Chateau MT, Scherrer K, Bureau JP.
Changes in the amount and distribution of prosomal subunits during the differentiation of U937 myeloid cells: high expression of p23K.
Cell Prolif. 1996 Nov;29(11):589-607.

Hieber AD, King TJ, Morioka S, Fukushima LH, Franke AA, Bertram JS.
Comparative effects of all-trans beta-carotene vs. 9-cis beta-carotene on carcinogen-induced neoplastic transformation and connexin 43 expression in murine 10T1/2 cells and on the differentiation of human keratinocytes.
Nutr Cancer. 2000;37(2):234-44.

Hirai A, Yano T, Nishikawa K, Suzuki K, Asano R, Satoh H, Hagiwara K, Yamasaki H.
Down-regulation of connexin 32 gene expression through DNA methylation in a human renal cell carcinoma cell.
Am J Nephrol. 2003 May-Jun;23(3):172-7. Epub 2003 Apr 10.

Hirotsune S, Yoshida N, Chen A, Garrett L, Sugiyama F, Takahashi S, Yagami K, Wynshaw-Boris A, Yoshiki A.
An expressed pseudogene regulates the messenger-RNA stability of its homologous coding gene.
Nature. 2003 May 1;423(6935):91-6.

Hirschi KK, Xu CE, Tsukamoto T, Sager R.
Gap junction genes Cx26 and Cx43 individually suppress the cancer phenotype of human mammary carcinoma cells and restore differentiation potential.
Cell Growth Differ. 1996 Jul;7(7):861-70.

Holm I, Mikhailov A, Jillson T, Rose B.
Dynamics of gap junctions observed in living cells with connexin43-GFP chimeric protein.
Eur J Cell Biol. 1999 Dec;78(12):856-66.

Husoy T, Mikalsen SO, Sanner T.
Phosphatase inhibitors, gap junctional intercellular communication and [125I]-EGF binding in hamster fibroblasts.
Carcinogenesis. 1993 Nov;14(11):2257-65.

Jongen WM, Fitzgerald DJ, Asamoto M, Piccoli C, Slaga TJ, Gros D, Takeichi M, Yamasaki H.
Regulation of connexin 43-mediated gap junctional intercellular communication by Ca2+ in mouse epidermal cells is controlled by E-cadherin.
J Cell Biol. 1991 Aug;114(3):545-55.

Jordan K, Solan JL, Dominguez M, Sia M, Hand A, Lampe PD, Laird DW.
Trafficking, assembly, and function of a connexin43-green fluorescent protein chimera in live mammalian cells.
Mol Biol Cell. 1999 Jun;10(6):2033-50.

Kamibayashi Y, Oyamada Y, Mori M, Oyamada M.
Aberrant expression of gap junction proteins (connexins) is associated with tumor progression during multistage mouse skin carcinogenesis in vivo.
Carcinogenesis. 1995 Jun;16(6):1287-97.

Kandouz M, Bier A, Carystinos GD, Alaoui-Jamali MA, Batist G.
Connexin43 pseudogene is expressed in tumor cells and inhibits growth.
Oncogene. 2004 Jun 10;23(27):4763-70.

Klann RC, Fitzgerald DJ, Piccoli C, Slaga TJ, Yamasaki H.
Gap-junctional intercellular communication in epidermal cell lines from selected stages of SENCAR mouse skin carcinogenesis.
Cancer Res. 1989 Feb 1;49(3):699-705.

Klaunig JE, Siglin JC, Schafer LD, Hartnett JA, Weghorst CM, Olson MJ, Hampton JA.
Correlation between species and tissue sensitivity to chemical carcinogenesis in rodents and the induction of DNA synthesis.
Prog Clin Biol Res. 1991;369:185-94.

Korneev SA, Park JH, O'Shea M.
Neuronal expression of neural nitric oxide synthase (nNOS) protein is suppressed by an antisense RNA transcribed from an NOS pseudogene.
J Neurosci. 1999 Sep 15;19(18):7711-20.

Kumatori A, Tanaka K, Inamura N, Sone S, Ogura T, Matsumoto T, Tachikawa T, Shin S, Ichihara A.
Abnormally high expression of proteasomes in human leukemic cells.
Proc Natl Acad Sci U S A. 1990 Sep;87(18):7071-5.

Laird DW, Castillo M, Kasprzak L.
Gap junction turnover, intracellular trafficking, and phosphorylation of connexin43 in brefeldin A-treated rat mammary tumor cells.
J Cell Biol. 1995 Dec;131(5):1193-203.

Lampe PD, Lau AF.
Regulation of gap junctions by phosphorylation of connexins.
Arch Biochem Biophys. 2000 Dec 15;384(2):205-15.

Lampe PD, Kurata WE, Warn-Cramer BJ, Lau AF.
Formation of a distinct connexin43 phosphoisoform in mitotic cells is dependent upon p34cdc2 kinase.
J Cell Sci. 1998 Mar;111 (Pt 6):833-41.

Lampe PD.
Analyzing phorbol ester effects on gap junctional communication: a dramatic inhibition of assembly.
J Cell Biol. 1994 Dec;127(6 Pt 2):1895-905.

Lau AF, Kanemitsu MY, Kurata WE, Danesh S, Boynton AL.
Epidermal growth factor disrupts gap-junctional communication and induces phosphorylation of connexin43 on serine.
Mol Biol Cell. 1992 Aug;3(8):865-74.

Lauf U, Giepmans BN, Lopez P, Braconnot S, Chen SC, Falk MM.
Dynamic trafficking and delivery of connexons to the plasma membrane and accretion to gap junctions in living cells.
Proc Natl Acad Sci U S A. 2002 Aug 6;99(16):10446-51. Epub 2002 Jul 29.

Leithe E, Rivedal E.
Epidermal growth factor regulates ubiquitination, internalization and proteasome-dependent degradation of connexin43.
J Cell Sci. 2004 Mar 1;117(Pt 7):1211-20. Epub 2004 Feb 17. Erratum in: J Cell Sci. 2004 Mar 15;117(8):1613.

Loewenstein WR.
Junctional intercellular communication: the cell-to-cell membrane channel.
Physiol Rev. 1981 Oct;61(4):829-913.

Lyakhovitsky A, Barzilai A, Fogel M, Trau H, Huszar M.
Expression of e-cadherin and beta-catenin in cutaneous squamous cell carcinoma and its precursors.
Am J Dermatopathol. 2004 Oct;26(5):372-8.

Markert CL.
Neoplasia: a disease of cell differentiation.
Cancer Res. 1968 Sep;28(9):1908-14.

Marques C, Pereira P, Taylor A, Liang JN, Reddy VN, Szweda LI, Shang F.
Ubiquitin-dependent lysosomal degradation of the HNE-modified proteins in lens epithelial cells.
FASEB J. 2004 Sep;18(12):1424-6. Epub 2004 Jul 9.

Martin PE, Blundell G, Ahmad S, Errington RJ, Evans WH.
Multiple pathways in the trafficking and assembly of connexin 26, 32 and 43 into gap junction intercellular communication channels.
J Cell Sci. 2001 Nov;114(Pt 21):3845-55.

Mege RM, Matsuzaki F, Gallin WJ, Goldberg JI, Cunningham BA, Edelman GM.
Construction of epithelioid sheets by transfection of mouse sarcoma cells with cDNAs for chicken cell adhesion molecules.
Proc Natl Acad Sci U S A. 1988 Oct;85(19):7274-8.

Mehta PP, Yamamoto M, Rose B.
Transcription of the gene for the gap junctional protein connexin43 and expression of functional cell-to-cell channels are regulated by cAMP.
Mol Biol Cell. 1992 Aug;3(8):839-50.

Mehta PP, Hotz-Wagenblatt A, Rose B, Shalloway D, Loewenstein WR.
Incorporation of the gene for a cell-cell channel protein into transformed cells leads to normalization of growth.
J Membr Biol. 1991 Dec;124(3):207-25.

Mehta PP, Bertram JS, Loewenstein WR.
The actions of retinoids on cellular growth correlate with their actions on gap junctional communication.
J Cell Biol. 1989 Mar;108(3):1053-65.

Mesnil M.
Connexins and cancer.
Biol Cell. 2002 Nov;94(7-8):493-500.

Mesnil M, Krutovskikh V, Piccoli C, Elfgang C, Traub O, Willecke K, Yamasaki H.
Negative growth control of HeLa cells by connexin genes: connexin species specificity.
Cancer Res. 1995 Feb 1;55(3):629-39.

Morin PJ, Sparks AB, Korinek V, Barker N, Clevers H, Vogelstein B, Kinzler KW.
Activation of beta-catenin-Tcf signaling in colon cancer by mutations in beta-catenin or APC.
Science. 1997 Mar 21;275(5307):1787-90.

Musil LS, Le AC, VanSlyke JK, Roberts LM.
Regulation of connexin degradation as a mechanism to increase gap junction assembly and function.
J Biol Chem. 2000 Aug 18;275(33):25207-15.

Musil LS, Cunningham BA, Edelman GM, Goodenough DA.
Differential phosphorylation of the gap junction protein connexin43 in junctional communication-competent and -deficient cell lines.
J Cell Biol. 1990 Nov;111(5 Pt 1):2077-88.

Musil LS, Beyer EC, Goodenough DA.
Expression of the gap junction protein connexin43 in embryonic chick lens: molecular cloning, ultrastructural localization, and post-translational phosphorylation.
J Membr Biol. 1990 Jun;116(2):163-75.

Naus CC, Elisevich K, Zhu D, Belliveau DJ, Del Maestro RF.
In vivo growth of C6 glioma cells transfected with connexin43 cDNA.
Cancer Res. 1992 Aug 1;52(15):4208-13.

Nishimura M, Saito T, Yamasaki H, Kudo R.
Suppression of gap junctional intercellular communication via 5' CpG island methylation in promoter region of E-cadherin gene in endometrial cancer cells.
Carcinogenesis. 2003 Oct;24(10):1615-23. Epub 2003 Aug 1.

Nowell PC.
The clonal evolution of tumor cell populations.
Science. 1976 Oct 1;194(4260):23-8.

Oyama T, Kanai Y, Ochiai A, Akimoto S, Oda T, Yanagihara K, Nagafuchi A, Tsukita S, Shibamoto S, Ito F, et al.
A truncated beta-catenin disrupts the interaction between E-cadherin and alpha-catenin: a cause of loss of intercellular adhesiveness in human cancer cell lines.
Cancer Res. 1994 Dec 1;54(23):6282-7.

Paulson AF, Lampe PD, Meyer RA, TenBroek E, Atkinson MM, Walseth TF, Johnson RG.
Cyclic AMP and LDL trigger a rapid enhancement in gap junction assembly through a stimulation of connexin trafficking.
J Cell Sci. 2000 Sep;113 (Pt 17):3037-49.

Petropoulos I, Conconi M, Wang X, Hoenel B, Bregegere F, Milner Y, Friguet B.
Increase of oxidatively modified protein is associated with a decrease of proteasome activity and content in aging epidermal cells.
J Gerontol A Biol Sci Med Sci. 2000 May;55(5):B220-7.

Pfeffer SR, Rothman JE.
Biosynthetic protein transport and sorting by the endoplasmic reticulum and Golgi.
Annu Rev Biochem. 1987;56:829-52.

Piek E, Heldin CH, Ten Dijke P.
Specificity, diversity, and regulation in TGF-beta superfamily signaling.
FASEB J. 1999 Dec;13(15):2105-24.

Pierce GB.
Neoplasms, differentiations and mutations.
Am J Pathol. 1974 Oct;77(1):103-118.

Pignatelli M, Ansari TW, Gunter P, Liu D, Hirano S, Takeichi M, Kloppel G, Lemoine NR.
Loss of membranous E-cadherin expression in pancreatic cancer: correlation with lymph node metastasis, high grade, and advanced stage.
J Pathol. 1994 Dec;174(4):243-8.

Potter VR.
Phenotypic diversity in experimental hepatomas: the concept of partially blocked ontogeny. The 10th Walter Hubert Lecture.
Br J Cancer. 1978 Jul;38(1):1-23.

Provost N, Moreau M, Leturque A, Nizard C.
Ultraviolet A radiation transiently disrupts gap junctional communication in human keratinocytes.
Am J Physiol Cell Physiol. 2003 Jan;284(1):C51-9. Epub 2002 Sep 4.

Qin H, Shao Q, Igdoura SA, Alaoui-Jamali MA, Laird DW.
Lysosomal and proteasomal degradation play distinct roles in the life cycle of Cx43 in gap junctional intercellular communication-deficient and –competent breast tumor cells.
J Biol Chem. 2003 Aug 8;278(32):30005-14. Epub 2003 May 26.

Ren P, de Feijter AW, Paul DL, Ruch RJ.
Enhancement of liver cell gap junction protein expression by glucocorticoids.
Carcinogenesis. 1994 Sep;15(9):1807-13.

Rock KL, Gramm C, Rothstein L, Clark K, Stein R, Dick L, Hwang D, Goldberg AL.
Inhibitors of the proteasome block the degradation of most cell proteins and the generation of peptides presented on MHC class I molecules.
Cell. 1994 Sep 9;78(5):761-71.

Rogers M, Berestecky JM, Hossain MZ, Guo HM, Kadle R, Nicholson BJ, Bertram JS.
Retinoid-enhanced gap junctional communication is achieved by increased levels of connexin 43 mRNA and protein.
Mol Carcinog. 1990;3(6):335-43.

Rothman JE, Wieland FT.
Protein sorting by transport vesicles.
Science. 1996 Apr 12;272(5259):227-34.

Rouan F, White TW, Brown N, Taylor AM, Lucke TW, Paul DL, Munro CS, Uitto J, Hodgins MB, Richard G.
Trans-dominant inhibition of connexin-43 by mutant connexin-26: implications for dominant connexin disorders affecting epidermal differentiation.
J Cell Sci. 2001 Jun;114(Pt 11):2105-13.

Ruch RJ, Cesen-Cummings K, Malkinson AM.
Role of gap junctions in lung neoplasia.
Exp Lung Res. 1998 Jul-Aug;24(4):523-39.

Ruch RJ.
The role of gap junctional intercellular communication in neoplasia.
Ann Clin Lab Sci. 1994 May-Jun;24(3):216-31

Ruch RJ, Cheng SJ, Klaunig JE.
Prevention of cytotoxicity and inhibition of intercellular communication by antioxidant catechins isolated from Chinese green tea.
Carcinogenesis. 1989 Jun;10(6):1003-8.

Saez JC, Martinez AD, Branes MC, Gonzalez HE.
Regulation of gap junctions by protein phosphorylation.
Braz J Med Biol Res. 1998 May;31(5):593-600.

Saunders MM, Seraj MJ, Li Z, Zhou Z, Winter CR, Welch DR, Donahue HJ.
Breast cancer metastatic potential correlates with a breakdown in homospecific and heterospecific gap junctional intercellular communication.
Cancer Res. 2001 Mar 1;61(5):1765-7.

Sigler K, Ruch RJ.
Enhancement of gap junctional intercellular communication in tumor promoter-treated cells by components of green tea.
Cancer Lett. 1993 Apr 15;69(1):15-9.

Stahl W, Sies H.
Bioactivity and protective effects of natural carotenoids.
Biochim Biophys Acta. 2005 May 30;1740(2):101-7. Epub 2004 Dec 28.

Stahl W, Nicolai S, Briviba K, Hanusch M, Broszeit G, Peters M, Martin HD, Sies H.
Biological activities of natural and synthetic carotenoids: induction of gap junctional communication and singlet oxygen quenching.
Carcinogenesis. 1997 Jan;18(1):89-92.

Stoebner PE, Lavabre-Bertrand T, Henry L, Guiraud I, Carillo S, Dandurand M, Joujoux JM, Bureau JP, Meunier L.
High plasma proteasome levels are detected in patients with metastatic malignant melanoma.
Br J Dermatol. 2005 May;152(5):948-53.

Stuhlmann D, Steinbrenner H, Wendlandt B, Mitic D, Sies H, Brenneisen P.
Paracrine effect of TGF-beta1 on downregulation of gap junctional intercellular communication between human dermal fibroblasts.
Biochem Biophys Res Commun. 2004 Jun 25;319(2):321-6.

Stuhlmann D, Ale-Agha N, Reinehr R, Steinbrenner H, Ramos MC, Sies H, Brenneisen P.
Modulation of homologous gap junctional intercellular communication of human dermal fibroblasts via a paracrine factor(s) generated by squamous tumor cells.
Carcinogenesis. 2003 Nov;24(11):1737-48. Epub 2003 Aug 29.

Suga Y, Takamori K, Ogawa H.
Skin proteasomes (high-molecular-weight protease): purification, enzymologic properties, gross structure, and tissue distribution.
J Invest Dermatol. 1993 Sep;101(3):346-51.

Swenson KI, Piwnica-Worms H, McNamee H, Paul DL.
Tyrosine phosphorylation of the gap junction protein connexin43 is required for the pp60v-src-induced inhibition of communication.
Cell Regul. 1990 Dec;1(13):989-1002.

Tada J, Hashimoto K.
Ultrastructural localization of gap junction protein connexin 43 in normal human skin, basal cell carcinoma, and squamous cell carcinoma.
J Cutan Pathol. 1997 Nov;24(10):628-35.

Tanaka T, Makita H, Ohnishi M, Mori H, Satoh K, Hara A.
Chemoprevention of rat oral carcinogenesis by naturally occurring xanthophylls, astaxanthin and canthaxanthin.
Cancer Res. 1995 Sep 15;55(18):4059-64.

TenBroek EM, Lampe PD, Solan JL, Reynhout JK, Johnson RG.
Ser364 of connexin43 and the upregulation of gap junction assembly by cAMP.
J Cell Biol. 2001 Dec 24;155(7):1307-18. Epub 2001 Dec 24.

Thomas T, Jordan K, Laird DW.
Role of cytoskeletal elements in the recruitment of Cx43-GFP and Cx26-YFP into gap junctions.
Cell Commun Adhes. 2001;8(4-6):231-6.

Till JE.
Stem cells in differentiation and neoplasia.
J Cell Physiol Suppl. 1982;1:3-11.

Traub O, Look J, Dermietzel R, Brummer F, Hulser D, Willecke K.
Comparative characterization of the 21-kD and 26-kD gap junction proteins in murine liver and cultured hepatocytes.
J Cell Biol. 1989 Mar;108(3):1039-51.

Trosko JE, Ruch RJ.
Cell-cell communication in carcinogenesis.
Front Biosci. 1998 Feb 15;3:d208-36.

Trosko JE, Goodman JI.
Intercellular communication may facilitate apoptosis: implications for tumor promotion.
Mol Carcinog. 1994 Sep;11(1):8-12.

Trosko JE, Chang CC, Madhukar BV.
Cell-to-cell communication: relationship of stem cells to the carcinogenic process.
Prog Clin Biol Res. 1990;331:259-76.

Valenti G, Procino G, Carmosino M, Frigeri A, Mannucci R, Nicoletti I, Svelto M.
The phosphatase inhibitor okadaic acid induces AQP2 translocation independently from AQP2 phosphorylation in renal collecting duct cells.
J Cell Sci. 2000 Jun;113 (Pt 11):1985-92.

van der Heyden MA, Rook MB, Hermans MM, Rijksen G, Boonstra J, Defize LH, Destree OH.
Identification of connexin43 as a functional target for Wnt signalling.
J Cell Sci. 1998 Jun;111 (Pt 12):1741-9.

VanSlyke JK, Musil LS.
Degradation of connexins from the plasma membrane is regulated by inhibitors of protein synthesis.
Cell Commun Adhes. 2003 Jul-Dec;10(4-6):329-33.

VanSlyke JK, Deschenes SM, Musil LS.
Intracellular transport, assembly, and degradation of wild-type and disease-linked mutant gap junction proteins.
Mol Biol Cell. 2000 Jun;11(6):1933-46.

Warn-Cramer BJ, Lampe PD, Kurata WE, Kanemitsu MY, Loo LW, Eckhart W, Lau AF.
Characterization of the mitogen-activated protein kinase phosphorylation sites on the connexin-43 gap junction protein.
J Biol Chem. 1996 Feb 16;271(7):3779-86.

Wei CJ, Francis R, Xu X, Lo CW.
Connexin43 associated with an N-cadherin-containing multiprotein complex is required for gap junction formation in NIH3T3 cells.
J Biol Chem. 2005 May 20;280(20):19925-36. Epub 2005 Feb 28.

Willecke K, Jungbluth S, Dahl E, Hennemann H, Heynkes R, Grzeschik KH.
Six genes of the human connexin gene family coding for gap junctional proteins are assigned to four different human chromosomes.
Eur J Cell Biol. 1990 Dec;53(2):275-80.

Yamasaki H, Omori Y, Zaidan-Dagli ML, Mironov N, Mesnil M, Krutovskikh V.
Genetic and epigenetic changes of intercellular communication genes during multistage carcinogenesis.
Cancer Detect Prev. 1999;23(4):273-9.

Yamasaki H, Mesnil M, Omori Y, Mironov N, Krutovskikh V.
Intercellular communication and carcinogenesis.
Mutat Res. 1995 Dec;333(1-2):181-8

Yamasaki H.
Gap junctional intercellular communication and carcinogenesis.
Carcinogenesis. 1990 Jul;11(7):1051-8.

Yano T, Ito F, Kobayashi K, Yonezawa Y, Suzuki K, Asano R, Hagiwara K, Nakazawa H, Toma H, Yamasaki H.
Hypermethylation of the CpG island of connexin 32, a candiate tumor suppressor gene in renal cell carcinomas from hemodialysis patients.
Cancer Lett. 2004 May 28;208(2):137-42.

Zhai Y, Wu R, Schwartz DR, Darrah D, Reed H, Kolligs FT, Nieman MT, Fearon ER, Cho KR.
Role of beta-catenin/T-cell factor-regulated genes in ovarian endometrioid adenocarcinomas.
Am J Pathol. 2002 Apr;160(4):1229-38.

Zhang LX, Cooney RV, Bertram JS.
Carotenoids up-regulate connexin43 gene expression independent of their provitamin A or antioxidant properties.
Cancer Res. 1992 Oct 15;52(20):5707-12.

Zhang ZQ, Zhang W, Wang NQ, Bani-Yaghoub M, Lin ZX, Naus CC.
Suppression of tumorigenicity of human lung carcinoma cells after transfection with connexin43.
Carcinogenesis. 1998 Nov;19(11):1889-94.

Zhu D, Caveney S, Kidder GM, Naus CC.
Transfection of C6 glioma cells with connexin 43 cDNA: analysis of expression, intercellular coupling, and cell proliferation.
Proc Natl Acad Sci U S A. 1991 Mar 1;88(5):1883-7.

General

Alberts Bruce et al.
Molecular Biology of the Cell, 4th ed.
Garland Science, 2002

Kreis and Vale
Extracellular matrix, Anchor, and Adhesion Proteins, 2nd ed.
Oxford University Press, 1999

Lewin Benjamin
Genes VII
Oxford University Press and Cell Press, 2000

Serban Nada
Pokretne i Nepokretne Celije (Serbian)
Savremena Administracija, 1996